

VIBRATIONAL RESPONSE OF STRUCTURES DUE TO
EXTERNAL DYNAMIC LOADING

IN PARTICULAR: INVESTIGATIONS OF THE BEHAVIOUR OF CROSS
BRACED WATER TOWERS IN EARTHQUAKES

A thesis presented for
the degree of Doctor of Philosophy
in Civil Engineering
in the University of Canterbury,
Christchurch, New Zealand.

by

R. SHEPHERD

1971

~~654.6~~
TA
654.6
.S548
1971
copy 1

ABSTRACT

A method of predicting the seismic response of cross braced elevated water tower structures, using an electronic digital computer to integrate the equations of motion of mathematical models of the system, is presented.

The validity of the models is established by experiments on a prototype water tower, which serve to verify the allowances made for the convective action of the water, and by tests on a simple braced frame, from which it is concluded that selected multiphase lateral stiffness characteristics can be achieved with satisfactory reliability.

The earthquake response of a typical elevated water tank, with braces having various elastic and post yield properties, is determined and conclusions are drawn regarding the desirable characteristics of this form of structure if it is to resist earthquakes effectively.

ACKNOWLEDGEMENTS

The author records with appreciation the assistance received from:

Professor R.H. Evans, Emeritus Professor of Civil Engineering, University of Leeds for the interest, guidance and encouragement which he has generously provided for many years;

the academic staff, graduate students and technicians of the Civil Engineering Department, University of Canterbury, particularly R.J. O'Driscoll, J.H. Wood, R.A.H. Donald, W.R. Walpole, G.K. Sidwell, R.E. McConnel and R.D. Sharpe, sometime graduate students, for their co-operation in analytical studies of mutual interest, A.J. Carr, Lecturer in Civil Engineering for advice on computing problems and F. Babonnick and A. Foot for assistance with the testing undertaken on braced frameworks;

Professors F.M. Henderson, acting Head of Department, 1968, and H.J. Hopkins permanent Head of the Civil Engineering Department, for making available technician assistance and technical resources to support the experiment phase of this work;

Mr R.J.P. Garden, Consulting Engineer, of Dunedin for drawing the author's attention to the possibilities of using multiphase cross-bracing in earthquake resistant design;

Professors G.W. Housner, D.E. Hudson and P.C. Jennings of the California Institute of Technology for their outstanding

contributions to Earthquake Engineering Research as a result of which the task of other workers in the field is so much less onerous;

Professor G.V. Berg of the University of Michigan for making available digitised records of strong motion earthquakes;

the staff of the University Computer Centre for their generous assistance with all aspects of the computer analyses undertaken;

Miss Kay E. Evans, for typing this thesis, and W. McClelland and H. Patterson for assistance with the figures.

TABLE OF CONTENTS

	Page
Abstract	(i)
Acknowledgements	(ii)
List of Tables	(vii)
List of Computer Programs	(vii)
List of Figures	(viii)
List of Symbols	(xii)
<u>Chapter One</u> Introduction	1
<u>Chapter Two</u> Two Mass Representation of an Elevated Water Tank	
II.1 Introduction	10
II.2 The Ilam Elevated Water Tower	10
II.3 Predicted Properties of the Ilam Water Tower	14
II.4 Measured Properties of the Ilam Water Tower	22
II.5 Comments on the Two Mass Modelling of Water Towers	26
<u>Chapter Three</u> Cross Bracing in Earthquake Resistant Structures	
III.1 Introduction	27
III.2 Cross Braced Panel Testing	29
III.3 Material Properties	37
III.4 Tests Undertaken	39
III.5 Comment on Cross Braced Panel Testing	62

Chapter Four Seismic Analyses by Digital Computer
Mathematical Modelling

IV.1	Introduction	63
IV.2	Mathematical Modelling of Structural Frameworks	64
IV.3	Determination of Elastic Dynamic Response of Multimass Systems by Numerical Integration	66
IV.4	Equation of Motion of a Yielding System	72
IV.5	Mathematical Model of an Elevated Water Tank	75

Chapter Five Computer Programs Used in the Analyses
of Cross Braced Frames

V.1	Stiffness Matrix Assembly Program	78
V.2	Normal Mode Properties Program	79
V.3	Damping Matrix Formulation Program	80
V.4	Matrix Inversion Program	80
V.5	Dynamic Elastic Response Program	80
V.6	Cross Braced Frame Dynamic Analysis Program (XBFRME)	81
V.6 (i)	KLAT	81
V.6 (ii)	Results of Validity Check on KLAT	86
V.6 (iii)	Main Program XBFRME	91
V.6 (vi)	Checks on XBFRME Program	102
V.7	Summary of the Use of Digital Computer Programs in the Determination of the Seismic Response of Elevated Water Tanks	104

Chapter Six Seismic Response Analysis

VI.1	Introduction	105
VI.2	The Structure Examined	105
VI.3	Digital Computer Analyses with No Convective Action of the Water	107
VI.4	Digital Computer Analyses Including Convective Action of the Water	119

Chapter Seven Review of Analyses Undertaken and
Comments on Applicability of the
Proposed Analysis Method

VII.1	Review of the Analyses Described in Chapter Six	132
VII.2	Consideration of Dissipated Energy as a Proportion of the Total Seismic Input Energy	141
VII.3	The Choice of Accelerogram	143
VII.4	Torsional Response Consideration	145
VII.5	Conclusion	147

APPENDICES

Appendix I	Calculations Undertaken in the Modelling of the Ilam Water Tower	152
Appendix II	Post Yield Axial Stiffness of Bracing Rods	154
Appendix III	Geometrical and Structural Properties of Test Frame	155
Appendix IV	Library Programs Used in the Analyses of Cross Braced Frameworks	158
Appendix V	Summary of Calculations Undertaken in Modelling the Three Storey Frame Shown in Figure 6.1.	172

REFERENCES		175
------------	--	-----

LIST OF TABLES

<u>Table</u>	<u>Title</u>	<u>Page</u>
1	Input and Output Data for MODANAL analysis of Ilam Water Tower	21
2	Comparison of Measured and Predicted Frequencies of the Ilam Water Tower	25
3	Summary of Material Properties of Bracing Rods	40
4	Results of MODANAL Analysis for Prototype Tank on Moran and Cheney Type Tower	121
5	Comparison of Extended Elastic Responses Neglecting Convective Action of the Water and Including this Effect	137

LIST OF COMPUTER PROGRAMS

<u>List</u>	<u>Program</u>	<u>Page</u>
1	MODANAL program	19
2	TRUEFORCE program	41
3	Subprogram KLAT	84
4	XBFRME Program	93
L.P.1	2-D STRUCTURE Program	159
L.P.2	Normal Modes Program	165
L.P.2A	Damping Matrix Program	167
L.P.3	Matrix Inversion Program	168
L.P.4	ELRES Program	169

LIST OF FIGURES

<u>Figure</u>	<u>Caption</u>	<u>Page</u>
2.1	Typical Elevated Water Tower	11
2.2	Two Mass Representation	11
2.3	Ilam Water Tower	12
2.4	Pull Back Testing of Ilam Water Tower	12
2.5	Section of Ilam Water Tower	13
2.6	Equivalent Dynamic System (After Housner)	16
2.7	Typical Theoretical Mode Shapes	20
2.8	Typical Oscilloscript Traces Recorded	24
3.1	Details of Hinged Knee Braced Frame	31
3.2	Details of Rigid Knee Braced Frame	32
3.3	Details of Racking Test Rig	34
3.4	Details of Racking Test Rig	35
3.5	Log-Log Plot of True-Stress, True-Strain for 0.25 in diameter mild steel bracing	38
3.6	True-Force, True-Deflection Curves for Mild Steel Bracing Rods after Yield	42
3.7	True-Force, True-Deflection Curves for Mild Steel Bracing Rods after Yield	43
3.8	Static Sidesway Stiffness Test - Unbraced Rigid Knee Portal	44
3.9	Static Sidesway Stiffness Test - Rigid Knee Portal braced with one 0.25 in diameter Mild Steel Rod	46
3.10	Static Sidesway Stiffness Test - Pinned Knee Portal, braced with diagonally opposed pre-stressed 0.25 in diameter Mild Steel Rods	48
3.11	Static Sidesway Stiffness Test - Pinned Knee Portal braced with diagonally opposed pre-stressed 0.25 in diameter Mild Steel Rods and parallel diagonally opposed 0.205 in diameter High Tensile Steel Rods	49

<u>Figure</u>	<u>Caption</u>	<u>Page</u>
3.12	Static Sidesway Stiffness Test - 3.5 cycles of loading, Pinned Knee Portal braced with diagonally opposed prestressed 0.25 in diameter mild steel rods and parallel diagonally opposed 0.205 in diameter high tensile rods	51
3.13	Static Sidesway Stiffness Test - 4.5 cycles of loading - Pinned Knee Portal braced with diagonally opposed prestressed 0.25 in diameter mild steel rods and parallel diagonally opposed 0.205 in diameter high tensile steel rods	52
3.14(a)	Static Sidesway Stiffness Test, 2 cycles of loading, Rigid Knee Portal braced with diagonally opposed prestressed 0.25 in diameter mild steel rods and parallel diagonally opposed 0.205 in diameter high tensile steel rods	54
3.14(b)	Third cycle of 3.14(a) Test	55
3.15	Cyclic Loading Test, Pinned Knee Portal braced with diagonally opposed 0.25 in diameter mild steel rods	58
3.16	Cyclic Loading Test, Pinned Knee Portal braced with 0.25 in diameter mild steel rods and 0.211 in diameter high tensile steel rods	60
3.17	Cyclic Loading Test, Rigid Knee Portal braced with 0.25 in diameter mild steel rods and 0.211 in diameter high tensile steel rods	61
4.1	Linear Acceleration Variation	76
4.2	Idealised Three Panel Elevated Water Tank	76
5.1	Flow Chart for Subprogram KLAT	82
5.2	Comparison of Experimental Sidesway Stiffness Test Results with those of KLAT for Pinned Knee braced frame	87
5.3	Comparison of Experimental Sidesway Stiffness Test Results with those of KLAT for rigid knee braced frame - first cycle	88
5.4	Comparison of Experimental Sidesway Stiffness Test Results with those of KLAT for rigid knee braced portal - continuation of Fig. 5.3 plot	90

<u>Figure</u>	<u>Caption</u>	<u>Page</u>
5.5	Flow Chart for Computer Program XBFRME	92
6.1	Elevated Water Tank Analysed	106
6.2	True Force/True Deflection Curves for Bracing Rods	109
6.3	Response of Extended Elastic, Undamped, Unbraced Frame supporting an empty tank	111
6.4	Response of Extended Elastic, 2% damped, Unbraced Frame supporting an empty tank	113
6.5	Response of Extended Elastic, undamped, Braced Frame supporting a full tank	114
6.6	Response of Extended Elastic, 2% damped (based on full stiffness) Braced Frame supporting a full tank	115
6.7	Response of Extended Elastic, 2% damped (based on unbraced frame stiffness) Braced Frame supporting a full tank	115
6.8	Response of system giving the plot in Fig. 6 and 7 but with 1.50 El Centro excitation in place of 1.0 El Centro	117
6.9	Response of Extended Elastic, 2% damped, Braced Frame supporting half a tank full of water	118
6.10	Response of 2% damped, bilinear Braced (with prestress) Frame supporting a full tank	120
6.11	Response of 2% damped, bilinear Braced Frame supporting half a tank full of water	118
6.12	Response of Extended Elastic, 2% damped, Braced Frame supporting a full tank of (convective) water	123
6.13	Response of Extended Elastic, 2% damped, Braced Frame supporting half a tank full of (convective) water	123
6.14	Response of 2% damped, bilinear Braced (with prestress) Frame supporting a full tank of (convective) water	125

<u>Figure</u>	<u>Caption</u>	<u>Page</u>
6.15	Response of system giving the plot in Fig. 6.14 but with 0.60 El Centro excitation in place of 1.0 El Centro	125
6.16	Response of 2% damped, bilinear Braced (no prestress) Frame supporting a full tank of convective water	126
6.17	Response of system giving the plot in Fig. 6.14 but with bottom bay bracing 2.82 in ² of M.S. and 2.0 in ² of H.T.S. each way	128
6.18	Response of system giving the plot in Fig. 6.17 but with only half a tank of (convective) water	128
6.19	Response of system giving the plot in Fig. 6.14 but with bottom bay bracing 2.41 in ² of M.S. and 0.049 in ² of H.T.S. each way	129
6.20	Response of system giving the plot in Fig. 6.14 but with bottom bay bracing 2.41 in ² of M.S. and 0.197 in ² of H.T.S. each way	129
6.21	Response of system giving the plot in Fig. 6.14 but with bottom bay bracing 2.41 in ² of M.S. and 0.440 in ² of H.T.S. each way	131
6.22	Response of system giving the plot in Fig. 6.14 but with bottom bay bracing 2.41 in ² of M.S. and 0.786 in ² of H.T.S. each way	131

LIST OF SYMBOLS

Note: A separate symbol table for the XBFRME computer program is given in section V.6(v) commencing on page 101.

A	integration constant or cross sectional area
$\{A\}$	vector used in numerical integration
B	integration constant
$\{B\}$	vector used in numerical integration
C	integration constant
$[C]$	damping matrix
c_r	damping coefficient
c_g	damping coefficient
$[D]$	matrix of pivots
d	displacement
d_1	column outside diameter
d_2	column inside diameter
d_{yb}	displacement to yield bracing
$\{d\}$	vector of distortions
\ddot{d}	acceleration
E	elastic modulus
e	base of Napierian logarithms
F	lateral force
$\{F\}$	vector of member forces
g	acceleration due to gravity
h	height of liquid in tank
h_1	height at which m_1 is considered to act

h_o	height at which m_o is considered to act
h_{so}	height of centre of mass position
I	second moment of area of section
$[K]$	stiffness matrix
$[K^*]$	matrix used in numerical integration
$[K]_{LAT}$	lateral stiffness matrix
K_o	strength coefficient
$\{k\}$	element stiffness matrix
k_1	effective spring stiffness of convective mass m_1
k_o	lateral stiffness of tower structure
k_{so}	lateral stiffness of mass m_{so}
L	length
$\{L\}$	vector of applied loads
$[M]$	mass matrix
m	total mass of liquid
m_1	mass of liquid acting convectively
m_o	mass of liquid acting with the structure
m_s	mass of structure
m_{so}	sum of m_o and m_s
n	strain hardening coefficient
n (subscript)	mode number
$[Q]$	multiplier matrix
$[Q^T]$	transform of $[Q]$
R	tank radius
s	engineering strain
t	time

t'	particular time
x	displacement
$\{x\}$	vector of mass displacements
x_1	displacement of mass m_1
x_{so}	displacement of mass m_{so}
\dot{x}	velocity
$\{\dot{x}\}$	vector of velocities
\dot{x}_t	velocity at time t
$\dot{x}_{t-\Delta t}$	velocity at time $t-\Delta t$
\ddot{x}	acceleration
$\{\ddot{x}\}$	vector of accelerations
\ddot{x}_g	base acceleration
\ddot{x}_t	acceleration at time t
$\ddot{x}_{t-\Delta t}$	acceleration at time $t-\Delta t$
$\{y\}$	vector of displacements
$\{\Delta R\}$	vector used in numerical integration
Δt	increment of time
$\{\Delta x\}$	vector of incremental displacements
$\{\Delta \dot{x}\}$	vector of incremental velocities
$\{\Delta \ddot{x}\}$	vector of incremental accelerations
ϵ_1	true strain
σ_1	true stress
σL	change in length
θ	angular distortion
ω	natural frequency of vibration

C H A P T E R O N E

INTRODUCTION

The problem of designing structures to minimise the effect of earthquakes has prompted extensive research in structural dynamics. The prediction of the elastic response of a structure to prescribed time varying loads or ground movements may readily be undertaken using the principles of general vibration theory^(1 & 2). However seismic disturbances are invariably unique and structures subjected to major earthquakes rarely behave in a linearly elastic manner. Thus the design problem is complicated by the indefinite nature of the disturbance and the complex behaviour of the structure.

Much attention has been devoted to the design of earthquake resistant multistorey framed structures and current earthquake resistant design philosophy involves the acceptance of two behaviour concepts. Buildings are assumed to resist small and medium seismic disturbances elastically, whereas plastic deformation is considered to provide collapse resistance to the near-catastrophic loading associated with a major earthquake⁽³⁾.

For the purposes of design it is usual to simulate dynamically induced earthquake loads by equivalent static forces. Current practice involves the calculation of the dynamic elastic properties of a proposed structure and the application of the response spectra, normal mode technique to the determination of the design loads^(4,5,6).

Allowance for the inelastic nature of the response at near-catastrophic loads is made by reducing the ordinates of the elastic response curves when deriving design spectra^(2,7,8).

So far as it has been possible to ascertain the procedure outlined above has been applied successfully to the seismic design of multi-storey framed structures.

However there are certain types of structure to which the method cannot be extended with impunity. A water tower is one such structure. Typically a braced steel framework is used to support a rectangular or cylindrical liquid storage tank and recognition that this form of structure differs substantially in its seismic response from multi-storey, multibay framed buildings is implied in earthquake resistant design codes⁽⁹⁾. The specified seismic design coefficients for water towers are of the order of twice those listed for buildings but this only partly reflects the development of a rational design procedure. The provisions are, in fact, somewhat arbitrary and progress towards a better justified design approach awaits an improved appreciation of the dynamic interaction of the elements comprising a water tower and the behaviour of the whole structure under earthquake loading.

Some thirty years ago considerable effort was expended in investigating the seismic behaviour of water towers. Jacobson⁽¹⁰⁾ used a large shaking table for experiments on model towers and similar work at M.I.T.⁽¹¹⁾ emphasized the necessity for a dynamic design approach to be adopted.

Westergaard's work⁽¹²⁾ on the changes of water pressure arising on dams due to earthquake motions was incorporated with the theory

developed from model considerations by Hoskings and Jacobson⁽¹³⁾ who found satisfactory agreement with theoretical results when the effective water mass acting in an impulsively loaded rectangular tank was measured. Carder⁽¹⁴⁾ tested steel water tanks by a series of pull back tests on the supporting towers and thereby studied the influence of foundation conditions, bracing properties and loading characteristics on the manner in which steel water towers vibrated with the object of determining their likely behaviour in an earthquake. An appreciation of the effect of initial tension in cross bracing rods were shown in the work of McLean and Moore⁽¹⁵⁾. They pointed out that in a laterally loaded three panel tower, having similar bracing in each panel, the upper tie rods buckled first, then the second panel rods and finally the diagonals in the lowest panel. A tower may pass through all stages in half a cycle of motion and as a result the period may be a composite of the four computed periods. Williams⁽¹⁶⁾ described investigations of the elastic behaviour of a cross braced elevated water tank and showed that for a single mass structure in near resonant conditions critical displacements may be built up before the type of ground motion changes.

Extensive model studies were undertaken by Ruge⁽¹⁷⁾ with the object of deriving data useful in the designing of seismically loaded water tanks. The concept of sacrificial cross bracing was discussed and he proposed the incorporation of specially designed spring elements in the structure, however only qualitative reference to damping and inelastic action was made. Ruge drew attention to the advantages gained by progressive rather than simultaneous failure of the

structural elements. Murphy⁽¹⁸⁾ carried out tests on an 84 ft. cross braced steel water tower at the Woburn Railway workshops at a result of which the natural period of vibration of the structure was determined. He suggested that the damage caused to the tower in the 1942 Wellington earthquake was consistent with that predictable using a Californian type response curve. Ulrich and Carder⁽¹⁹⁾ discussed the increase in stiffness and decrease in damping observed in tests of a cross braced water tower when loose tie rods had been tightened. They submitted that their observations supported the idea that if a structure becomes damaged by a strong earthquake the period will probably increase because of the loss of rigidity and as the elastic resilience is partly destroyed the internal damping will be somewhat higher and this serve to protect the structure, partly offsetting its damaged condition. The behaviour of typical elevated water tanks in the 1952 Californian earthquake was described by Steinbrugge and Moran⁽²⁰⁾. They reported stretching of anchor bolts and bracing rods and the complete collapse of some tanks. They deduced the modes of failure and inferred that torsional motion had occurred in some cases. Steinbrugge and Moran observed that wind braced tanks had not behaved satisfactorily whereas those designed for seismic loading had behaved better. They concluded that the currently effective design coefficients were not too large and that more study of the seismic response of cross braced elevated water towers was needed. After analysing the behaviour of water tank structures in the 1952 Californian earthquake Moran and Cheney⁽²¹⁾ reported satisfactory correlation between the behaviour

predicted using the response spectrum approach and the actual damage sustained.

Steinbrugge and Flores⁽²²⁾ described the stretching of cross bracing in elevated water tank towers resulting from the 1960 Chilean earthquake and Clough and Jenschke⁽²³⁾ carried out computer analyses of cross braced frames based on the steel frame buildings at the University of Concepcion in which diagonal bracing was incorporated. After this was broken the unbraced structure resisted the earthquakes occurring on the following day with no further structural damage thus giving rise to the question of whether the bracing was either necessary or beneficial. A digital computer study was made of the strengthening effect of the diagonal bracing when the buildings were subjected to ground motions of three different earthquakes. Results indicated that for some earthquakes the bracing may be beneficial whereas in other cases the bracing induced forces in the frame which exceed the strength of the braced structure. Thus the bracing may actually result in the structure being less earthquake resistant than if it was unbraced. Housner⁽²⁴⁾ has proposed a method of limit design based on the energy input by recorded strong ground motions. The velocity response spectra concept was used to define the energy fed into a structure and part of this energy was assumed to be dissipated by yielding of the structure. Housner showed that a cross braced tower designed to resist, at the limit of its elastic range, an equivalent static load of 0.125 g will be safe in a disturbance which would produce 0.40 g in an elastic structure, providing that the bracing rods may be permitted to stretch.

A method of determining the hydrodynamic pressures developed in a fluid container subjected to horizontal accelerations has also been proposed by Housner⁽²⁵⁾. The simplifications of earlier work including that of Jacobsen⁽²⁶⁾ and Graham and Rodriguez⁽²⁷⁾ involves some approximation but the technique is considered sufficiently accurate for seismic design use⁽²⁸⁾. Both Cloud⁽²⁹⁾ and Blume⁽³⁰⁾ have reported reasonable correlation between the observed behaviour of water tanks and the vibrational characteristics predicted using Housner's method. In addition satisfactory agreement between the behaviour of petroleum storage tanks in the 1964 Alaskan earthquake and the trends expected from theoretical considerations based on Housner's work has been demonstrated⁽³¹⁾.

However the considerable progress which has been achieved in the last decade in understanding the behaviour of buildings subjected to seismic loads has not been made in the fields of other structures such as elevated water tank towers and bridges. During this period substantial research effort expended on laboratory and site measurements, paralleled by significant theoretical investigations, has enabled much to be learnt of the dynamic characteristics of buildings in both the elastic and inelastic ranges. A more realistic approach towards the solution of the earthquake design problem for buildings is consequently being developed. The large proportion of papers describing investigations of building problems, in comparison with the handful of papers relating to elevated water tank towers, presented to the World Earthquake Engineering Conferences emphasises the relatively small effort being expended on these more specialised

structures.

Chandrasekaran and Krishna⁽³²⁾ have reported on experimental and analytical investigations of the seismic behaviour of reinforced concrete water towers. They recommended incorporation of diagonal steel braces in concrete frame towers to improve the strong motion response and suggested that a reinforced concrete elevated water tank may be analysed satisfactorily as a single degree of freedom system. This simplification was also used by Ramiah and Gupta⁽³³⁾ whereas Sonobe and Nishikawa⁽³⁴⁾, Infrim and Bratu⁽³⁵⁾ and Garcia⁽³⁶⁾ have advocated a two degree of freedom representation.

The computer simulation techniques which have been applied widely to building seismic response analysis in the last decade have received scant attention by those concerned with the earthquake behaviour of elevated liquid storage tanks. However Hanson and Fan⁽³⁷⁾ have used a digital computer to examine the effect of minimum cross bracing on the inelastic response of multistorey buildings and have shown that significant reductions in the ductility and energy absorption capacity requirements of the main frame members may be achieved by the provision of suitable diagonal members.

The principle of supplying load resistance by direct tension or compression members rather than by elements acting primarily in bending is not in itself new⁽³⁸⁾. The problems which may arise due to incorrect design of a braced framework are well recognised^(39,40). Also the concept that a braced frame may ride out a strong motion earthquake by progressive weakening of the structure has been suggested previously⁽⁴¹⁾. Nevertheless an examination of the seismic

behaviour of a range of cross braced elevated water tower structures using an electronic digital computer simulation technique does not appear to have been undertaken. The feasibility of providing expendable cross bracing and of predicting the response of elevated water tower structures which incorporated such structural components appears worthy of study and this consideration prompted the investigation described in this thesis.

In Chapter Two the mass representation of a water tower system, involving allowance for the convective motion of the fluid, is described and the validity of the model is substantiated by the results of a simple dynamic test on a prestressed concrete elevated water tank on the Ilam site of the University of Canterbury.

The concept of multiphase cross bracing is discussed in Chapter Three. Experiments undertaken on a simple cross braced frame are described and from these it is concluded that selected multiphase response may be achieved reliably in cross braced frames if sufficient attention is given to the determination of the material characteristics and to the structural detailing.

The seismic analysis of structures using digital computer mathematical modelling techniques is outlined in Chapter Four and, in particular, the calculation of the earthquake response of a yielding system by numerical integration of the appropriate equations of motion is described. The application of this analysis method to the determination of the displacement response of elevated water tanks supported on cross braced tower structures, to digitised seismic ground accelerations is explained.

Digital computer programs used in this analysis procedure are outlined in Chapter Five and the specially written cross braced frame dynamic analysis program XBFRME is described in detail. Results of verification checks on this program are given and some limitations of the mathematical model on which it is based are discussed.

Moran and Cheney's 100,000 (U.S.) gallon water tank supported on a three storey, single bay, cross braced frame, 105 ft. high, is used as the basis for the series of seismic response predictions described in Chapter Six. Differences in the response are determined between the situation in which entirely elastic response is assumed, and those in which multiphase response of the bracing elements is taken into account. Also the effects are examined of varying the levels of prestress and changing other aspects of the bracing system.

In Chapter Seven the investigation described in this thesis is reviewed and certain suggestions for the improved design of seismic resistant cross braced elevated water tank structures are presented.

The Appendices include descriptions of the calculations undertaken in modelling both the Ilam and the Moran and Cheney water towers, details of the geometric and structural properties of the test frames and lists of the library digital computer programs used in the analyses.

C H A P T E R T W O

TWO MASS REPRESENTATION OF AN ELEVATED WATER TANKII.1 Introduction

A typical elevated water tank is shown diagrammatically in Figure 2.1. To expedite computer simulation studies it is convenient to initially invoke the two degree of freedom representation^(35,36) and to replace the contents of the tank by an equivalent sprung mass m_1 , corresponding to the sloshing part of the liquid, and a second component m_0 corresponding to that portion of the tank contents which moves with the structure, the mass of which is designated by m_s in Figure 2.2.

The effective spring stiffness k_1 may be determined from considerations of the geometric properties of the tank⁽²⁸⁾ and the tower stiffness k_0 may be derived from the tower properties using standard structural analysis techniques.

The opportunity was taken to verify this two mass representation of a water tower system by comparing the predicted and measured dynamic characteristics of a prestressed concrete water tower on the Ilam site of the University of Canterbury.

II.2 The Elevated Water Tower

The structure examined is a prestressed concrete tubular tower supporting a cylindrical reinforced concrete tank and is shown in

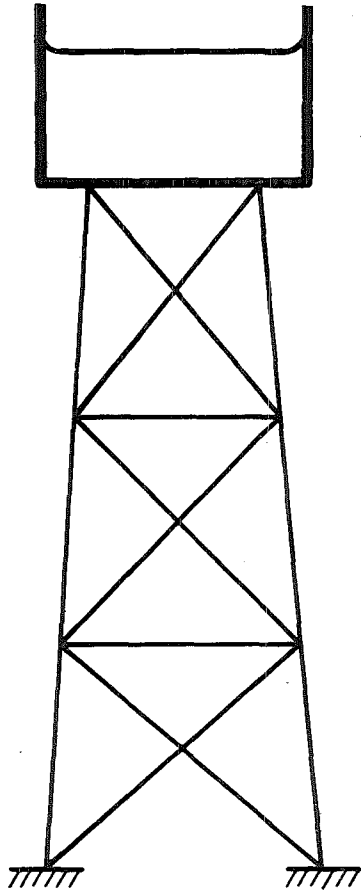


Fig.2.1: TYPICAL ELEVATED
WATER TOWER

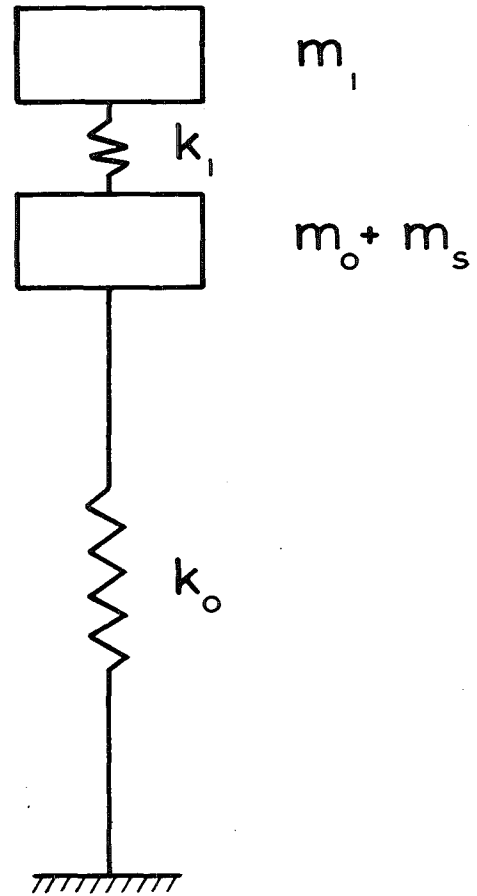


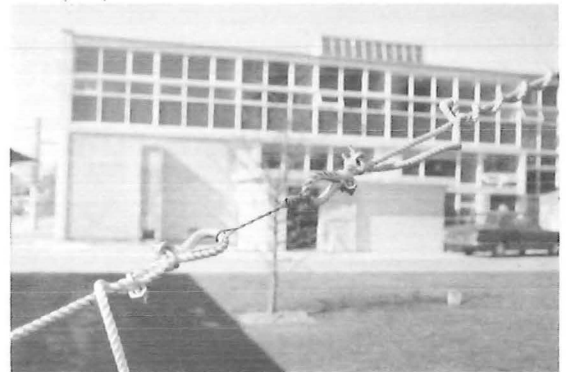
Fig. 2.2 : TWO MASS
REPRESENTATION



Fig.2.3-Ilam water tower.



(i)



(ii)



(iii)



(iv)

Fig.2.4 – Pull back testing of Ilam water tower.

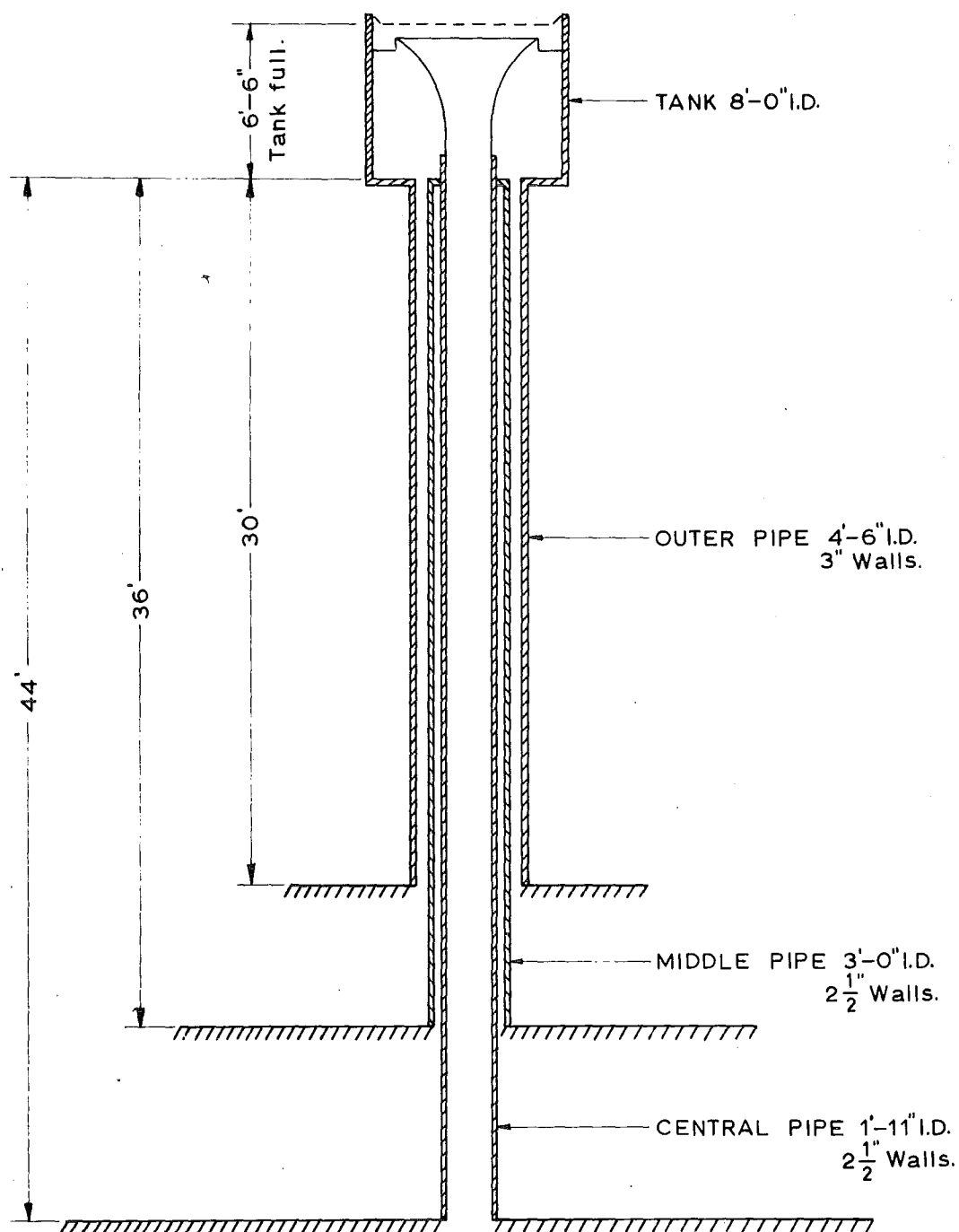


Fig. 2.5 : SECTION OF ILAM WATER TOWER

Figure 2.3. As is indicated in Figure 2.5 two concentric internal tubes form an integral part of the structure and consequently will assist in resisting lateral loads. Under normal operating conditions the tank serves to provide a constant head supply of water and the volume between the tubes is full of water.

II.3 Predicted Properties of the Ilam Water Tower

The dynamic characteristics of the elevated water tower were calculated using Housner's method^(25,28). The method of determining the hydrodynamic behaviour of the liquid container involves some approximation but the results are considered sufficiently accurate for seismic design use.

The fluid is separated into impulsive and convective parts. Then impulsive pressures are those associated with the forces of inertia produced by impulsive movements of the walls of the container, the pressures developed being directly proportional to the acceleration of the container walls. Convective pressures are those produced by the oscillation of the fluid and are thus the consequences of the impulsive pressures.

The equivalent dynamic system for a liquid storage tank is shown in Figure 2.6. The tank with an oscillating liquid surface is shown in Figure 2.6(a). The equivalent system is shown in Figure 2.6(b) where m_0 and m_1 produce dynamic forces equivalent to those produced by the liquid.

The mass m_0 exerts a maximum horizontal force directly proportional to the maximum acceleration of the tank bottom, at a height

h_o (see Figure 2.6(b) and thus contributes to the overturning moment in the tank.

The mass m_1 acting as a solid oscillating mass flexibly connected to the walls and located at a height h_1 also contributes to the overturning moment acting on the tank. The value of the overturning moment is computed by increasing the vertical arms to allow for the moment of the dynamic forces acting on the bottom. Thus each moment arm h_o and h_1 has two distinct values, the smaller being used to evaluate the bending moment on a plane just above the bottom, and the larger value to determine the overturning moment on a plane just below the bottom. The first case may be designated by the subscript ebp (excluding bottom pressure) and the second by the subscript ibp (including bottom pressure). Where there is a risk that the tank wall may buckle⁽³¹⁾ the ebp moment is important. In the case of the particular concrete tank under consideration the ibp value will be of greater significance.

The mass of the tank and accessories may be accounted for by increasing m_o where necessary.

The determination of the masses m_o and m_1 , the moment arms h_o and h_1 and the effective spring stiffness k_1 may be readily undertaken following Housner's work as is indicated below.

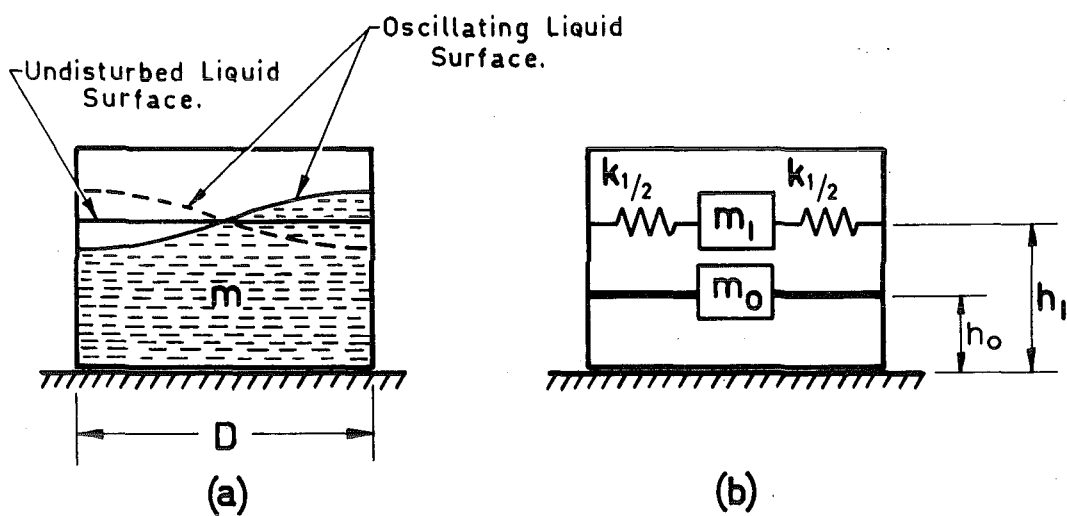


FIGURE 2.6
(After Housner)

Computation Procedure (summarised from reference 25)

Cylindrical tank case.

(a) Calculation of Impulsive Force

Steps (1) Determine the equivalent impulsive mass m_o

$$m_o = \frac{\tanh \sqrt{3} R/h}{\sqrt{3} R/h} \cdot m$$

where R is the tank radius

h is the liquid height

m is the total mass of liquid

(2) Determine the effective height h_o

$$h_o = \frac{3h}{8} \left[1 + \frac{4}{3} \left(\frac{\sqrt{3} R/h}{\tanh \sqrt{3} R/h} - 1 \right) \right]$$

(3) Add m_o to the mass of the structure m_s to obtain m_{so}

(4) Determine centre of mass position h_{so}

$$h_{so} = \frac{m_o h_o + m_s h_s}{m_{so}}$$

(b) Calculation of Convective Force

(5) Determine the equivalent convective mass m_1

$$m_1 = 0.387 R/h \cdot \tanh (1.84 h/R) \cdot m$$

(6) Determine the effective height h_1

$$h_1 = h \left[1 - \frac{\cosh \sqrt{27/8} h/R - 135/88}{\sqrt{27/8} h/R \sinh \sqrt{27/8} h/R} \right]$$

(c) Calculation of normal mode properties

- (7) Compute the lateral stiffness of the water tower i.e. the elastic load/deflection characteristic of the mass centre point (at height h_{so} above the bottom of the tank.)

- (8) Determine the equivalent spring stiffness k_1

$$k_1 = 5.4 \frac{m_1^2 g h}{m R^2}$$

- (9) Compute the normal mode frequencies and displaced shapes for the two-mass coupled system.

$$\omega^2 = \frac{1}{2} \left[\left(\frac{k_{so} + k_1}{m_{so}} + \frac{k_1}{m_1} \right) \pm \sqrt{\left(\frac{k_{so} + k_1}{m_{so}} + \frac{k_1}{m_1} \right)^2 - \frac{4k_{so} k_1}{m_{so} m_1}} \right]$$

where ω is the natural frequency (radians/sec)

$$\text{also } \frac{x_{so}}{x_1} = 1 - \frac{m_1 \omega^2}{k_1}$$

where $\frac{x_{so}}{x_1}$ is the displacement ratio of the total impulsive mass.

The computer program MODANAL (list 1) was written to expedite the computation of the modal properties of a two mass representation of an elevated water tower using Housner's equations. The input data includes geometric and mass properties of the tower and the lateral stiffness of the structure with respect to the mass centroid. The output includes the natural frequencies and associated displaced shapes of the two modes of vibration (see Figure 2.7). Typical

PROGRAM MODANAL
THIS PROGRAM COMPUTES THE MODAL PROPERTIES OF A
TWO MASS REPRESENTATION OF AN ELEVATED WATER TOWER
USING HOUSNER'S EQUATIONS

```

REAL M,MS,KSO,MSO,K1,M1
55 N=1
  READ(5,1,END=99) M,R,H,MS,KSO,G,HS
  1 FORMAT(7G10.0)
  RATIO=R/H
  RAT=SQRT(3.)*RATIO
  MO=TANH(RAT)/RAT*M
  MO CALCULATED
  TRAT=3.*RATIO
  HO=.375*H*(1.+4.*(RAT/TANH(RAT)-1.)/3.)
  HO CALCULATED
  MSO=MS+MO
  MSO CALCULATED
  HSO=(MO*HO+MS*HS)/MSO
  HSO CALCULATED
  M1=0.387*RATIO*TANH(1.84/RATIO)*M
  M1 CALCULATED
  HRAT=SQRT(3.375)/RATIO
  H1=H*(1.-(COSH(HRAT)-135./88.)/(HRAT*SINH(HRAT)))
  H1 CALCULATED
  K1=5.4*M1**2*G*H/(M*R**2)
  K1 CALCULATED
  DISC=SQRT(((KSO+K1)/MSO+K1/M1)**2-4.*KSO*K1/(MSO*M1))
  IF(DISC.LT.0.0) GO TO 88
  CONST=(KSO+K1)/MSO+K1/M1
  WTW01=(CONST-DISC)/2.
  WTW02=(CONST+DISC)/2.
  IF(WTW01.LT.0.0.OR.WTW02.LT.0.0) GO TO 88
  XSOX11=1.-M1*WTW01/K1
  XSOX12=1.-M1*WTW02/K1
  W1=SQRT(WTW01)/6.284
  W2=SQRT(WTW02)/6.284
44 WRITE(6,999)
  WRITE(6,2) M
  WRITE(6,3) R
  WRITE(6,4) H
  WRITE(6,5) MS
  WRITE(6,6) KSO
  WRITE(6,7) G
  WRITE(6,8) HS
  2 FORMAT(///25X,'M = ',E12.4,' LBS/G'//)
  3 FORMAT(25X,'R = ',E12.4,' FEET'//)
  4 FORMAT(25X,'H = ',E12.4,' FEET'//)
  5 FORMAT(25X,'MS = ',E12.4,' LBS/G'//)
  6 FORMAT(25X,'KSO = ',E12.4,' LBS/FOOT'//)
  7 FORMAT(25X,'G = ',E12.4,' GRAVACCN'//)
  8 FORMAT(25X,'HS = ',E12.4,' FEET'////)
  WRITE(6,10) MSO
  WRITE(6,15) HSO
  WRITE(6,20) M1
  WRITE(6,25) H1
  WRITE(6,30) K1

```

```

GO TO (66,77),N
66 WRITE(6,35) W1
  WRITE(6,40) XSOX11
  WRITE(6,45) W2
  WRITE(6,40) XSOX12
  GO TO 55
77 WRITE(6,45)
  GO TO 55
10 FORMAT(///25X,'MSO = ',E12.4,' LBS/G'//)
15 FORMAT(25X,'HSO = ',E12.4,' FEET'//)
20 FORMAT(25X,'M1 = ',E12.4,' LBS/G'//)
25 FORMAT(25X,'H1 = ',E12.4,' FEET'//)
30 FORMAT(25X,'K1 = ',E12.4,' LBS/FOOT'//)
35 FORMAT(25X,'W1 = ',E12.4,' CYCLES/SEC'//)
40 FORMAT(25X,'XSO = ',E12.4//)
45 FORMAT(25X,'W2 = ',E12.4,' CYCLES/SEC'//)
50 FORMAT(25X,'ERROR IN CALCULATING FREQUENCY'//)
999 FORMAT(///25X,'*****')
88 N=2
  GO TO 44
99 STOP
END

```

TYPICAL INPUT DATA

0.0	4.	0.0	700.	650000.	32.2	2.
196.	4.	2.0	700.	650000.	32.2	2.
340.	4.	3.5	700.	650000.	32.2	2.
490.	4.	5.0	700.	650000.	32.2	2.
638.	4.	6.5	700.	650000.	32.2	2.

LIST 1

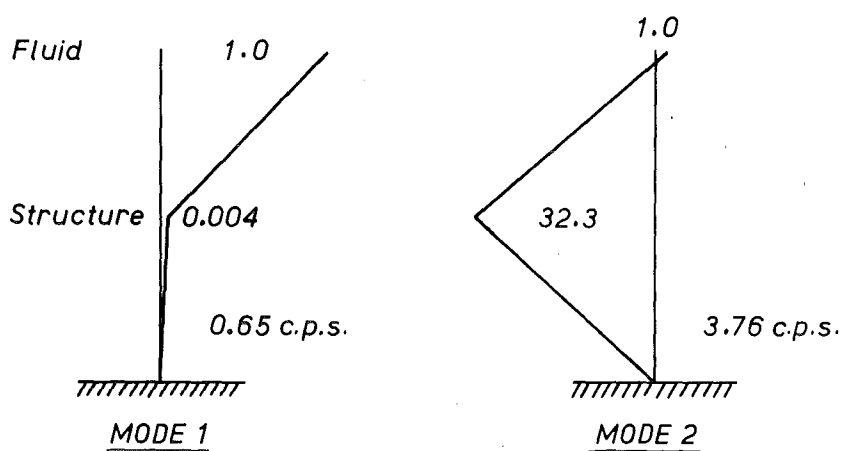


Figure 2.7: TYPICAL THEORETICAL MODE SHAPES

INPUT							OUTPUT								
FLUID MASS	TANK RADIUS	FLUID HEIGHT	STRUCT- URAL MASS	STRUCT- URAL STIFF- NESS	GRAVITY ACC $\frac{N}{G}$	STRUCT- URE C.G. HEIGHT	TOTAL INERTIA MASS	INERTIA MASS HEIGHT	CONVECT- IVE MASS	CONVECT- IVE MASS HEIGHT	EFFECT- IVE UPPER SPRING STIFF- NESS	FIRST MODE FRE- QUENCY	DISPLACE- MENT RATIO	SECOND MODE FRE- QUENCY	DISPLACE- MENT RATIO
M LBS/G	R FT	H FT	MS LBS/G	KSO KIPS/FT	G FT/SEC ²	HS FT	MSO LBS/G	HSO FT	M1 LBS/G	H1 FT	K1 KIPS/FT	W1 C.P.S.	XSO	W2 C.P.S.	XSO
638	4.0	6.5	545	650	32.2	2.0	1016	2.7	151	4.7	2.53	0.65	0.004	4.0	-37
490	4.0	5.0	545	650	32.2	2.0	856	2.5	149	3.5	2.45	0.64	0.004	4.4	-45
340	4.0	3.5	545	650	32.2	2.0	710	2.3	139	2.5	2.16	0.62	0.003	4.8	-58
196	4.0	2.0	545	650	32.2	2.0	601	2.1	110	2.2	1.35	0.56	0.002	5.2	-88
0	4.0	0.0	545	650	32.2	2.0	545	2.0	0	0	0	0	1.0	5.5	1.0
638	4.0	6.5	700	650	32.2	2.0	1171	2.6	151	4.7	2.53	0.65	0.004	3.8	-32
490	4.0	5.0	700	650	32.2	2.0	1011	2.4	149	3.5	2.45	0.64	0.004	4.0	-38
340	4.0	3.5	700	650	32.2	2.0	865	2.2	139	2.5	2.16	0.63	0.003	4.4	-48
196	4.0	2.0	700	650	32.2	2.0	756	2.1	110	2.2	1.35	0.55	0.002	4.7	-70
0	4.0	0	700	650	32.2	2.0	700	2.0	0	0	0	0	1.0	4.8	1.0
638	4.0	6.5	800	650	32.2	2.0	1271	2.6	151	4.7	2.53	0.65	0.004	3.6	-30
490	4.0	5.0	800	650	32.2	2.0	1111	2.4	149	3.5	2.45	0.64	0.004	3.9	-35
340	4.0	3.5	800	650	32.2	2.0	965	2.2	139	2.5	2.16	0.63	0.003	4.1	-43
196	4.0	2.0	800	650	32.2	2.0	856	2.1	110	2.2	1.35	0.56	0.002	4.4	-61
0	4.0	0	800	650	32.2	2.0	800	2.0	0	0	0	0	1.0	4.5	1.0

TABLE 1—Typical input and output data for MODANAL
analysis of Ilam water tower

input and output is shown in Table 1. A summary of the preliminary calculations undertaken in the modelling of the tower shown in Figure 2.3 is presented in Appendix I and the predicted significant translation vibration frequencies of the structure, corresponding to the tank being filled with water to selected levels, are presented in Table 2.

II.4 Measured Properties of the Ilam Water Tower

A simple pull-back test was carried out on the tower. The structure was deflected laterally by applying a load immediately below the tank through a 0.5 in. diameter nylon rope anchored both to a hoist at ground level and to a steel collar fixed round the tower (Figure 2.4(i)). The rope was tensioned using the hoist and quick release was achieved by cutting a 10 gauge mild steel wire link inserted in the length (Figure 2.4(ii)). The sections on either side of the wire link were anchored to reduce the hazard arising from back lash as the link was severed. (Figure 2.4(iii)).

The motion of the tower was recorded by a horizontal displacement meter (Figure 2.4(iv)), developed for use in the small amplitude dynamic testing of multistorey buildings⁽⁴²⁾, coupled to a pen recorder.

The meter is essentially an inverted pendulum enclosed in a cylindrical housing which is sealed onto the base plate and filled with silicon oil. The relative movement between the pendulum and the housing is detected by a Philips PR 9310 inductive pickup connected to Philips PR 3304 direct reading measuring bridge which

serves to amplify the transducer signal before it is recorded on a Philips PT 2108 oscilloscript. A maximum magnification of 24,000 may be obtained using this equipment, a 1 mm division on the recording paper corresponding to a meter base displacement of 4.16×10^{-5} mm. In practice the meter was calibrated on a shaking table to establish the variation in response characteristic with both temperature and frequency.

A series of pull-back tests were undertaken, the depth of water in the tank being varied between 0 and 6.5 ft. A typical free vibration oscilloscript trace is shown in Figure 2.8(a) and a portion of a trace obtained when the tower was excited by the action of the pump which circulates water up the outer tubes of the tower to spill over the internal weir at approximately 7 cusecs is shown in Figure 2.8(b). A pronounced beat effect is evident on the second trace. The recorded frequency of 4 c.p.s. evident on both traces is that of the second mode of the system, the configuration in which the structural movement predominates (see Figure 2.7). The percentage equivalent viscous critical damping was determined from the decay of the free vibration as 1.3%.

Subsequently hand shaking tests, similar to those used in building excitation⁽⁴³⁾ were used to determine the "sloshing" frequency of the water inside the tank. Recording was undertaken in a similar manner to that used in the pull-back tests. A range of water depths were again investigated and the results are presented in Table 2.

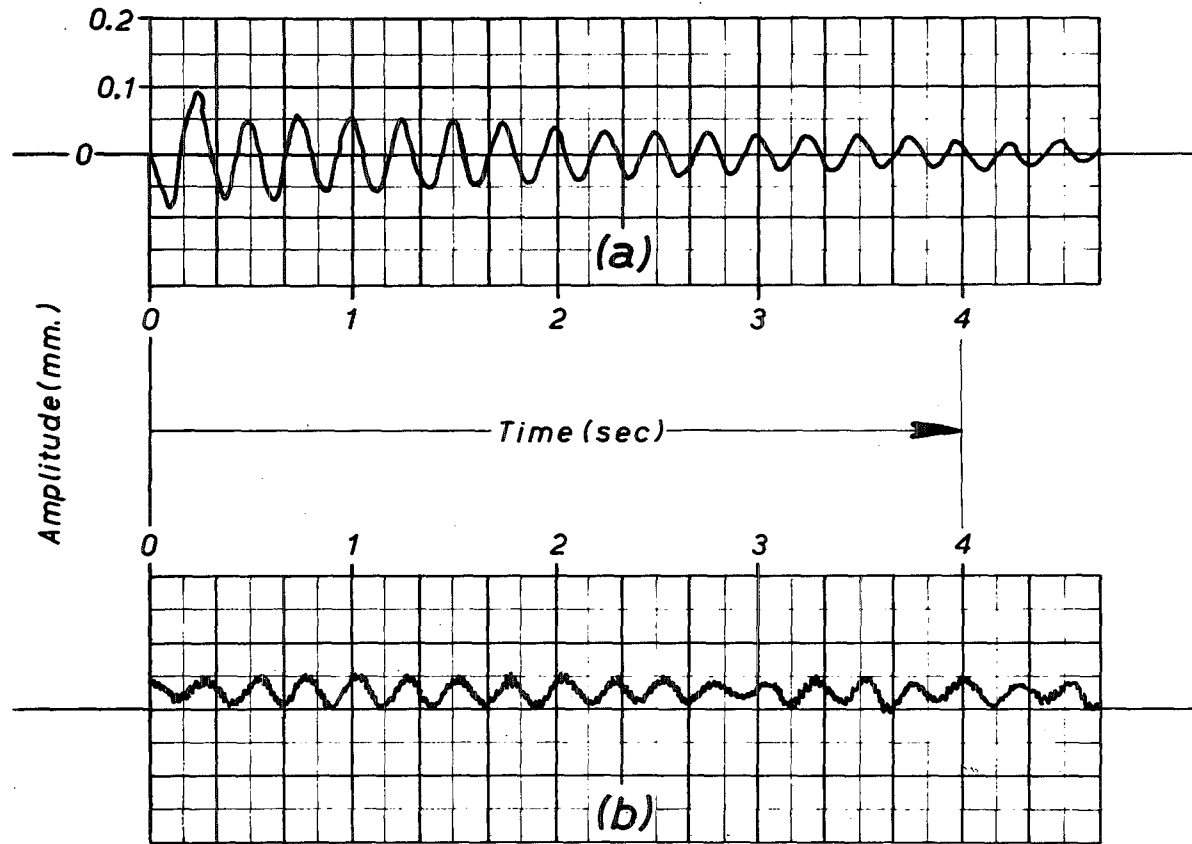


Figure 2.8: TYPICAL OSCILLOSCRIPT TRACES RECORDED ON
ILAM WATER TOWER
(a) Decay Curve (b) Vibration induced by pumping

Fluid Depth	MODE 1		MODE 2			
	MODANAL Values	Experi- mental Values	MODANAL Analysis Results For Structural Mass MS			Experi- mental Values
			MS=545	700	800	
ft.	c.p.s.	c.p.s.	c.p.s.	c.p.s.	c.p.s.	c.p.s.
6.5	0.65	0.64	4.0	3.8	3.6	4.0
5.0	0.64	0.62	4.4	4.1	4.0	4.25
3.5	0.63	0.60	4.8	4.4	4.1	4.5
2.0	0.56	0.55	5.2	4.7	4.4	4.76
0	0	0	5.5	4.8	4.5	4.9

Table 2. Comparison of measured and predicted frequencies of Ilam water tank structure.

II.5 Comment on the Two Mass Modelling of Water Towers

Where the primary objective is to determine a two degree of freedom system equivalent to a particular elevated water tower it is evident that the Housner analysis method may be conveniently programmed for digital computer execution and that a program such as MODANAL enables sensitivity analyses to be readily undertaken (see the results presented in Table 1 corresponding to variations in the quantity of water in the selected tank and to changes in the effective mass of the structural system.)

The testing undertaken on the Ilam water tower indicates that the use of a two mass representation will enable satisfactory predictions of the frequency properties to be made, particularly when this is essentially a preliminary step in the modelling of the system with the object of carrying out more complex analyses as described in the following chapters. The relatively small discrepancies between the measured and calculated frequency values can be accounted for by the hindering of the convective movement of the water by the internal weir structure. This would not be present in a typical elevated water storage tank and even better correlation could reasonably be expected in more usual configurations.

C H A P T E R T H R E E

CROSS BRACING IN EARTHQUAKE RESISTANT STRUCTURESIII.1 Introduction

Current earthquake resistant design philosophy requires structures to resist minor earthquakes without damage (i.e. elastically), to resist moderate earthquakes without structural damage but with some non-structural damage and to resist major earthquakes without catastrophic collapse but with some structural damage (i.e. inelastic deformation).

The use of cross bracing to resist lateral forces is an obvious method of providing economic stiffening in a tower structure. Increased rigidity may be achieved efficiently, in terms of material usage, in otherwise light and fairly flexible frameworks. Fifty years ago, when rigidity was considered to be of paramount importance in seismic design, cross bracing was extensively used. Certainly stiff structures do not normally suffer extensive secondary damage in small or moderate earthquakes but a growing awareness that more flexible structures tended to attract less inertia load in an earthquake disturbance, coupled with the understanding of the need for ductile characteristics, prompted the use of rigid jointed unbraced frameworks for building frames to such an extent that only in relatively light-tower structures, such as those used to support elevated water tanks, has cross bracing

continued to be generally used. In the last two or three years diagonal bracing has reappeared in several notable new buildings including the Alcoa building in San Francisco's Golden Gateway Centre and the 100 storey John Hancock building in Chicago. Nevertheless, the architectural disadvantages of bracing, coupled with some problems encountered in ensuring adequate structural integrity, appear likely to limit the use of bracing to semi-industrial structures such as elevated water tank towers. For this reason in this study consideration of the application of cross bracing is restricted to a basically simple, single bay, multistorey framework supporting a liquid storage tank.

The concept of two phase seismic response is implicit in the current seismic design philosophy outlined above. This mode of behaviour can readily be encouraged in braced frameworks by correct provision of ductile (and expendable) bracing elements inserted in an otherwise elastic frame. In the case of a braced tower with essentially rigid joints, the structure may be designed to have expendable bracing which will yield in a major seismic disturbance, thereby absorbing energy and at the same time increasing the flexibility of the structure so that the residual ductile, moment resisting frame can then survive the earthquake, despite having experienced substantial lateral displacements, by virtue of its own resistance. In the case of a braced tower with essentially pinned joints the bracing may itself be of a two phase nature, possibly provided by the use of pairs of parallel braces, one of each of which is designed

to remain elastic under all anticipated loading conditions and the second one being selected with the intention that it should yield and finally break in a major earthquake.

In parallel with the analytical study of this expendable bracing concept it was considered necessary to examine certain practical aspects of incorporating cross bracing of the type envisaged in a civil engineering structure. Consequently a feasibility study was undertaken. The simplest possible cross braced panel, consisting of a two dimensional rectangular steel frame braced with diagonal members, was modelled physically and subjected to selected racking tests. The object was to establish that behaviour of the type conceived can be obtained in a practical situation without resort to assembly techniques which might prove unrealistic and to confirm that the actual load deflection characteristics correlate satisfactorily with those predicted.

III.2 Cross Braced Panel Testing

Initially a series of simple rectangular portal frames of 5 ft. 0 in. leg and beam length and of 4 in. x 2.5 in. x 6.5 lb/ft. section R.S.J., both with and without bracing, were subjected to racking loads applied through a horizontal jack bearing against the top of the leg, in line with the centre line of the beam. Secondary effects, including deformation perpendicular to the plane of the frame and local stress concentrations around the knee prevented any meaningful behaviour patterns being established but as a result of this preliminary experimental work a better controlled series of tests

was subsequently undertaken. These are described below.

In order to facilitate laboratory testing with readily available equipment a standard braced panel fabricated from 3 in. x 2 in. x 4.5 lb/ft. R.S.J. section was selected (see Figures 3.1 and 3.2). This configuration allowed the detailing to be representative of that encountered in full scale steel frameworks without requiring particularly elaborate facilities to enable such a frame to be racked in the post-elastic range.

The span of the frame was chosen to conform to the 15 in. pitch of the holding down sockets on the test floor used and a further consideration in selecting the frame size was the availability of a variable displacement dynamic loading machine which had been constructed for, and used in, a dynamic study of structural concrete⁽⁴⁴⁾. This machine is capable of applying reversed cyclic loading at frequencies between 0.5 and 5.0 c.p.s. with a maximum force output of 4 ton, a maximum throw of 3 in. (i.e. 6 in. double amplitude) but with a limitation on the torque on the main drive shaft of 4.9 ton.in. As it was intended to use this machine to cyclically load the braced panels they were proportioned accordingly.

To overcome the difficulties encountered in the preliminary testing when the racking load was applied to the face of the section at the knee position, a load link consisting of two parallel 3 in. x 0.5 in. mild steel arms, pinned to the centre of the beam, was used. (See Figures 3.3(i) and 3.3(ii)). This enabled lateral loads to be applied along the centre line of the beam section without stress concentrations being introduced at one knee position and the

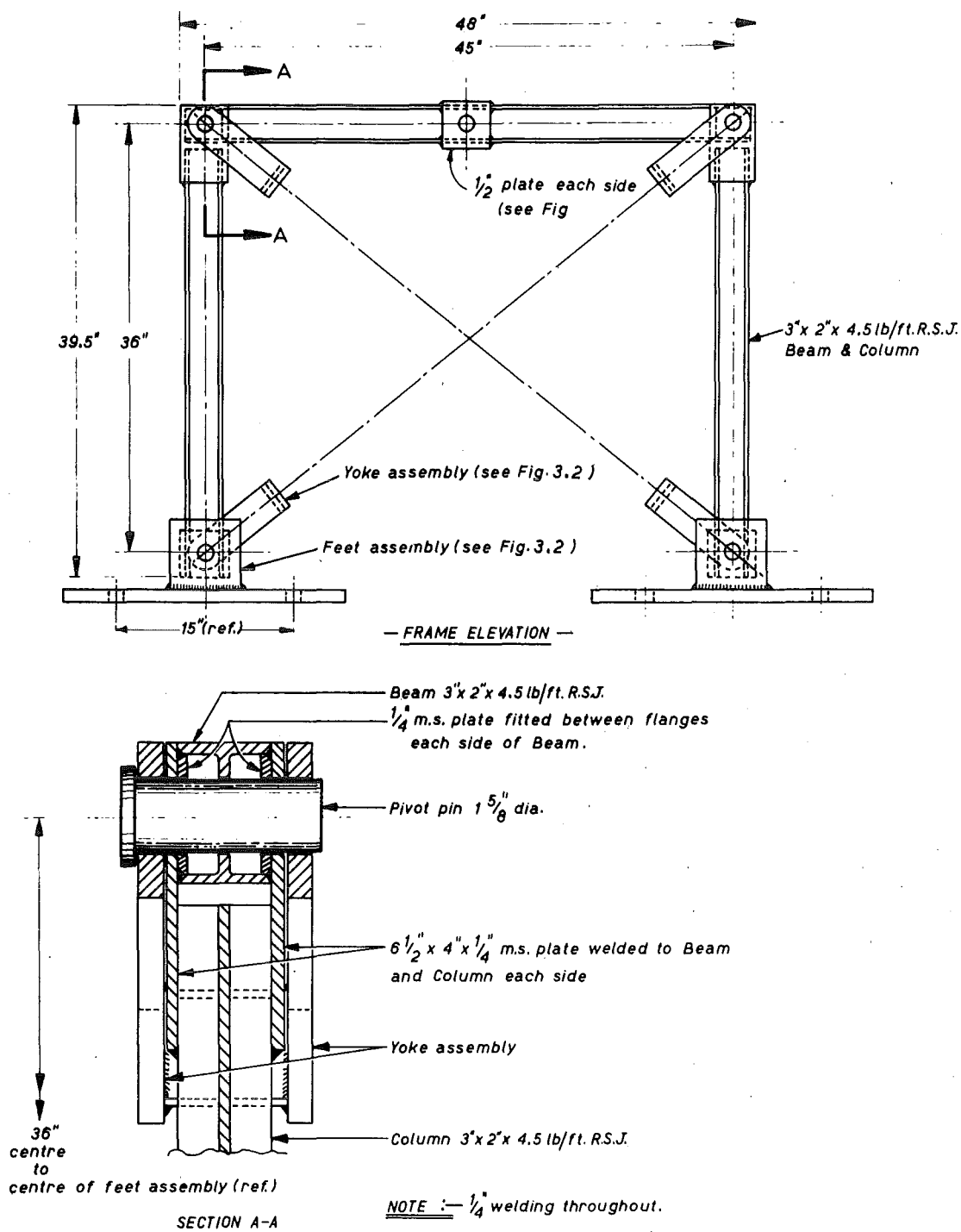


Figure 3.1: DETAILS OF HINGED KNEE BRACED PORTAL

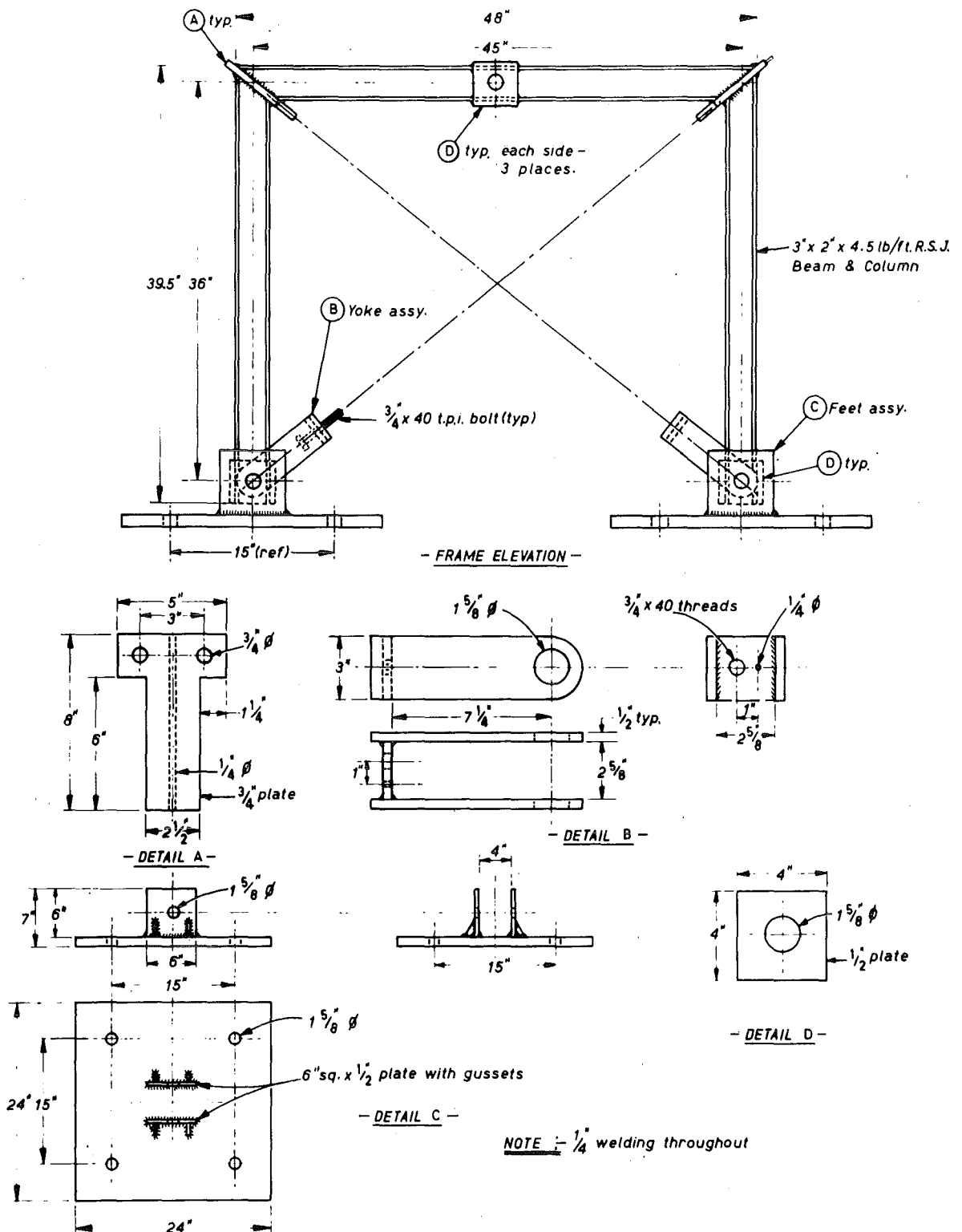


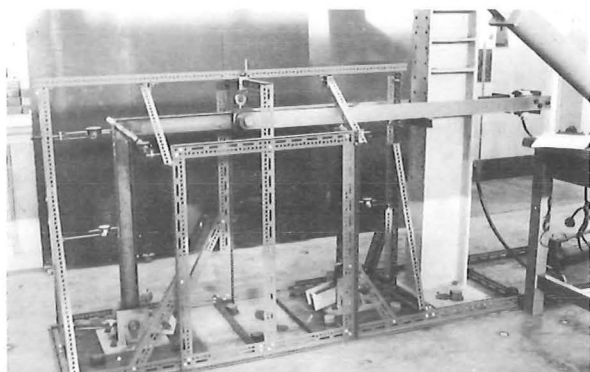
Figure 3.2: DETAILS OF RIGID KNEE BRACED FRAME

system was considered to adequately represent the inertia load situation developed in a prototype panel by earthquake movement.

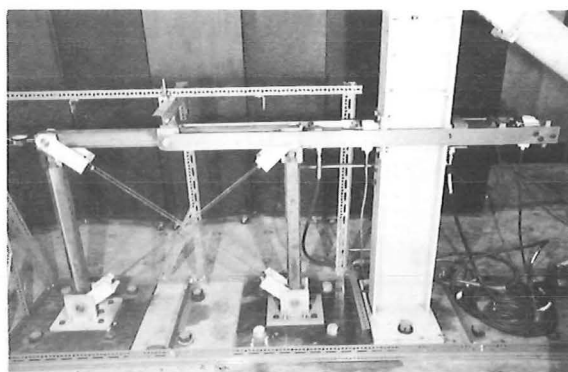
For the series of static tests undertaken provision was made to load the link in either tension or compression by means of a 10 ton Simplex hydraulic jack (model RC 106) activated by a Simplex two way hand pump. The jack reacted against a substantial laterally braced vertical cantilever (Figure 3.3(iii)) and was mounted in series with a 10 ton Philips 9266/10 load cell connected to a model 120 Budd strain gauge bridge, to enable the applied load to be determined.

When the test frames were racked by the dynamic loading machine (Figures 3.4(i) and 3.4(ii)) the load link was also used but in this case it was pinned to the machine cross head (Figure 3.4(iii)) which itself incorporates a load cell so that the transmitted axial force was again determined by means of a strain gauge bridge.

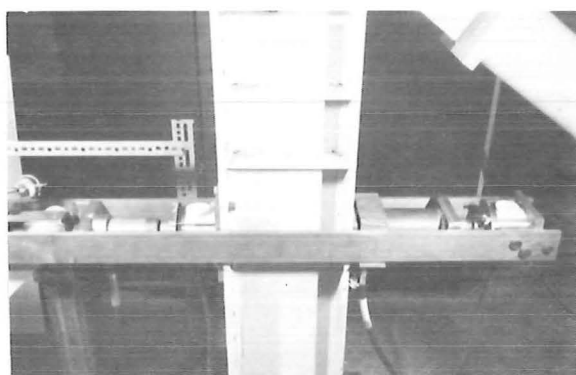
The deformation of the frame was measured by a series of 2 in. travel Mercer model Alpha 22(a) dial gauges and, in the dynamic testing, by deflection gauges consisting of strain gauged spring steel cantilever of 10 in. length and 0.5 in. x 0.0625 in. section. (See Figures 3.4(iv) and 3.4(v)). These were clamped to vertical supports bolted to the strong floor and connected to the frame under test through twin universal joints at the free ends. When recording dynamic loads and displacements, provision was made to connect the strain gauges in the load cell and the deflection gauges through Philips PR9304 bridges to a Riken Denshi X-Y Plotter Model F-3B, F-2



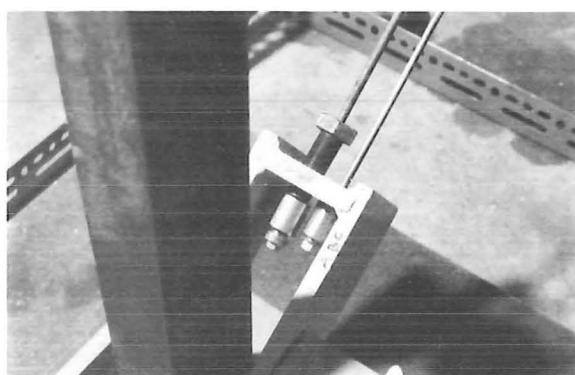
(i)



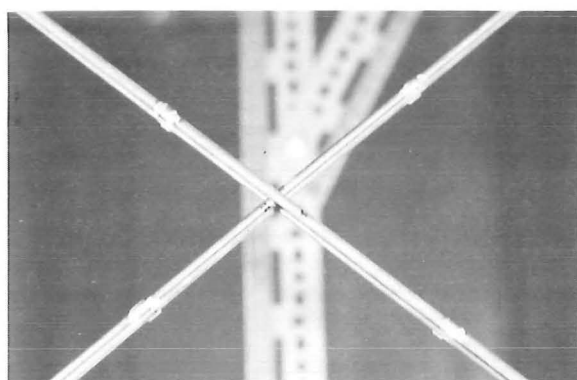
(ii)



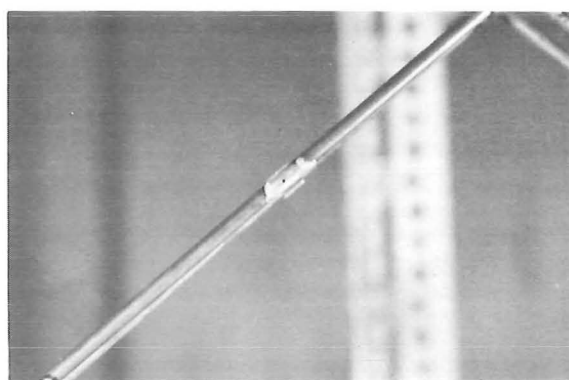
(iii)



(iv)

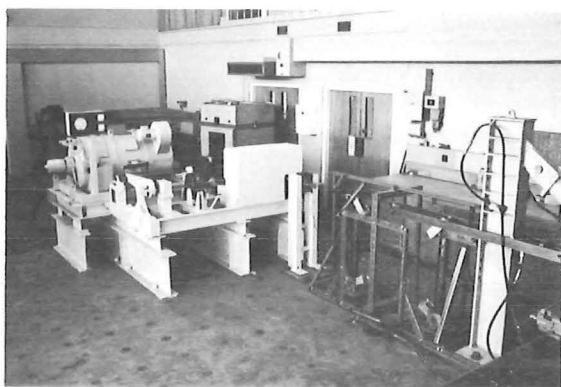


(v)



(vi)

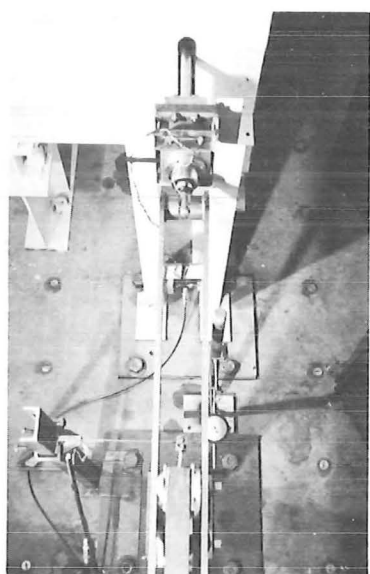
Fig.3.3—Details of racking test rig.



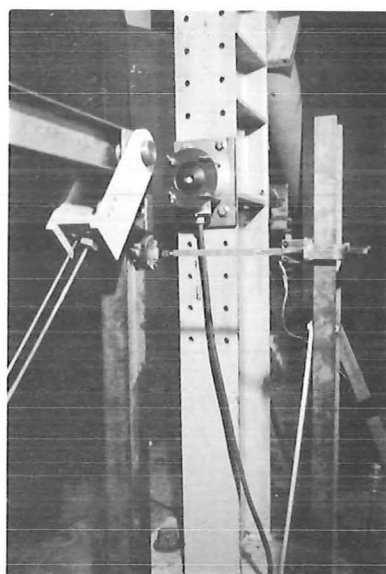
(i)



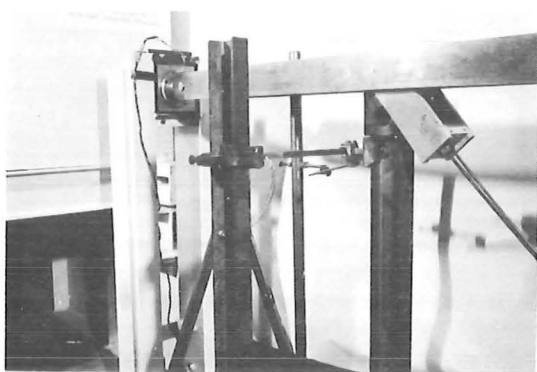
(ii)



(iii)



(iv)



(v)



(vi)

Fig. 3.4—Details of racking test rig.

on which Load/Deflection curves were recorded. (Figure 3.4(vi)).

Two methods were used to determine the strains in the circular section bracing rods. Standard Philips PR 9814 wire resistance strain gauges were glued to the surface of the rods in pairs on diametrically opposed positions and each pair was wired in series to ensure that axial, rather than bending, distortions were measured. In addition 8 in. Demac gauges were used to determine the rod strains, the Demac points being fixed to the rods using wax (see Figures 3.3(v) and 3.3(vi)). The relative merits of these two strain measuring techniques, as applied in the tests made, are discussed below.

The bracing rods were secured in the frame in several different ways. Some of the rods used initially had plates welded to each end so that they could be bolted to the knee stiffening plate at the upper end and to the stirrup at the lower one. Other rods were anchored by passing them through holes in the stiffening plates and in the stirrups, standard prestressing anchorages being used to secure the rods. (See Figure 3.3(iv)). In the later stages of testing the hinged panels, stirrups were used at both the upper and lower ends of the bracing and in all cases a drilled adjustment bolt was used between the anchorage and the plate through which the rod passed to facilitate the seating of the grips and to enable any slack which occurred during testing to be taken up.

III.3 Material Properties

Since it was intended to load the frames and bracing both in the elastic range and beyond yield, properties of the steel elements used were established in a series of tensile tests on specimens prepared and proportioned in accordance with BS18:1962. Several rectangular cross section specimens were cut from the web of the R.S.J. section adjacent to the lengths used in fabricating the portals, and sets of circular cross section test pieces were prepared from lengths of the rods used as bracing. A 25,000 lb. capacity Avery Universal testing machine was used to apply the tensile loads and the strains were recorded using a 2 in. gauge length Baty mechanical strain gauge. Properties established included the elastic modulus, the first yield strain, the true stress/true strain post yield relationship and the ultimate load.

The need to verify the properties of the materials used was demonstrated by the first rod tested which, although supplied as "mild steel" exhibited very little ductility consistent with the material having been cold worked.

Following the work of Erasmus⁽⁴⁵⁾ essentially bilinear load/deflection models of axially loaded mild steel braces may be derived from consideration of true force, true deflection curves⁽⁴⁶⁾ and hence the material properties measured in this study were used to establish the elastic stiffness and effective post-yield elastic stiffness of the bracing elements (see Appendix II).

A typical plot of log true stress against log true strain is presented in Figure 3.5 and from this and a similar graph for the

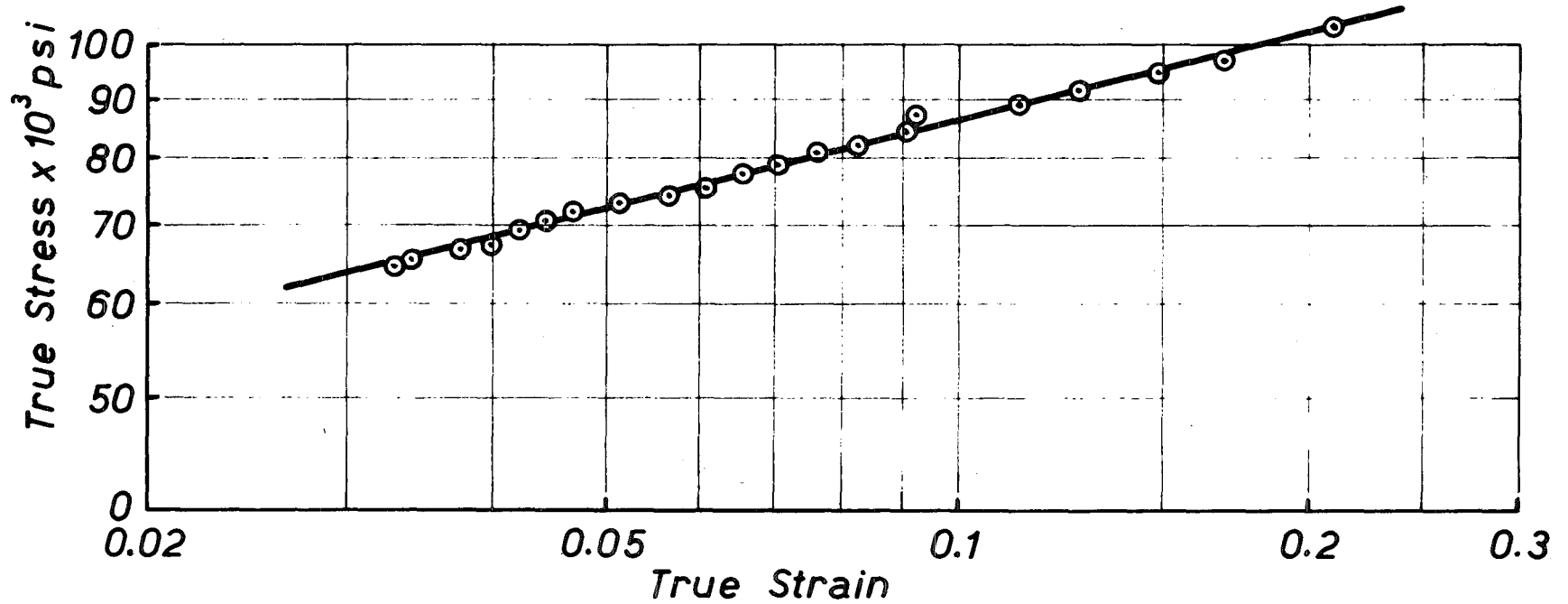


Fig.3.5 : LOG-LOG PLOT OF TRUE-STRESS, TRUE-STRAIN
FOR 0.25 in. dia. MILD STEEL BRACING

thicker bracing the values of strain hardening exponent n and strength coefficient K were determined for the mild steel braces. A summary of the bracing rods' material properties is presented in Table 3. The testing of the joist material indicated that the section was of typical low carbon steel having a Young's modulus of 28×10^6 lbs/in.² and a yield level of 43,500 lbs/in.².

A simple digital computer program TRUEFORCE (list 2), based on the expression for true force developed in Appendix II, was used to calculate the post yield forces in the bracing rods for selected lateral deflections of the test portal and the results of these computations are shown in Figures 3.6 and 3.7.

III.4 Tests Undertaken

An initial static racking test was undertaken on an unbraced rigid knee portal in the rig shown in Figure 3.3(i) to establish that the difficulties experienced in the preliminary experimental work, brought about by distortion of the frame perpendicular to its own plane and by upward deflection of the base plates, had been satisfactorily overcome. This was confirmed. The jack loads were limited to those corresponding to 0.5 in deflection to avoid inelastic straining of the frame and the load/deflection plot (Figure 3.8) enabled a value of stiffness of 4,600 lb/in. to be determined. This correlates satisfactorily with the theoretical value of 4,570 lb/in. (See Appendix III).

A second static racking test on a rigid knee portal braced with one 0.25 in. diameter mild steel rod enabled the bilinear

Dia- meter (ins)	Bracing	Young's Modulus (lbs/in ²) $\times 10^6$	Elastic Limit Strain	Strain Hardening Exponents n	Strength Co- efficient K _o	Ultimate Tensile Load (lbs)
	Type					
0.25	M.S.	31.2	0.00186	0.25	154,000	2,940
0.375	M.S.	29.6	0.00189	0.28	132,000	6,860
0.205	H.T.S.	28.9	0.008	-	-	7,670
0.211	H.T.S.	29.2	0.008	-	-	7,780

Table 3. Summary of Material Properties of Bracing Rods.

```

C          PROGRAM TRUEFORCE
C      THIS PROGRAM COMPUTES THE TRUE FORCE
C      IN A PLASTICALLY DEFORMING BRACE WHEN
C      A DEFINED TRUE DEFLECTION IS IMPOSED
C
      REAL BLC,ABO,DL,APDL,FA,FKO,TRFCR
6 READ(5,1) BLC,ABO,DL,APDL,FA,FKO
1 FORMAT(6G10.0)
WRITE(6,2) BLC,ABO,DL,APDL,FA,FKO
2 FORMAT(25X,'INPUT DATA ECHC CHECK',6G10.3///)
ADL=DL
5 BLI=BLC+ADL
ABI=ABO*BLC/BLI
TRFCR=ABI*FKO*((ALOG(BLI/BLC))**FA)
WRITE(6,3) ADL
3 FORMAT(25X,'TRUE DEFLECTION = ',E12.4,'INCHES'///)
WRITE(6,4) TRFCR
4 FORMAT(25X,'TRUE FORCE = ',E12.4,'LBS.'////)
ADL=ADL+DL
IF((APDL-ADL).GE.0) GO TO 5
GO TO 6
END

```

INPUT DATA ECHC CHECK 45.0 0.490E-01 0.782E-01 2.00 0.250 0.154E 06

TYPICAL OUTPUT

TRUE DEFLECTION = 0.7820E-01INCHES

TRUE FORCE = 0.1537E 04LBS.

TRUE DEFLECTION = 0.1564E 00INCHES

TRUE FORCE = 0.1825E 04LBS.

TRUE DEFLECTION = 0.2346E 00INCHES

TRUE FORCE = 0.2016E 04LBS.

TRUE DEFLECTION = 0.3128E 00INCHES

TRUE FORCE = 0.2162E 04LBS.

LIST 2

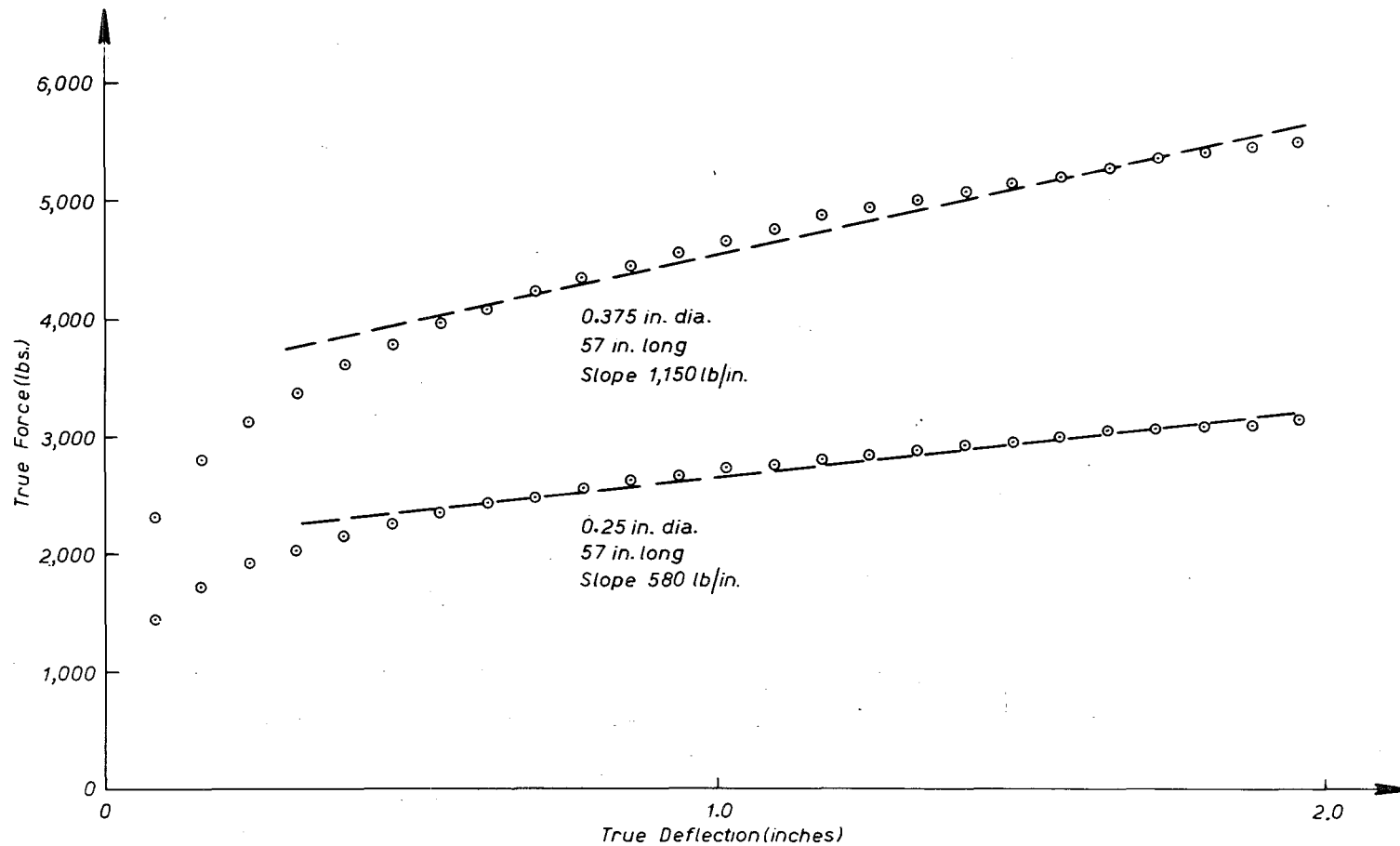


Fig.3.6: TRUE FORCE / TRUE DEFLECTION CURVES FOR MILD STEEL BRACING RODS AFTER YIELD

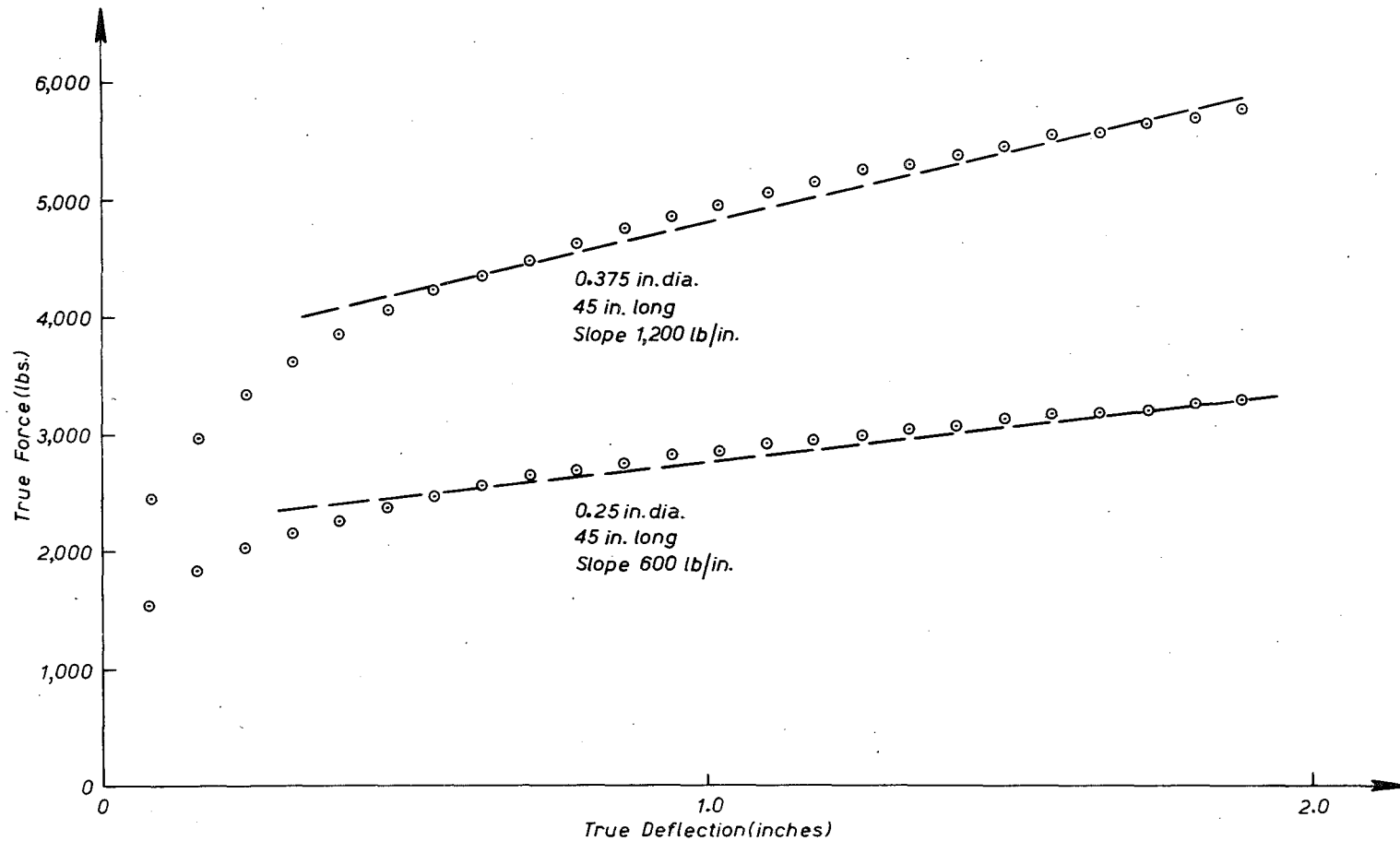


Fig. 3.7: TRUE FORCE / TRUE DEFLECTION CURVES FOR MILD STEEL BRACING RODS AFTER YIELD

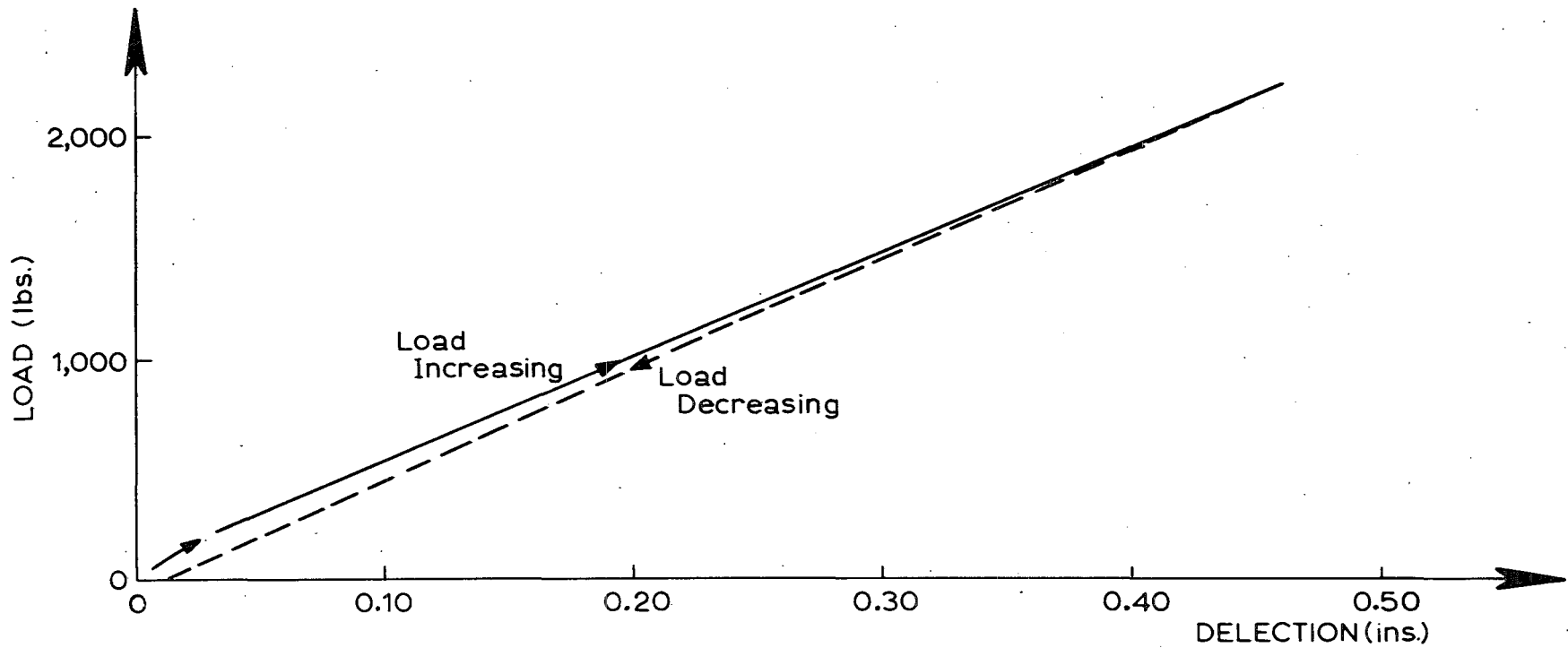


Fig. 3.8: STATIC SIDESWAY STIFFNESS TEST—UNBRACED RIGID KNEE PORTAL

load/deflection graph shown in Figure 3.9 to be obtained. The initial experimental stiffness of 20,000 lb/in. compares reasonably well with the theoretical value (4,570 lb/in. for the bare frame plus 16,350 lb/in. for the bracing giving a total of 20,920 lb/in.) and the slope of the second section of the graph, 5,000 lb/in., correlates well with the predicted value (4,570 lb/in. for the bare frame plus 580 lb/in. for the post yield axial stiffness of the bracing, see Figure 3.6, giving a total of 5070 lb/in.).

As had been anticipated, considerable difficulty was experienced at the start of the test on the braced frame in adjusting the bracing to take up the slack in the anchorages and to be "just tight" at the commencement of the racking test. After many attempts to overcome this problem a satisfactory technique was devised. This involved repeated tensioning and releasing of the bracing by means of the adjustment screw at the lower end, until readings across the Demac gauge points indicated that no further slip in the anchorage was occurring (confirmed by a linear increase in strain reading resulting from equal incremental rotations of the adjustment screw) and finally the screw was adjusted to the position at which strain readings taken across the Demac points indicated that the "just tight" condition existed.

A subsequent static racking test on a pinned knee frame braced with one 0.25 in. diameter mild steel rod indicated that the elastic lateral stiffness was 16,700 lb/in. When the same frame was braced with two diagonally opposed 0.25 in. diameter mild steel rods, with equal residual prestress achieved through use of the adjustment screws

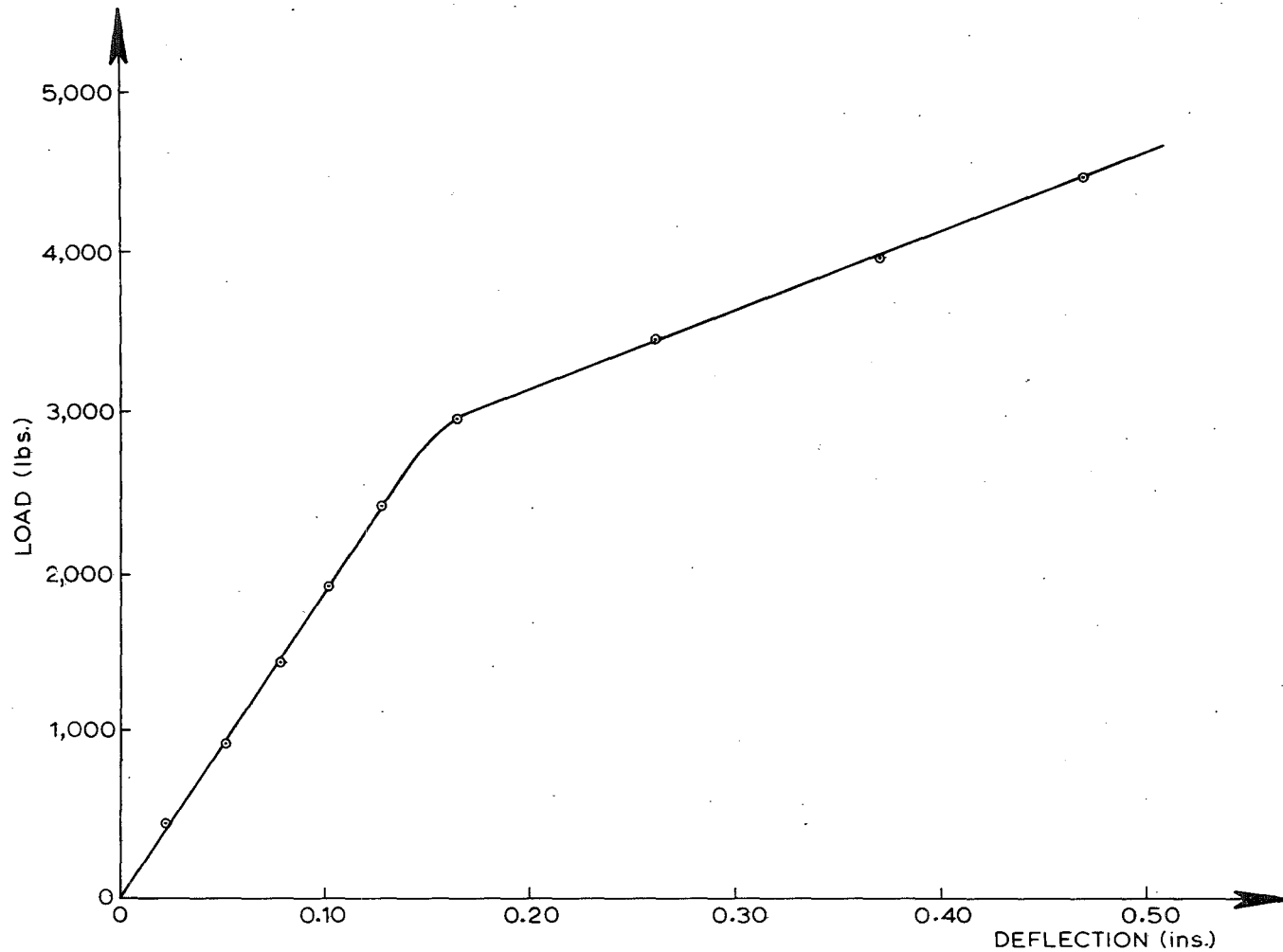


Fig. 3.9: STATIC SIDESWAY STIFFNESS TEST RIGID KNEE PORTAL BRACED WITH ONE 0.25 in. dia. M.S. ROD.

after the initial slack in the anchorages had been removed, the load/deflection curve shown in Figure 3.10 was determined experimentally. This confirmed the expected behaviour and, in particular, illustrated the increased stiffness conferred by the prestressed member, the return to the characteristics of a frame with a single brace when the second rod became just slack on losing its prestress and the onset of yield in the tensioned rod at a value of racking force consistent with the incremental load due to the racking being superimposed on the initial prestress in the rod.

A static racking test on a pinned knee frame braced with two diagonally opposed 0.205 in. diameter high tensile steel rods as well as two mild steel rods, all four rods being initially prestressed, enabled the load/deflection curve shown in Figure 3.11 to be obtained. The initial stiffness of 55,000 lb/in. correlates well with the theoretical value (33,000 lb/in. plus 10,300 lb/in. for each of the two H.T.S. rods), the stiffness of 10,700 lb/in. corresponds to the situation which only one (yielding) mild steel rod (of computed stiffness 580 lb/in.) and one high tensile steel rod (computed stiffness 10,300 lb/in.) are together resisting the sidesway, and the 600 lb/in. stiffness corresponds to the situation in which only one yielding mild steel rod remains active. Confirmation that two of the rods went slack soon after point I on the curve, that the tensioned mild steel rod commenced yielding just above point I and had reached a fully yielding state and point II and that the tensioned high tension steel rod fractured at point III was

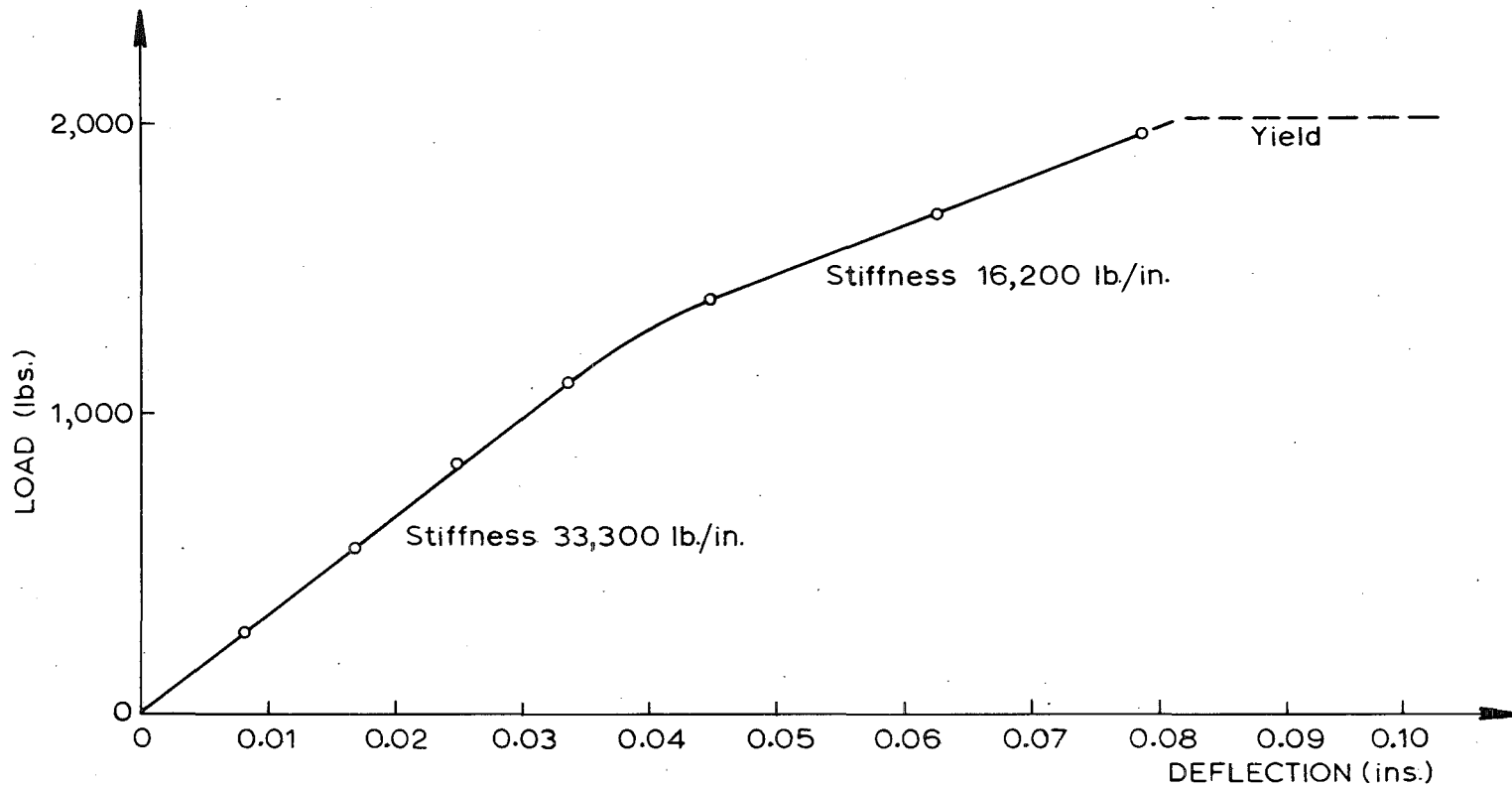


Fig. 3.10: STATIC SIDESWAY STIFFNESS TEST PINNED KNEE PORTAL BRACED WITH DIAGONALLY OPPOSED PRESTRESSED 0.25dia. M.S. RODS.

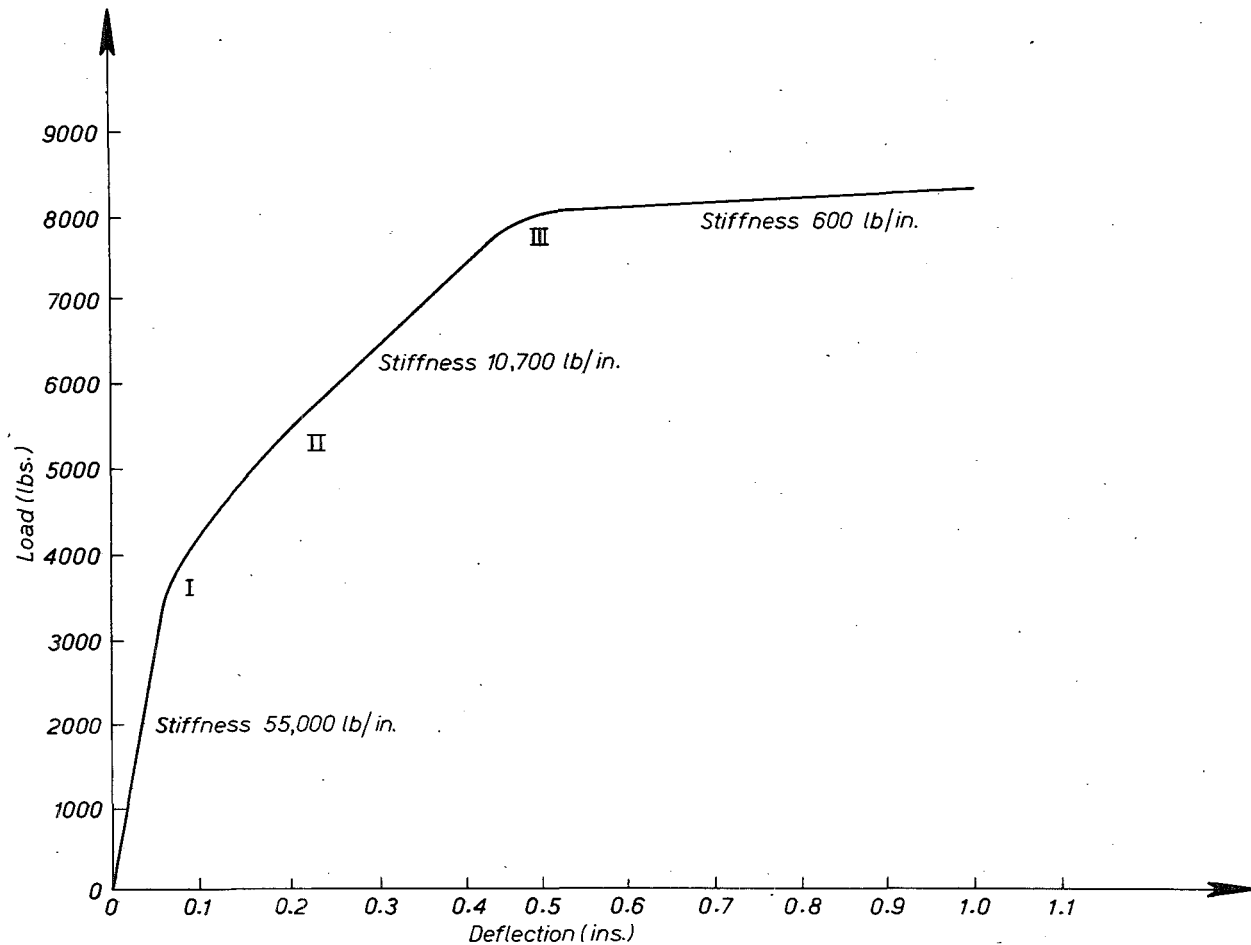
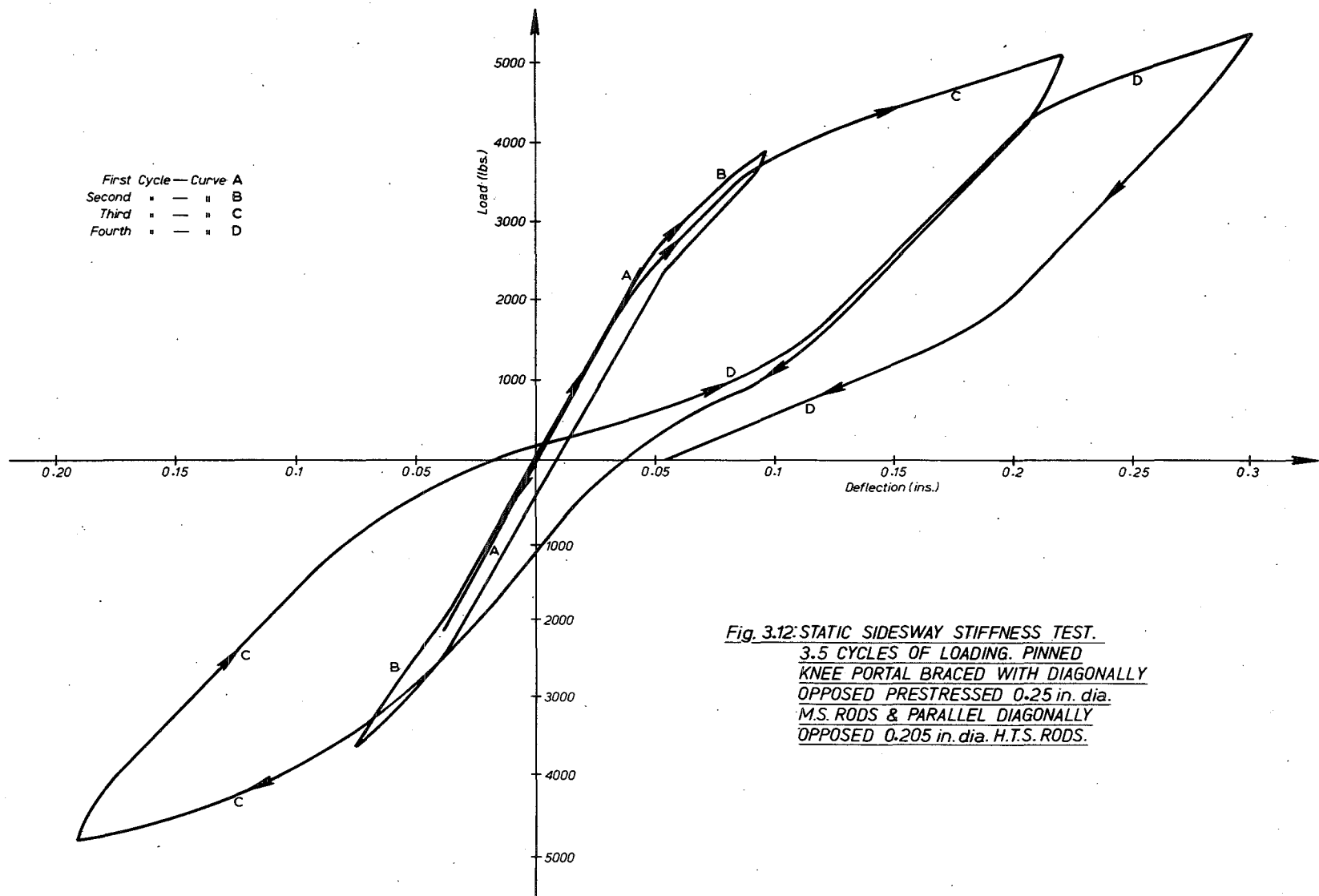


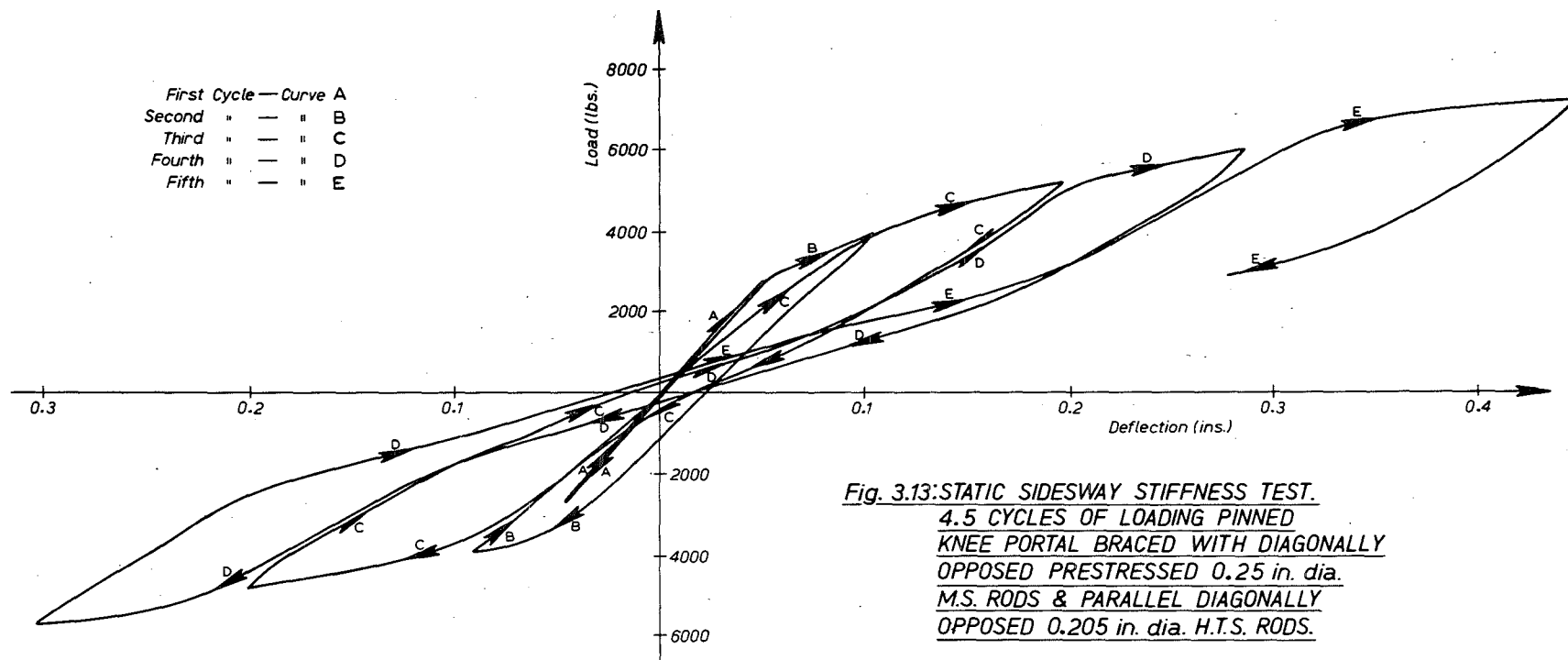
Fig. 3.11: STATIC SIDESWAY STIFFNESS TEST. PINNED KNEE PORTAL BRACED WITH DIAGONALLY OPPOSED PRESTRESSED 0.25 in. dia. M.S. RODS AND PARALLEL DIAGONALLY OPPOSED 0.205 in. dia. H.T.S. RODS.

provided by the Demac gauge readings which were undertaken throughout the test. These readings were found to be almost indispensable in interpreting the sequence of behaviour in this and similar tests.

Several static racking tests involving reversed (cyclic) loading were subsequently undertaken on the pinned knee frame braced with four prestressed rods. Typical behaviour patterns are shown in Figure 3.12 and 3.13. In Figure 3.12, 3.5 cycles of loading were imposed. In cycle A the system retained its initial characteristics throughout. No rods completely lost their prestress nor did any yield; the constant stiffness of 55,000 lb/in. determined experimentally correlating satisfactorily with the predicted value. In cycle B the initial prestress in the mild steel rod was eliminated at a sway of 0.05 in. and consequently this rod became slack; the high tensile steel rod followed this behaviour pattern at almost the same value of sway and consequently the slope of the upper section of the cycle B curve (27,000 lb/in.) represents the situation in which the pinned knee frame is braced with the two tensioned rods acting alone. On removal and subsequent reversal of load the cycle B curve returns along lines of similar gradient, corresponding to the participation of either two or four bracing rods, producing an essentially bilinear trace. Since no yielding of the rods was evident it is concluded that the failure of the downward trace to superimpose on the upward one is primarily due to the inevitable slack in the pinned frame. This feature shows up again at the bottom of cycle B curve.

Cycles C and D exhibited essentially trilinear characteristics.





The slopes corresponding to 55,000 lb/in. and 27,000 lb/in. stiffnesses reflecting the participation of four and two braces respectively, acting elastically, and the slopes of 10,500 lb/in. results from the yielding of the tensioned mild steel braces leaving one high tensile steel rod to provide the majority of the sway resistance (combined computed stiffness of 10,880 lb/in.). The width of the C and D cycle curves can be accounted for primarily by the yielding of the tensioned mild steel bracing rods; this action provides the major part of the energy absorbing property of the system.

After replacing the bracing members and reintroducing prestress into them by following the setting up procedure described earlier, 4.5 cycles of loading were applied to the pinned knee frame with the result shown in Figure 3.13. Characteristic slope values of 55,000 lb/in., 10,500 lb/in. and 27,000 lb/in. were again established and, as in the 3.5 cycle test, in each case these may be satisfactorily related to the state of participation and of stress of the bracing members.

Static racking tests involving reversed (cyclic) loading or braced rigid knee frames were also carried out. Typical results are shown in Figures 3.14(a) and 3.14(b). A rigid knee frame was prestressed with two pairs of diagonally opposed rods, as in the earlier tests on the pinned frame, and the results of the first two cycles of loading are presented in Figure 3.14(a). The slope of the first - entirely elastic - cycle of 57,500 lb/in. correlates satisfactorily with the predicted value (53,600 lb/in. for the bracing plus 4,570 lb/in. for the bare frame) and the characteristic slopes of 12,000 lb/in. and

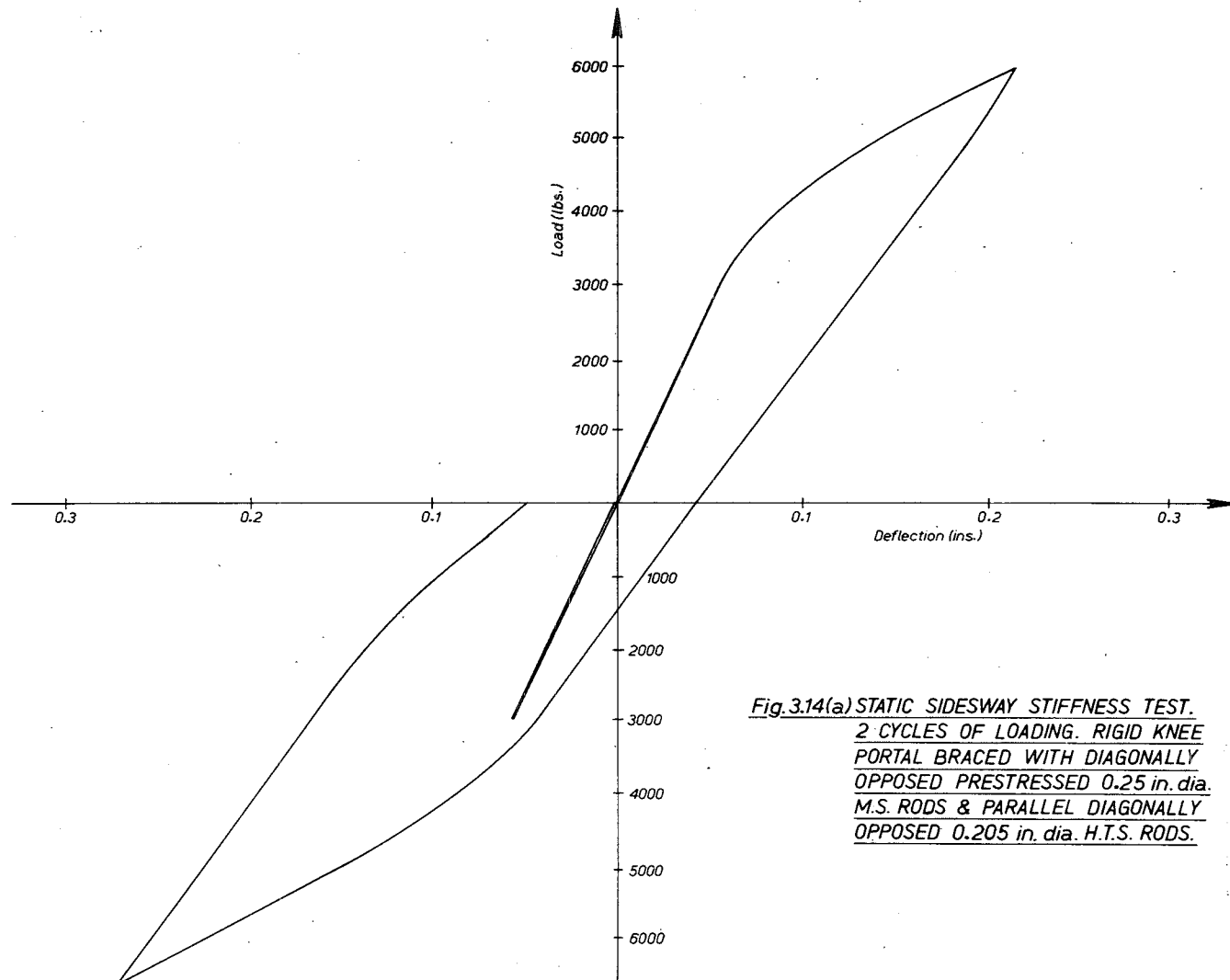
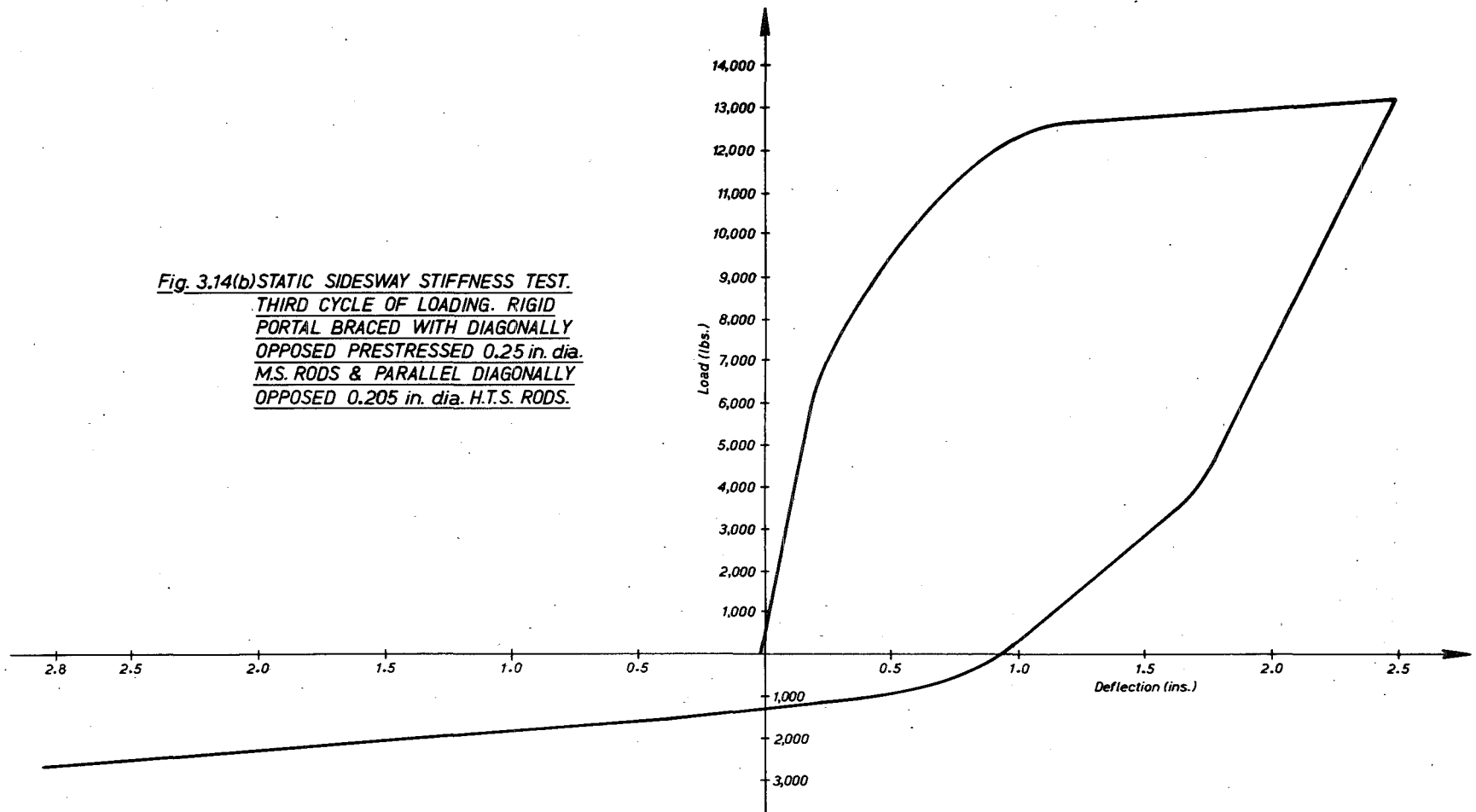


Fig. 3.14(a) STATIC SIDESWAY STIFFNESS TEST.
2 CYCLES OF LOADING. RIGID KNEE
PORTAL BRACED WITH DIAGONALLY
OPPOSED PRESTRESSED 0.25 in. dia.
M.S. RODS & PARALLEL DIAGONALLY
OPPOSED 0.205 in. dia. H.T.S. RODS.

Fig. 3.14(b) STATIC SIDESWAY STIFFNESS TEST.
THIRD CYCLE OF LOADING. RIGID
PORTAL BRACED WITH DIAGONALLY
OPPOSED PRESTRESSED 0.25 in. dia.
M.S. RODS & PARALLEL DIAGONALLY
OPPOSED 0.205 in. dia. H.T.S. RODS.



34,000 lb/in. exhibited by the second cycle of loading correspond to the situations in which the sidesway is resisted in the first case by a yielding frame and a yielding mild steel rod (580 lb/in.) acting in parallel with one high tensile steel rod (10,300 lb/in.) and in the second case by one mild steel rod and one high tensile steel rod together with the frame, all acting elastically (16,300 lb/in. plus 10,300 lb/in. plus 4,570 lb/in.). Subsequent cyclic loading of this frame resulted in the curve presented in Figure 3.14(b) being obtained. In this case the very large deflections both made deflection measurement difficult and resulted in almost continuously varying inelastic characteristics being determined, as distinct from phased inelastic behaviour. The essentially linear portions of the curve having slopes of 21,000 lb/in., 12,000 lb/in. and 300 lb/in. are difficult to relate satisfactorily to the calculated element stiffness values although the 12,000 lb/in. stiffness corresponds to the sidesway being resisted by one high tensile rod assisted by a yielding frame and a yielding mild steel rod. One high tensile rod fractured at the top of the loading cycle and the effect of this was to jar the whole rig and to necessitate the resetting of the dial gauges. Consequently some doubt exists in the relationships of the later readings to the earlier ones.

Subsequent to the static reversed (cyclic) loading experiments, a series of braced frames were tested using the dynamic loading machine. Since this is basically a controlled displacement device, as distinct from a controlled load testing machine, it proved to be of only limited use in complementing the experiments undertaken

statically. Nevertheless its availability prompted a series of tests on both pinned and rigid knee frames braced with diagonally opposed pairs of rods. The machine was run at a constant speed throughout, to provide a connecting rod frequency of 2.2 c.p.s. which was selected to lie within the normally accepted range of earthquake induced vibration and the frames were subjected to cyclic displacements through a range of selected amplitudes. The normal test pattern involved increasing, and in some cases subsequently decreasing, the amplitudes by equal steps and recording the sidesway load/deflection characteristics on the X-Y plotter.

Several typical recorded curves are presented in Figure 3.15. Curve (i) shows a single cycle of a test of a pinned knee portal braced with one 0.25 in. diameter mild steel rod in each direction. As a result of previous loading and consequent yielding of the bracing about 0.3 in. of slack exists on each side of the initial undeflected position. Hence the rods only contribute stiffness in the extremities of the oscillation when an experimental value of stiffness corresponding satisfactorily to the calculated one was observed. Curves (ii) to (vii) in Figure 3.15 illustrate the effect of increasing the amplitude of movement applied by the test machine at a constant rate. The gradient of the top of each loop corresponds to the stiffness of the yielding mild steel brace and the essentially bilinear nature of the response of this system is once again apparent. In curve (viii) in Figure 3.15 the load/deflection loop corresponding to the last cycle in the overlaying group of curves is recorded.

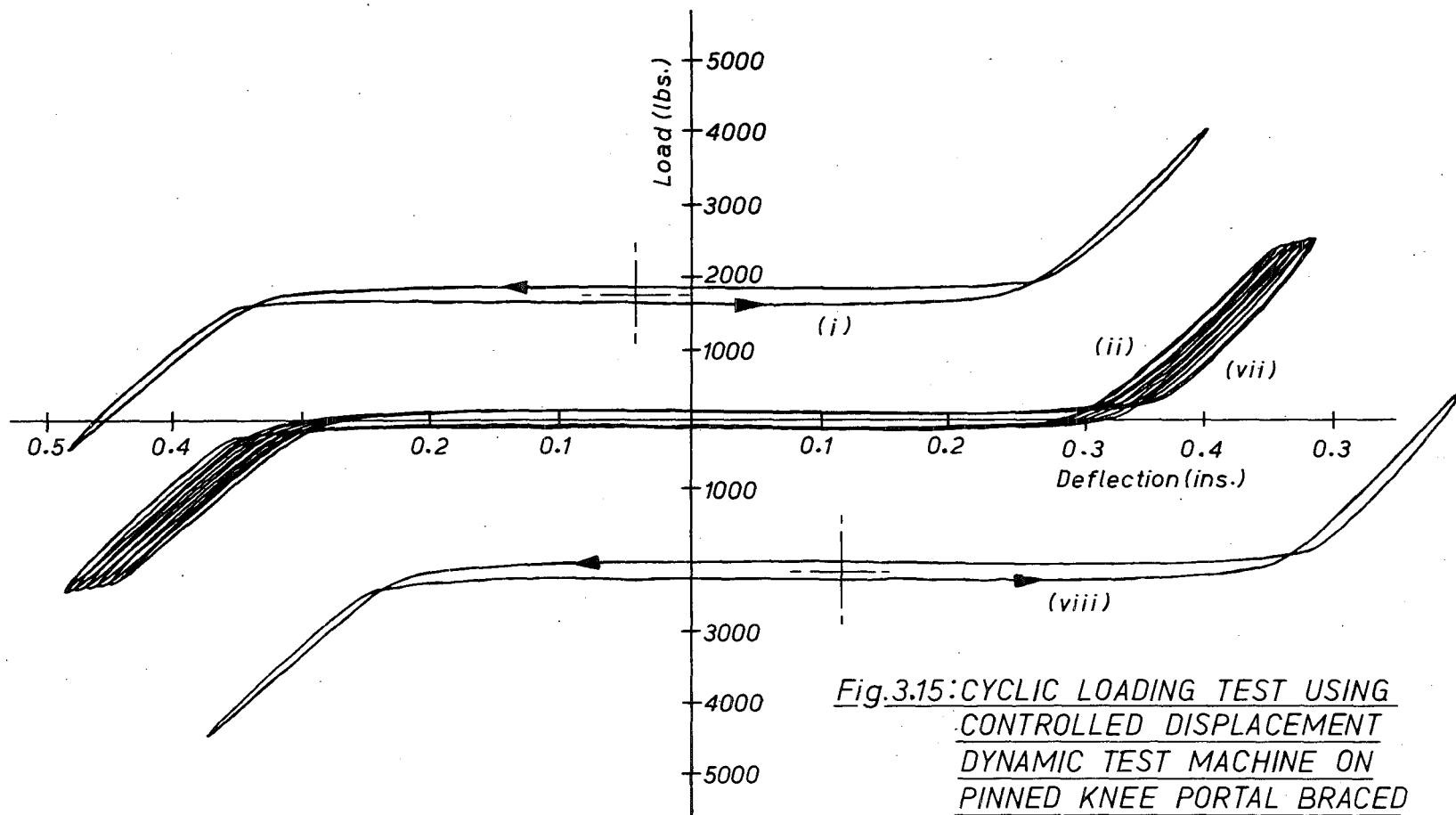


Fig.3.15:CYCLIC LOADING TEST USING
CONTROLLED DISPLACEMENT
DYNAMIC TEST MACHINE ON
PINNED KNEE PORTAL BRACED
WITH TWO DIAGONALLY OPPOSED
0.25 in. dia. M.S. RODS.

The result of four cycles of loading of a pinned knee frame, braced with one pair of 0.25 in. diameter mild steel rods and one pair of 0.211 in. diameter high tensile steel rods, is shown in Figure 3.16. The loading machine was adjusted at a constant rate to give four loops of decreasing amplitude subsequent to the braced frame having been vibrated through displacements of considerably larger amplitudes. The characteristics of a stiffening system are apparent from the curves; the first gradient on the rising section of each loop corresponds to the situation in which one 0.211 in. diameter high tensile steel brace acting alone supplies the sidesway stiffness (computed at 10,900 lb/in.) and the steeper slope is appropriate to the configuration in which one mild steel brace is also acting (the slack in the mild steel braces arising from previous yielding having been taken up in the first portion of the sway movement).

The curve in Figure 3.17 was recorded during a cyclic loading test on a rigid knee frame braced with both mild steel and high tensile steel rods. A stiffening characteristic is once more evident. Again this is due to the participation at the extremities of the oscillatory movement of the previously yielded mild steel rods. The gradient across the major portion of the curve (15,800 lb/in.) correlates with the computed value of 10,900 lb/in. (for the high tensile steel rod) plus 4,570 lb/in. (for the bare frame). The steeply rising section of the loading cycle (slope 32,000 lb/in.) compares satisfactorily with the predicted value made up of 10,900 lb/in. and 4,570 lb/in. plus 16,700 lb/in. for the

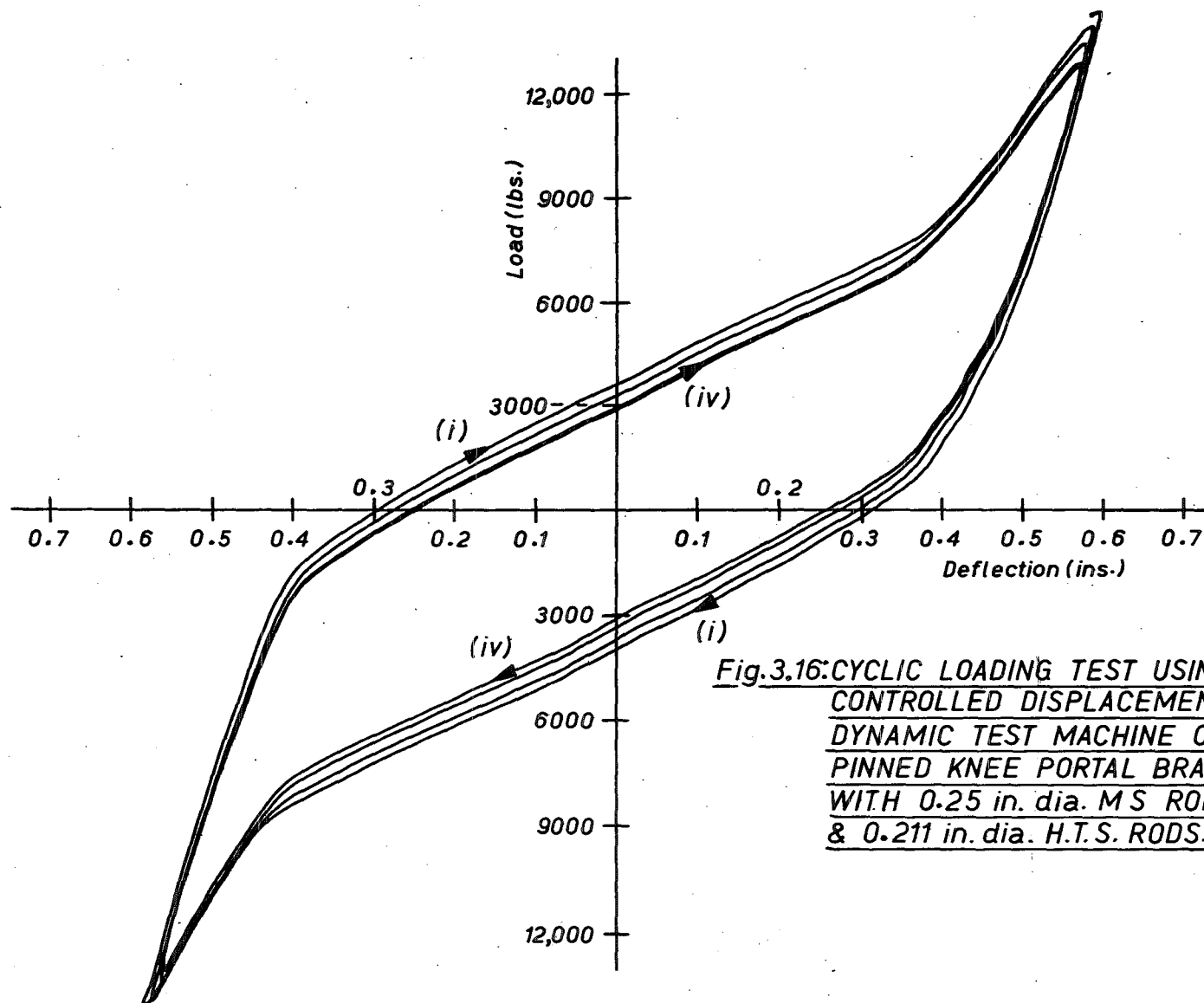


Fig.3.16: CYCLIC LOADING TEST USING
CONTROLLED DISPLACEMENT
DYNAMIC TEST MACHINE ON
PINNED KNEE PORTAL BRACED
WITH 0.25 in. dia. M.S. RODS
& 0.211 in. dia. H.T.S. RODS.

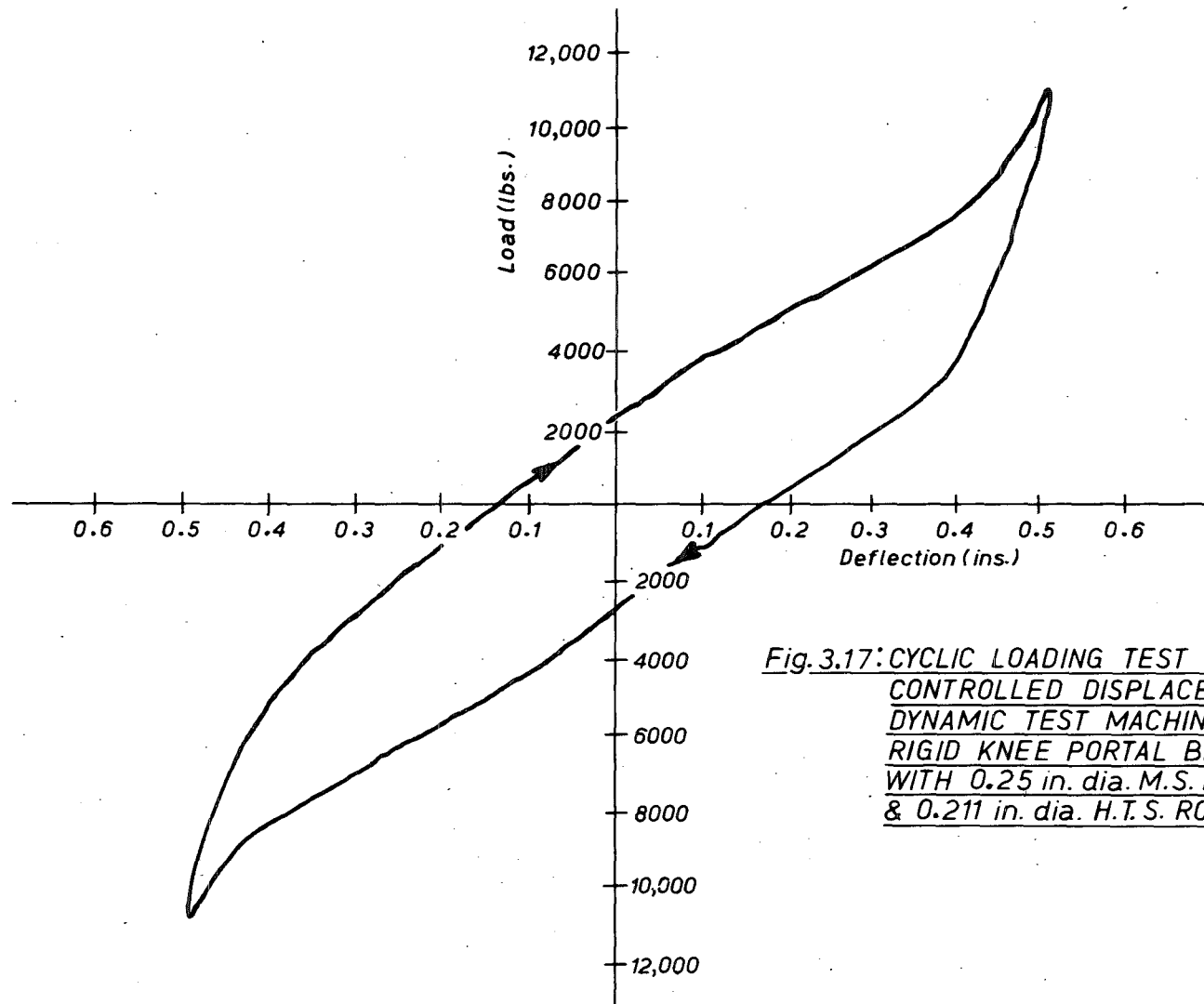


Fig. 3.17: CYCLIC LOADING TEST USING
CONTROLLED DISPLACEMENT
DYNAMIC TEST MACHINE ON
RIGID KNEE PORTAL BRACED
WITH 0.25 in. dia. M.S. RODS
& 0.211 in. dia. H.T.S. RODS.

tensioned mild steel brace.

III.5 Comment on Cross Braced Panel Testing

Points established as a result of the testing included the fact that, once a satisfactory technique had been developed, no real problem was encountered in ensuring that the bracing anchorages were secure or in introducing a chosen level of prestress into the braces. Another point worthy of recording was that in the testing undertaken in the static rig the readings made on the bracing rod Demac gauges proved to be of great assistance when the load/deflection curves were being interpreted. These readings were notably more reliable than those made using the wire resistance strain gauges, probably because of the problems arising from local flexing and yielding of the rods under the resistance strain gauges.

The tests established that selected multiphase response may be achieved reliably in cross braced frames by the choice of suitable bracing and that, in particular, a significant variation in sidesway load/deflection characteristics may be obtained by the use of sacrificial members, possibly combined with initial prestress in some or all of the braces. It has been shown to be a practical possibility to produce a braced frame which is relatively stiff under small sidesway, which becomes more flexible at larger deflections and concurrently exhibits ductile properties, but which has a reserve of energy absorption capacity coupled with the ability to stiffen up again at near destructive levels of sidesway.

C H A P T E R F O U R

SEISMIC ANALYSES BY DIGITAL COMPUTER MATHEMATICAL MODELLINGIV.1 Introduction

The increasing availability of electronic digital computers throughout the last twenty years has prompted the solution of many previously intractable problems, one of which is the analysis of the response of structures to time varying ground disturbances resulting from earthquakes. Early attempts to apply digital computers to structural engineering problems almost invariably involved programming the previously well tried manual methods of analysis, whereas much more efficient computer orientated techniques were subsequently devised. To some extent this pattern was reflected in the particular application to seismic response calculations. The response spectra, normal mode approach⁽⁴⁷⁾ was developed a generation ago in an attempt to simplify earthquake response analyses^(48,49,50,51) and initial applications of digital computers in earthquake engineering involved their use to determine response spectra⁽⁵²⁾ and modal properties⁽⁶⁾. However digital computers have made the direct numerical integration of the equations of motion of multidegree of freedom system a practical proposition. This fact has prompted the use of a numerical integration approach to seismic analysis calculations, particularly to inelastic response calculations^(53,54) where the system is assumed to behave in a linear elastic manner during each

time increment used in the stepwise numerical integration process and the non linear behaviour is determined as the response of a sequence of successively differing systems.

IV.2 Mathematical Modelling of Structural Frameworks

The steps involved in mathematical modelling of a structure and the solution of the distribution of member forces and distortions resulting from a chosen applied load may be summarised as:-

- (1) Idealisation of the structure to a system readily represented mathematically
- (2) Evaluation of the structural properties of the elements
- (3) Combination of the element characteristics to determine the properties of the complete system
- (4) Solution of the equations describing the load/distortion relationships of the complete system so determining the deformations (or forces) resulting from the applied loading
- (5) Calculation of the effects on individual members of the applied loading.

In the case of plain frameworks step (1) consists of idealising the structure to a series of one dimensional elements, the properties of which are assumed to be concentrated along the centre-line axis. These elements are considered to be connected together at the joints or nodal points where the mass of the structure is assumed to be concentrated and where inter-element continuity is enforced.

Step (2) involves the determination of stiffness (or flexibility)

coefficients making use of the elastic properties of the element material and the geometric characteristics (length, area, orientation). Typically Slope/Deflection relationships are invoked to determine element stiffness matrices $[k]$ which consist of arrays of element stiffness values each being the force required to produce unit deformation for a particular degree of freedom^(55,56). These element stiffness characteristics may subsequently be combined to determine the stiffness of the complete framework by summing the stiffnesses of the ends of all members meeting at a joint (and making allowance for the carry-over effect to adjacent joints). In matrix algebra terms step (3) results in the calculation of a frame stiffness matrix $[K]$ consisting of an array of stiffnesses each relating the force acting in the sense of a particular degree of freedom to the corresponding unit deformation.

The equation relating the applied loading system $\{L\}$ to the distortion of the whole structure $\{d\}$ namely

$$\{L\} = [K] \cdot \{d\}$$

may be solved in step (4) by inversion, iteration or relaxation techniques⁽⁵⁷⁾. Once the distortion of the whole structure under the chosen loading has been established, in terms of deflections and rotations in the senses of the degrees of freedom originally selected, back substitution in the element stiffness relationships enables the individual member forces to be determined.

In matrix terms this step (5) may be expressed

$$\{F\} = [k] \cdot \{d\}$$

where $\{F\}$ is the column matrix of member forces.

The inherent nature of the seismic analysis problem, involving time varying ground deformation, necessitates the inclusion of both mass parameters and some allowance for the energy absorbing capacity of the structural system. The lumping of masses at the node points, as outlined in discussing step (1) above, is convenient and reasonably realistic for many civil engineering structures but it is not always possible to justify the frequently used representation of the energy dissipation by an equivalent viscous damping factor. Certainly the manipulation of the mathematical model so devised is relatively easy and, for small values of damping, the concept of equivalent viscous damping is of value⁽⁵⁸⁾ but in the study of the seismic response of certain structural systems, including water towers which have yielding braces equivalent viscous damping is an inadequate representation of the energy absorption⁽⁵⁹⁾. Consideration of the actual load/deflection properties of the structure is a necessary prerequisite to valid response predictions of such systems and the mathematical model must include provision for this.

IV.3 Determination of Elastic Dynamic Response of Multi-Mass Systems by Numerical Integration

If consideration of deflections is limited to one degree of freedom only, the equation describing the dynamic equilibrium of a multi-mass system subjected to earthquake ground motion may be

written

$$[M] \cdot \{\ddot{x}\} + [C] \cdot \{\dot{x}\} + [K]_{LAT} \cdot \{x\} = -[M] \cdot \ddot{x}_g \quad \dots 4(1)$$

where $[M]$ is the diagonal matrix of the lumped masses

$[C]$ is the equivalent viscous damping matrix

$[K]_{LAT}$ is the lateral stiffness matrix of the system
i.e. the section of the complete stiffness matrix
appropriate to the degree of freedom considered.

$\{x\}$ is the column vector of the mass displacements in
the sense of the degree of freedom considered,
(measured relative to the base of the structure).

\ddot{x}_g is the base acceleration (i.e. the acceleration of
the ground)

$\{\dot{}\}$ derivative with respect to time

$\{\ddot{}\}$ second derivative with respect to time.

This equation may be solved by direct numerical integration using a step-by-step process. Several numerical integration processes may be used. Essentially all involve the calculation of values of displacement, velocity and acceleration of the system at selected time intervals. The selection of an optimum integration step interval must take into account the particular method used as it significantly effects the stability of the process.

Digital computer structural analysis techniques characteristically require substantial allocation of storage to that part of the process which involves the mathematical modelling of the structure. This is

particularly so in investigations of post-elastic behaviour and in many practical cases the computer size critically restricts the adequate representation of the system. Consequently, since the numerical analysis has to be treated as a peripheral problem to that of simulating the structural system it is desirable to use an integration procedure which involves small storage requirements provided that it is adequate for the analysis being undertaken. Primarily for this reason the numerical integration techniques based on the work of Newmark⁽⁶⁰⁾ are preferred to other methods such as those of Kutta⁽⁶¹⁾ and Nordsieck⁽⁶²⁾.

An investigation⁽⁶³⁾ of various possible variations of the Newmark linear variation in acceleration method was prompted by the necessity to use an IBM 360/44 computer which has a single precision 32 bit word length and operates in hexadecimal arithmetic and it was established that if the integration time step interval is sufficiently small and if sufficient significant figures are used in the calculations, the more involved techniques provide little practical advantage. Consequently the linear variation in acceleration method was used in this investigation. The assumption of linear acceleration variation enables two equations to be set up relating displacement and velocity at time t in terms of the acceleration at time t and the displacement, velocity and acceleration at time $t-\Delta t$ where Δt is a time interval.

From Figure 4.1

$$\ddot{x} = \ddot{x}_{t-\Delta t} + A t' \quad \dots 4(2)$$

where A is an integration constant.

Integrating with respect to time,

$$\dot{x} = B + \ddot{x}_{t-\Delta t} t' + \frac{1}{2} A t'^2 \quad \dots 4(3)$$

where B is an integration constant

$$\text{at } t' = 0, \dot{x} = \dot{x}_{t-\Delta t} = B$$

Integrating again with respect to time,

$$x = C + \dot{x}_{t-\Delta t} t' + \frac{1}{2} \ddot{x}_{t-\Delta t} t'^2 + \frac{1}{6} A t'^3 \quad \dots 4(4)$$

where C is an integration constant

$$\text{at } t' = 0, x = x_{t-\Delta t} = C$$

$$\text{Now at } t' = \Delta t, \ddot{x}_{t'} = \ddot{x}_t$$

$$\text{Therefore } \ddot{x}_t = \ddot{x}_{t-\Delta t} + A \Delta t$$

$$\text{and } A = \frac{\ddot{x}_t - \ddot{x}_{t-\Delta t}}{\Delta t}$$

Hence substituting for A , B and C and setting $t' = \Delta t$

two equations are obtained, one for velocity

$$\dot{x}_t = \dot{x}_{t-\Delta t} + \frac{\Delta t}{2} \ddot{x}_{t-\Delta t} + \frac{\Delta t}{2} \ddot{x}_t \quad \dots 4(5)$$

and the other for displacement

$$x_t = x_{t-\Delta t} + \Delta t \dot{x}_{t-\Delta t} + \frac{\Delta t^2}{3} \ddot{x}_{t-\Delta t} + \frac{\Delta t^2}{6} \ddot{x}_t \quad \dots 4(6)$$

If these expressions are substituted into the original dynamic equilibrium equation 4(1) an expression for $\{\ddot{x}\}_t$ can be determined. Thus providing that the initial displacement and velocity are postulated and that correct stiffness and damping matrices are available, the numerical integration may be carried out. If it is assumed that the system is initially at rest,

$$\{x\}_0 = \{\dot{x}\}_0 = 0$$

and the initial acceleration of the system is then equal to the initial exciting acceleration.

The appropriate stiffness matrix may be derived from the overall stiffness matrix $[K]$ which can be assembled by the standard direct stiffness method.

In the mathematical modelling of the elastic system the damping is usually assumed to be of viscous form and the damping matrix $[C]$ may be set up by assuming two sets of dampers, one associated with the springs and the other with the masses.

$$\text{i.e. } [C] = c_r[M] + c_g[K] \quad \dots 4(7)$$

where c_r and c_g are damping coefficients.

It may be shown⁽⁶⁴⁾ that

$$(c_g \omega_n^2 + c_r)_{nn} = C_n (2\omega_n) \quad \dots 4(8)$$

where C_n is the ratio of actual to critical damping in mode n and ω_n is the natural frequency of node n . This equation involves only the natural frequency and consequently the damping

coefficients and proportion of critical damping in each mode are directly related. The two coefficients may be adjusted until a reasonable value is obtained for the damping in each of two modes, in seismic analysis normally the lowest two, providing that the modal frequencies are known. Thus the establishment of the damping matrix requires the prior determination of the modal frequencies. This may be readily undertaken using the system stiffness properties previously discussed in the following manner.

Combining the elastic relation between applied loads $\{L\}$ and distortions $\{d\}$

$$\text{i.e. } \{L\} = [K] \cdot \{d\} \quad \dots 4(9)$$

with the harmonic condition

$$\ddot{d} = -\omega_n^2 \{d\} \quad \dots 4(10)$$

and substituting in the dynamic equilibrium equation

$$\{L\} = -[M] \{\ddot{d}\} \quad \dots 4(11)$$

the expression

$$[M] \cdot \omega_n^2 \cdot \{d\} = [K]_{LAT} \cdot \{d\} \quad \dots 4(12)$$

may be obtained.

An iterative solution⁽⁶⁵⁾ of this equation will yield the higher mode characteristics first whereas the lower mode properties are of much greater significance in seismic analysis since almost all of the total structural response is contained in the lowest three normal modes.

Consequently the last expression is usually rearranged to give

$$\frac{1}{\omega_n^2} \cdot \{d\} = [K]_{LAT}^{-1} \cdot [M] \cdot \{d\} \quad \dots 4(13)$$

and an iterative solution of this will yield the fundamental mode properties first, followed by the higher mode characteristics in ascending order.

In summary then, after the structure has been idealised the analysis procedure described above initially involves the evaluation of the stiffness properties of the system, followed by a modal analysis. The damping characteristics are then determined and, together with the stiffness properties, are used in the numerical integration procedure to determine the elastic dynamic response to the earthquake disturbance. A numerical example of this procedure is presented in Chapter Six.

IV.4 Equations of Motion of A Yielding System

In the subsequent analyses of cross braced frames having yielding members it is assumed that, under seismic loading, the vertical and rotational inertia forces are negligible so that only the horizontal inertia forces are considered.

The equation of dynamic equilibrium of a multimass viscously damped, elastic system subjected to external excitation viz;

$$[M] \cdot \{\ddot{x}\} + [C] \cdot \{\dot{x}\} + [K]_{LAT} \cdot \{x\} = -[M] \cdot \ddot{x}_g \quad \dots 4(14)$$

is actually nonlinear in the case of yielding systems because the stiffness is dependent on the magnitude of the response. However when it is assumed that the restoring force remains linear over a short step interval Δt then

$$[M] \cdot \{\Delta \ddot{x}\} + [C] \cdot \{\Delta \dot{x}\} + [K]_{LAT} \cdot \{\Delta x\} = -[M] \cdot \Delta \ddot{x}_g \quad \dots 4(15)$$

represents the set of linear equations which may be solved by numerical integration techniques.

Then, from equation 4(6),

$$\begin{aligned} \{\Delta x\} &= \Delta t \cdot \{\dot{x}\}_{t-\Delta t} + \frac{\Delta t^2}{3} \cdot \{\ddot{x}\}_{t-\Delta t} + \frac{\Delta t^2}{6} \cdot \{\ddot{x}\}_t \\ &= \Delta t \cdot \{\dot{x}\}_{t-\Delta t} + \frac{\Delta t^2}{2} \cdot \{\ddot{x}\}_{t-\Delta t} + \frac{\Delta t^2}{6} \cdot \{\Delta \ddot{x}\} \quad \dots 4(16) \end{aligned}$$

and, from equation 4(5),

$$\begin{aligned} \{\Delta \dot{x}\} &= \frac{\Delta t}{2} \cdot \{\ddot{x}\}_{t-\Delta t} + \frac{\Delta t}{2} \cdot \{\ddot{x}\}_t \\ &= \Delta t \cdot \{\ddot{x}\}_{t-\Delta t} + \frac{\Delta t}{2} \cdot \{\Delta \ddot{x}\} \quad \dots 4(17) \end{aligned}$$

Solving equation 4(16) for $\{\Delta \ddot{x}\}$ gives

$$\begin{aligned} \{\Delta \ddot{x}\} &= \frac{6}{\Delta t^2} \cdot \{\Delta x\} - \frac{6}{\Delta t} \cdot \{\dot{x}\}_{t-\Delta t} - 3 \cdot \{\ddot{x}\}_{t-\Delta t} \\ &= \frac{6}{\Delta t^2} \cdot \{\Delta x\} + \{A\} \quad \dots 4(18) \end{aligned}$$

where

$$\{A\} = -\frac{6}{\Delta t} \cdot \{\dot{x}\}_{t-\Delta t} - 3 \cdot \{\ddot{x}\}_{t-\Delta t} \quad \dots 4(19)$$

and substituting in equation 4(17) for $\{\Delta \ddot{x}\}$ gives

$$\begin{aligned}
 \{\Delta \dot{x}\} &= \Delta t \cdot \{\ddot{x}\}_{t-\Delta t} + \frac{3}{\Delta t} \cdot \{\Delta x\} - 3 \cdot \{\dot{x}\}_{t-\Delta t} - \frac{3}{2} \Delta t \cdot \{\ddot{x}\}_{t-\Delta t} \\
 &= \frac{3}{\Delta t} \cdot \{\Delta x\} - 3 \cdot \{\dot{x}\}_{t-\Delta t} - \frac{\Delta t}{2} \{\ddot{x}\}_{t-\Delta t} \\
 &= \frac{3}{\Delta t} \cdot \{\Delta x\} + \{B\} \quad \dots 4(20)
 \end{aligned}$$

where

$$\{B\} = -3 \cdot \{\dot{x}\}_{t-\Delta t} - \frac{\Delta t}{2} \{\ddot{x}\}_{t-\Delta t} \quad \dots 4(21)$$

These expressions for $\{\Delta \dot{x}\}$ and $\{\Delta \ddot{x}\}$ may be substituted in equation 4(15) to give a matrix equation which may be solved for $\{\Delta x\}$

$$\text{i.e.} \quad [K^*] \cdot \{\Delta x\} = \{\Delta R\} \quad \dots 4(22)$$

$$\text{where} \quad [K^*] = \left[\frac{6}{\Delta t^2} \cdot [M] + \frac{3}{\Delta t} \cdot [C] + [K]_{LAT} \right] \quad \dots 4(23)$$

$$\text{and} \quad \{\Delta R\} = - \left\{ \Delta \ddot{x}_g \cdot [M] + [M] \cdot \{A\} + [C] \cdot \{B\} \right\} \quad \dots 4(24)$$

The numerical process used involves initialising the values of the relative velocity and displacement vectors to zero, assuming the system is initially at rest. Then

$$\{\ddot{x}_0\} = - \ddot{x}_g \cdot \{1\} \quad \dots 4(25)$$

and the following steps are executed repeatedly

$$\begin{aligned}
 \{A\} &= -\frac{6}{\Delta t} \cdot \{\dot{x}\} - 3 \cdot \{\ddot{x}\} \\
 \{B\} &= -3 \cdot \{\dot{x}\} - \frac{\Delta t}{2} \{\ddot{x}\} \\
 \{\Delta R\} &= -\left\{ \Delta \ddot{x}_g \cdot [M] + [M] \cdot \{A\} + [C] \cdot \{B\} \right\} \\
 [K^*] &= \left[\frac{6}{\Delta t^2} \cdot [M] + \frac{3}{\Delta t} \cdot [C] + [K]_{LAT} \right] \\
 \{\Delta x\} &= [K^*]^{-1} \cdot \{\Delta R\} \\
 \{x\} &= \{x\} + \{\Delta x\} \\
 \{\dot{x}\} &= \{\dot{x}\} + \frac{3}{\Delta t} \cdot \{\Delta x\} + \{B\} \\
 \{\ddot{x}\} &= \{\ddot{x}\} + \frac{6}{\Delta t^2} \{x\} + \{A\}
 \end{aligned}$$

The matrix $[K^*]$ is set up on the first pass and is used repeatedly until the lateral stiffness of the system changes when it is modified to allow for yielding or fractured members.

IV.5 Mathematical Model of an Elevated Water Tank

For the purpose of seismic response calculation an elevated water tank supported on a braced framework can be modelled (see Figure 4.2) as a two mass system (representing the convective and impulsive effects of the water as described in Chapter Two, the mass m_1 being the convective mass, m_o the impulsive mass and m_s the mass of the tank structure), carried on an idealised frame of members whose own mass is lumped at the beam positions (M_1 , M_2 , M_3 in Figure 4.2). The system shown, in which the elevation of the tower has three braced panels, then becomes one of four discrete masses, M_1 , M_2 , $M_3 + m_s + m_o$ and m_1

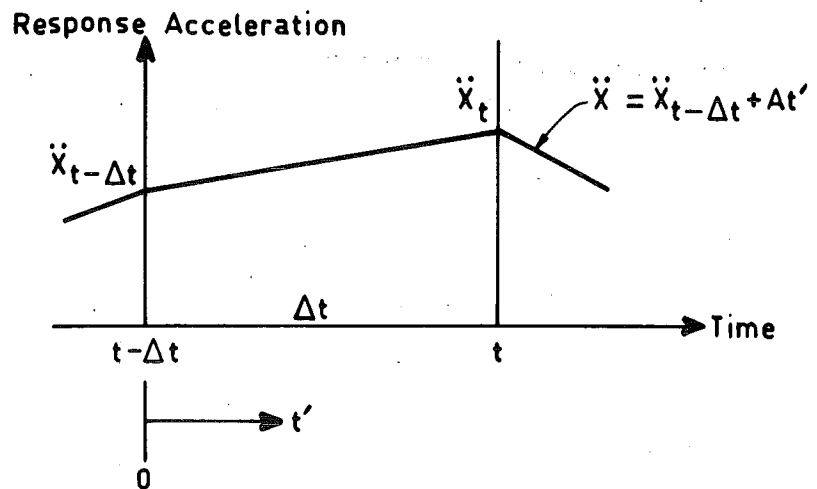


Fig.4.1—LINEAR ACCELERATION VARIATION

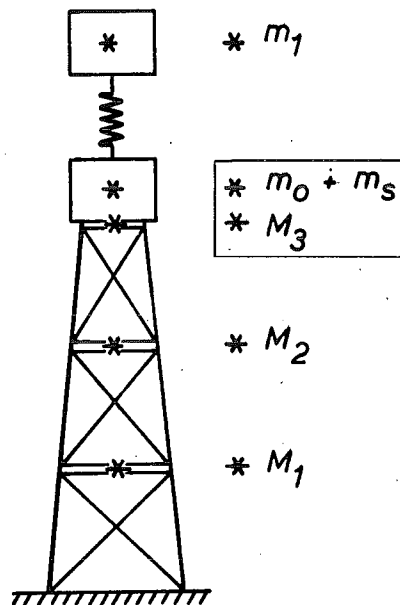


Fig 4.2 — IDEALISED THREE PANEL
ELEVATED WATER TANK

connected by links which are essentially elastic but which, in the case of the panel links, have stiffnesses which vary with lateral displacement as the bracing members slacken, yield or fracture.

Equations representing this system may be set up and solved by numerical integration techniques as described earlier in this chapter, using digitised ground accelerations as the excitation, and the displacement response of the structure to earthquakes may thus be determined.

C H A P T E R F I V E

COMPUTER PROGRAMS USED IN THE ANALYSES OF CROSS BRACED FRAMESV.1 Stiffness Matrix Assembly Program

The determination of the frame stiffness matrices appropriate to the cross braced towers examined was undertaken using the '2-D Structure' program lodged in the University of Canterbury Civil Engineering Department's computer program library. This program enables the joint displacements and element forces in any two dimensional structure composed of an arbitrary assemblage of one and two dimensional elements to be calculated. The stiffness matrix $[K]$ is assembled using the Direct Stiffness Method⁽⁶⁶⁾ and the equation $\{L\} = [K] \{d\}$ is solved by first decomposing the stiffness matrix viz:-

$$[K] = [Q] [D] [Q^T]$$

where $[D]$ is the matrix of pivots

and $[Q]$ is the lower triangular matrix of multipliers.

The solution for the displacements then follows a two step operation⁽⁶⁷⁾, first the forward reduction of the applied load vector $\{L\}$ to give the vector $\{y\}$

$$[Q] \cdot [D] \cdot \{y\} = \{L\}$$

followed by the back substitution for the displacement $\{d\}$

$$[Q^T] \cdot \{d\} = \{y\}$$

The particular application of this program to the calculation of a frame stiffness matrix involves the determination of the deformations occurring when unit actions are applied at the node points. A listing of the program, together with typical output and details of the frame analysed, is presented in Appendix IV, section LP 1.

V.2 Normal Mode Properties Program

The normal mode properties of the structures studied were established using the Civil Engineering Department's computer library program 'Normal Mode Properties from F_{LAT} '. This program enables the eigenvalue, eigenvector analysis to be undertaken by an iterative technique⁽⁶⁵⁾ using the lateral flexibility and mass properties as input and in addition to calculating the normal mode frequencies and displaced shapes, also computes the 1 g displacements and subsequently the maximum seismic displacements and inter storey shears (assuming the structure to remain fully elastic) resulting from the application of the Skinner response spectrum⁽⁶⁸⁾.

In the application of this program to the study of braced frameworks the primary use was to determine the characteristic mode frequencies. A listing of the program, together with typical output is presented in Appendix IV, section LP 2.

V.3 Damping Matrix Formulation Program

Damping coefficients and damping matrices used in subsequent analyses were calculated using the library program 'DAMPING MATRIX'. Based on the application of equation 4(8) (section IV.3) this program enables the damping characteristics of a multimass system to be determined in such a manner that the fractions of critical damping in the first two modes are set at specified values. A list of the program is presented in Appendix IV, section LP 2A.

V.4 Matrix Inversion Program

Since the normal mode properties program requires as input the appropriate lateral flexibility matrix and the stiffness matrix assembly program which was used enabled determination of the lateral stiffness matrix of those frames examined, it was necessary to undertake inversion of some matrices in the course of the analysis procedure adopted. A simple matrix inversion program, based on the Gauss-Jordan elimination technique was used and is listed in Appendix IV, section LP 3.

V.5 Dynamic Elastic Response Program

In order to determine the elastic seismic response for purposes of partially verifying the functioning of the main program used in cross braced frame analysis which is described subsequently the elastic response analysis program ELRES lodged in the Civil Engineering Department's computer library was used.

Developed by Walpole⁽⁶⁹⁾ this program uses a numerical integration procedure based on the Newmark constant linear acceleration

method applied to equation 4(1) to calculate the elastic response of a multi-mass system to Berg format earthquake records. Input includes details of the discrete masses, the lateral stiffness matrix, the damping matrix, the selected time step for the integration process and the digitised earthquake record. The output is in the form of a table presenting the displacements of each mass at each time step and a summary of the maximum displacement undergone by each mass and the time at which this occurs. A listing of the program, together with typical output is presented in Appendix IV, section LP 4.

V.6 Cross Braced Frame Dynamic Analysis Program (XBFRME)

The seismic response of an elevated water tank, supported on cross braced towers having bracing with prestressed and yielding characteristics, was calculated using a specially written digital computer program XBFRME. This program consists of a series of subprograms and subroutines, each of which is described separately below. A complete listing of XBFRME is presented in LIST 4.

V.6 (i) KLAT

The first main sub-section of XBFRME consists of a frame lateral matrix assembly program in which particular provision is made for the characteristics of the cross bracing members. A flow chart for KLAT is presented in Figure 5.1 and a listing of a stand-alone version is given in LIST 3.

After setting up arrays and initialising vectors, the program determines the initial stiffness characteristics of the cross bracing

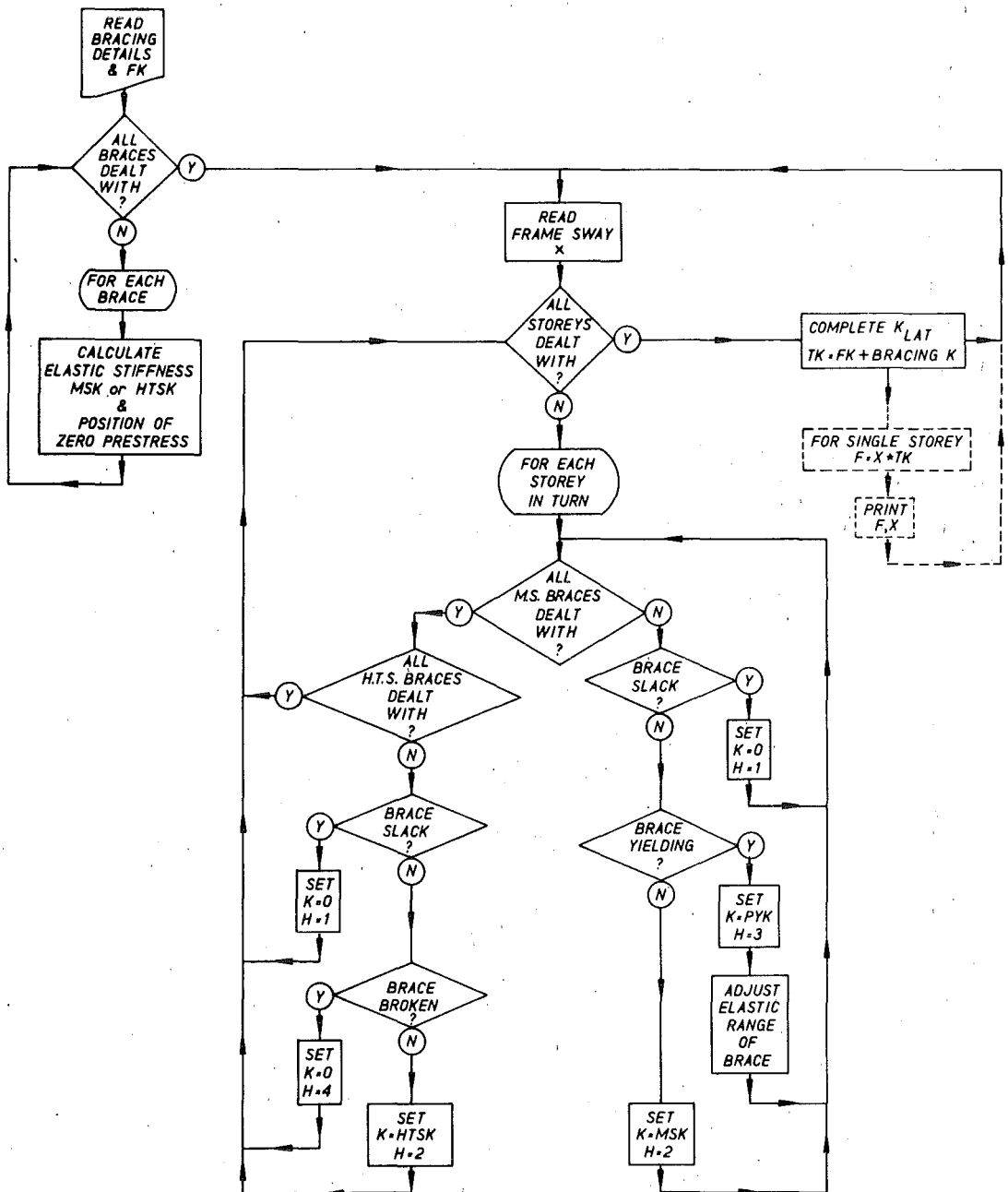


Fig.5.1 : FLOW CHART FOR SUBPROGRAM 'KLAT'

members in a loop which causes the bracing details to be read, the stiffnesses to be computed and the positions of the frame corresponding to the various prestressed members just becoming slack to be calculated.

After reading in the deflected shape of the frame a check is made on each bracing member to determine whether, in the case of the mild steel braces, slackness or yielding has been induced or, in the case of the high tensile steel members, slackness or fracture has been caused. If a mild steel rod has yielded an appropriate adjustment to the effective elastic range of the rod, as defined by the overall frame position, is made. In each case the appropriate stiffness value is selected for each rod, according to its load state, and the history indicator is set.

The total stiffness matrix for the braced frame is formed from the initially read bare frame stiffness, and the bracing rod contributions are determined in this KLAT program. New deflections are read in and the check cycle is repeated to establish whether the new positions of the frame induce slackness, yielding or fracture. When necessary the total frame stiffness is recomputed and the history records are updated. The reading of new deflections is then repeated as often as required and the cycle continued.

For purposes of checking out the validity of the KLAT program an extra instruction, requiring the computation of the sidesway force corresponding to the input sidesway distortion, was added to the program and the values of both force and deflection were printed out at each step. This enabled the results of the mathematical

```

C
C
C      SUBPROGRAM KLAT
C
C      DETERMINATION OF BRACED FRAME STIFFNESS CHARACTERISTICS
C
      REAL*4 MS1PYK(10)
      REAL*4 MS2PYK(10)
      DIMENSION AMS1K(10),AMS2K(10),FMS1K(10),FMS2K(10), AMS1P(10),AMS2P(10),AMS1DY(10),AMS2DY(10),AMS1DN(10),AMS2DN(10),HMS1(10),HMS2(10),HTS1K(10),HTS2K(10),HMS1P(10),HTS2P(10),HTS1DU(10),HTS2DU(10),HTS1U(10),HTS2U(10),HMS1S(10),HMS2S(10),HTF(10),HTS1DU(10),HTS2DU(10),FK(10,10),TK(10,10),STRS(10),ANGLE(10),X(10),ADJ(10),FHTS1K(10),FHTS2K(10),
      6PX(10)
      INTEGER HMS1, HMS2, HMS1S, HMS2S, NS, STOREY, HTF
      READ(5,100) NS
      READ(5,100) NS
      FORMAT(10I5)
100
C
C      HISTORY CODE 1 = SLACK, 2 = ELASTIC, 3 = YIELDING, 4 = BROKEN
C      INITIALISE HISTORY CONDITIONS
      DO 1 I=1,NS
      HMS1(I)=2
      HMS2(I)=2
      HMS1S(I)=2
      HMS2S(I)=2
1      HTF(I)=2222
C      INITIALISE KNOWN VECTORS
      DO 2 I=1,NS
      X(I)=0.
      PX(I)=0.0
      AMS1DN(I)=0.
      AMS2DN(I)=0.
      DO 2 J=1,NS
      YK(I,J)=0.
      AY=0.0
2
C
C      HEAD LATERAL FRAME STIFFNESS MATRIX (K)LAT ( FOR UNBRACED FRAME )
C
      READ(5,200) ((FK(L,J), L=1,NS),J=1,NS)
200 FORMAT(10G10.3)
      WRITE(6,201)
201 FORMAT(1H1,55X,21HINPUT DATA CHECK/56X,21(1H-1///
130X,39HUNBRACED FRAME LATERAL STIFFNESS MATRIX//)
      WRITE(6,202) ((FK(L,J),L=1,NS),J=1,NS)
202 FORMAT(50X,F12.6)
C
C      READ BRACING DETAILS AND COMPLTE BRACED FRAME STIFFNESS
C
      DO 3 I=1,NS
      BRACING MILD STEEL ONE ( BOTTOM LEFT TO TOP RIGHT)
      BRACING MILD STEEL TWO ( TOP LEFT TO BOTTOM RIGHT)
      READ(5,200) A,ZL,AMS1P(I),AMS1Y(I),MS1PYK(I),ANG,EMS
      WRITE(6,203)
203 FORMAT(1H1,60X,15HBRACING DETAILS//)
      WRITE(6,200) A,ZL,AMS1P(I),AMS1Y(I),MS1PYK(I),ANG,EMS
      ANG=ANG*3.1415926/180.
      AMS1K(I)=EMS*A/ZL*CCS(ANG)*COS(ANG)
      READ(5,200) A,ZL,AMS2P(I),AMS2Y(I),MS2PYK(I),ANG,EMS
      WRITE(6,200) A,ZL,AMS2P(I),AMS2Y(I),MS2PYK(I),ANG,EMS

```

```

      ANG=ANG*3.1415926/180.
      AMS2K(I)=EMS*A/ZL*CCS(ANG)*COS(ANG)
      BRACING HIGH TENSILE STEEL ONE ( BOTTOM LEFT TO TOP RIGHT )
      BRACING HIGH TENSILE STEEL TWO ( TOP LEFT TO BOTTOM RIGHT )
      READ(5,200) A,ZL,HTS1P(I),HTS1U(I),ANG,EHT
      WRITE(6,200) A,ZL,HTS1P(I),HTS1U(I),ANG,EHT
      ANG=ANG*3.1415926/180.
      HTS1K(I)=EHT*A/ZL*CCS(ANG)*COS(ANG)
      READ(5,200) A,ZL,HTS2P(I),HTS2U(I),ANG,EHT
      WRITE(6,200) A,ZL,HTS2P(I),HTS2U(I),ANG,EHT
      ANG=ANG*3.1415926/180.
      HTS2K(I)=EHT*A/ZL*CCS(ANG)*COS(ANG)
      ADJUST FOR LOSS OF PRESTRESS OR FOR YIELDING IF NECESSARY
      AMS1DO(I)=AMS1P(I)/AMS1K(I)
      AMS2DO(I)=AMS2P(I)/AMS2K(I)
      HTS1DO(I)=HTS1P(I)/HTS1K(I)
      HTS2DO(I)=HTS2P(I)/HTS2K(I)
      AMS1DN(I)=AMS1DO(I)
      AMS2DN(I)=AMS2DO(I)
      FMS1K(I)=AMS1K(I)
      FMS2K(I)=AMS2K(I)
      FHTS1K(I)=HTS1K(I)
      FHTS2K(I)=HTS2K(I)
3      CONTINUE
C
C      ADJUST FOR LOSS OF PRESTRESS OR FOR YIELDING IN M.S. IF NECESSARY
C      ADJUST FOR LOSS OF PRESTRESS OR FOR FRACTURE IN H.T.S. DITTC
C      SNAW OF TOP OF BRACED PANEL TO RIGHT RELATIVE TO BASE
C      IS POSITIVE X
C      THE INTERSTOREY DRIFT EQUALS X(I) MINUS X(I-1)
C
C      MILD STEEL BRACING ONE
C      FIRST, LOSS OF PRESTRESS DUE TO BRACING GOING SLACK
C
      READ(5,200) (X(I),I=1,NS)
      DO 5 I=1,NS
      XIO=X(I-1)
      IF(I.EQ.1)XIO=0
      AMS1K(I)=FMS1K(I)
      HMS1(I)=2
      R=X(I)-XIO-AMS1DN(I)
      IF(R.GE.0.0) GO TO 10
      AMS1K(I)=0.0
      HMS1(I)=1
10      CONTINUE
C      SECOND QUERY IF YIELD HAS TAKEN PLACE
      AMS1DY(I)=(AMS1Y(I)/FMS1K(I))+AMS1DN(I)
      C=X(I)-XIO-AMS1DY(I)
      IF(C.LT.0.0) GO TO 20
      AMS1K(I)=MS1PYK(I)
      HMS1(I)=3
C      FOLLOWING YIELD ADJUSTMENT OF ELASTIC RANGE POSITION NECESSARY
      ADJ(I)=X(I)-XIO-AMS1DY(I)
      AMS1DN(I)=AMS1DN(I)+ADJ(I)
20      CONTINUE
      WRITE(6,300)AMS1K(I)
300 FORMAT(70X,G10.3)
C      MILD STEEL BRACING TWO
      AMS2K(I)=FMS2K(I)
      HMS2(I)=2
      BR=X(I)-XIO-AMS2DN(I)

```

```

      IF(BB.LE.0.0) GC TO 30
      AMS2K(I)=0.0
      HMS2(I)=1
30  CCNTINUE
      AMS2DY(I)=(-AMS2Y(I)/FMS2K(I))+AMS2DN(I)
      CC=X(I)-XIO-AMS2DY(I)
      IF(CC.GT.0.0) GC TO 40
      AMS2K(I)=MS2PYK(I)
      HMS2(I)=3
      ACJ(I)=X(I)-XIO-AMS2DY(I)
      AMS2DN(I)=AMS2DN(I)+ADJ(I)
40  CCNTINUE
      WRITE(6,300)AMS2K(I)
C   HIGH TENSILE STEEL BRACING CNE
      IF(MHTS1(I).GT.3) GC TO 60
      HTS1K(I)=FHTS1K(I)
      HHTS1(I)=2
      BBB=X(I)-XIO-HTS1DO(I)
      IF(BBB.GE.0.0) GO TO 50
      HTS1K(I)=0.0
      HHTS1(I)=1
50  CCNTINUE
      HTS1DU(I)=(HTS1U(I)/FHTS1K(I))+HTS1DO(I)
      CCC=X(I)-XIO-HTS1DU(I)
      IF(CCC.LE.0.0) GO TO 60
      HTS1K(I)=0.0
      HHTS1(I)=4
60  CCNTINUE
      WRITE(6,300)HTS1K(I)
C   HIGH TENSILE STEEL BRACING TWC
      IF(MHTS2(I).GT.3) GO TO 80
      HTS2K(I)=FHTS2K(I)
      HHTS2(I)=2
      BBBB=X(I)-XIO-HTS2DO(I)
      IF(BBBB.LE.0.0) GO TO 70
      HTS2K(I)=0.0
      HHTS2(I)=1
70  CCNTINUE
      HTS2DU(I)=(-HTS2U(I)/FHTS2K(I))+HTS2DO(I)
      CCCC=X(I)-XIO-HTS2DU(I)
      IF(CCCC.GE.0.0) GO TO 80
      HTS2K(I)=0.0
      HHTS2(I)=4
80  CCNTINUE
      WRITE(6,300)HTS2K(I)
C   FROM TOTAL STIFFNESS MATRIX
C
C   DC 4 L=1,NS
C   DC 4 J=1,NS
4   TK(L,J)=FK(L,J)
      TK(1,1)=TK(1,1)+AMS1K(1)+AMS2K(1)+HTS1K(1)+HTS2K(1)
      IF(NS.EQ.1) GO TO 5
      DC 6 L=2,NS
      AA=AMS1K(L)+AMS2K(L)+HTS1K(L)+HTS2K(L)
      TK(L-1,L-1)=TK(L-1,L-1)+AA
      TK(L-1,L)=TK(L-1,L)-AA
      TK(L,L-1)=TK(L,L-1)-AA
6   TK(L,L)=TK(L,L)+AA
5   CCNTINUE

```

```

      WRITE(6,200)TK
      DC 210 I=1,NS
      F(I)=F(I)+TK(L,J)*(X(I)-PX(I))
      PX(I)=X(I)
210 HTF(I)=1000*HMS1(I)+100*HMS2(I)+10*MHTS1(I)+MHTS2(I)
204 FORMAT(2F12.6,I10)
      WRITE(6,204) (F(I),I=1,NS),(X(I),I=1,NS),(HTF(I),I=1,NS)
      GC TO 7
      ENC

```

RS
RS
RS
RS
RS
RS
RS
RS

LIST 3

(continued)

model analysis undertaken using KLAT to be compared directly with the experiments conducted on the single bay braced frames which are reported in Chapter Three.

V.6 (ii) Results of validity check on KLAT

A comparison of the results determined using KLAT with those obtained in a static sidesway stiffness test on a pinned knee frame braced with pairs of diagonally opposed prestressed mild steel and high tensile steel rods is presented in Figure 5.2. To assist identification the curves were deliberately separated by setting the yield level of the mild steel rods 200 lbs lower, in the mathematical analysis, than the true value. This effect is cumulative so that the traces tend to diverge as the loading cycle progresses but it is evident that the mathematical model adequately describes the cross braced framework, particularly in the increasing-load sections of the curves. The slackness which was evident in the experimental frame testing is difficult to represent in the mathematical model and the fact that this is not allowed for in the program accounts for the divergence in the curves on the decreasing-load sections of the cycles. Nevertheless the similarity in the shapes and in particular the slopes, serves to verify the use of the model set up in KLAT as a reasonable representation of the cross braced frame tested.

Some limitations of the mathematical model were examined and the results are presented diagrammatically in Figures 5.3 and 5.4. In analysing the rigid knee braced frame (Figure 5.3) the full curve

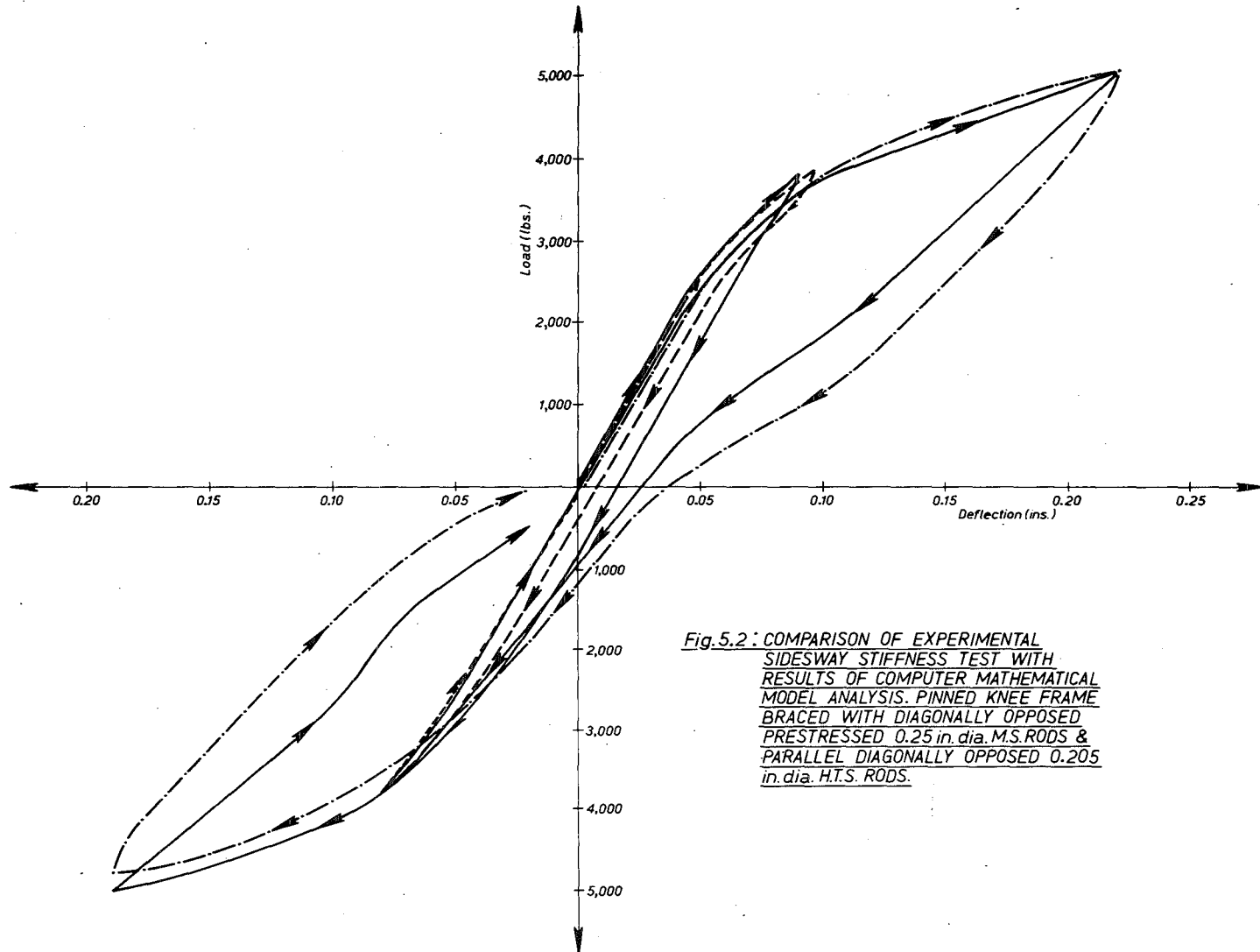
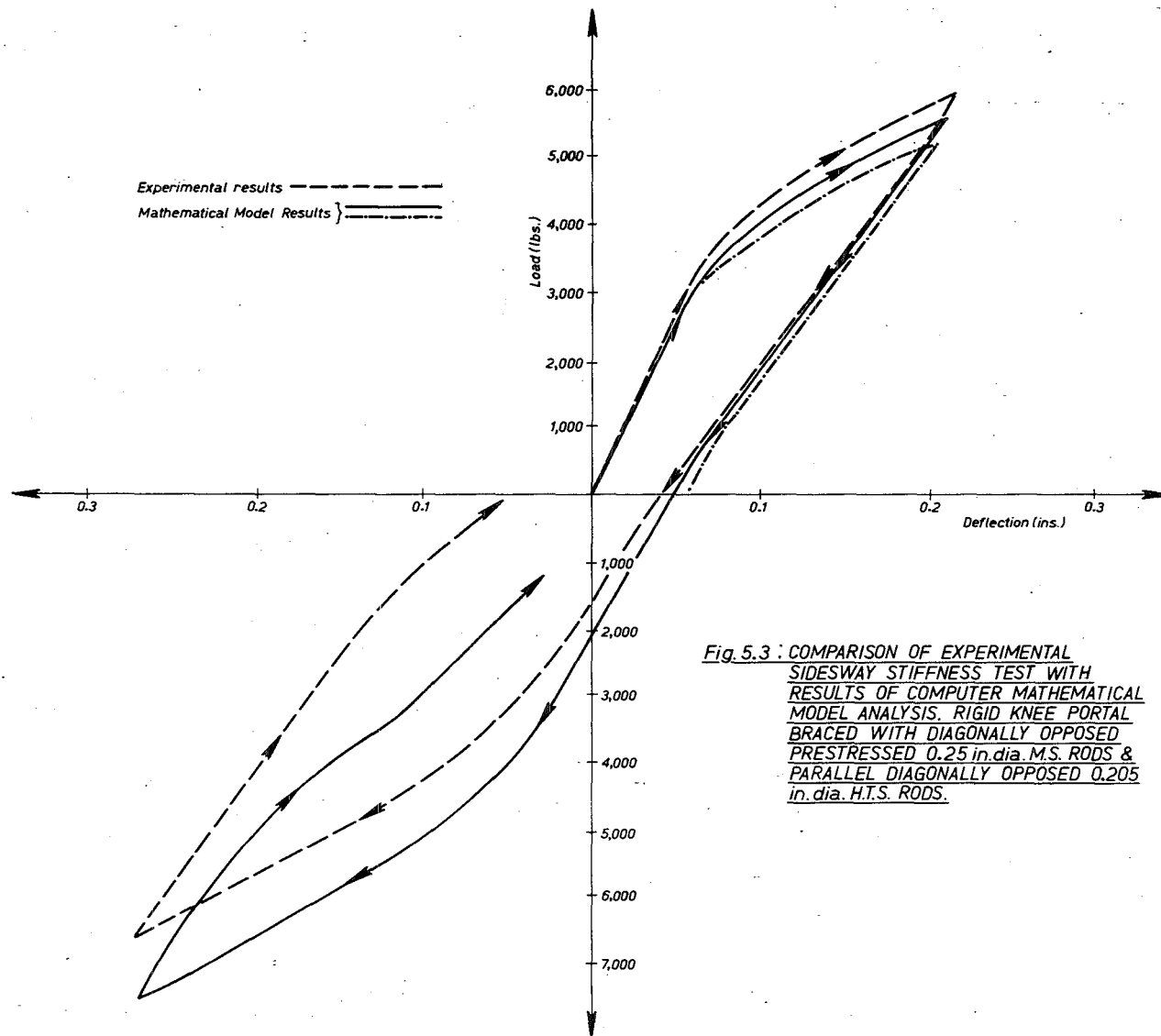


Fig. 5.2: COMPARISON OF EXPERIMENTAL SIDESWAY STIFFNESS TEST WITH RESULTS OF COMPUTER MATHEMATICAL MODEL ANALYSIS. PINNED KNEE FRAME BRACED WITH DIAGONALLY OPPOSED PRESTRESSED 0.25 in. dia. M.S. RODS & PARALLEL DIAGONALLY OPPOSED 0.205 in. dia. H.T.S. RODS.



was obtained using a reduced yield level (to separate the curve from the experimental one) and a displacement step interval of 0.03 inch. The curve denoted by crosses was obtained using identical data but with a displacement step interval of 0.01 inch. The effect of the step interval being large is to increase the apparent load on the system along those sections of the curve where the stiffness is in fact falling off, since the curve is built up progressively by projecting across the step interval at a gradient defined by the last value of stiffness. It was not expected that the displacement step interval would be large enough to cause significant errors in the dynamic analysis since the magnitude of the displacement increment is limited by the small integration time step but the result of this preliminary investigation emphasised the need to avoid large step intervals.

The comparison of results obtained in another of the experimental sidesway stiffness tests described in Chapter Three with those obtained using the KLAT program drew attention to another limitation of the mathematical model. As is shown in Figure 5.4, the model does not adequately represent the braced frame beyond about 0.8 in. sidesway. This is undoubtedly because the assumption of a constant post yield stiffness for the remaining active bracing rod becomes invalid at this level of sidesway. Provision could have been made in the program for suitable modification of the element stiffness values at this order of deflection but since it was felt that inter-storey sways of this proportion were generally unacceptable for reasons of instability and other generally neglected, second order effects, an

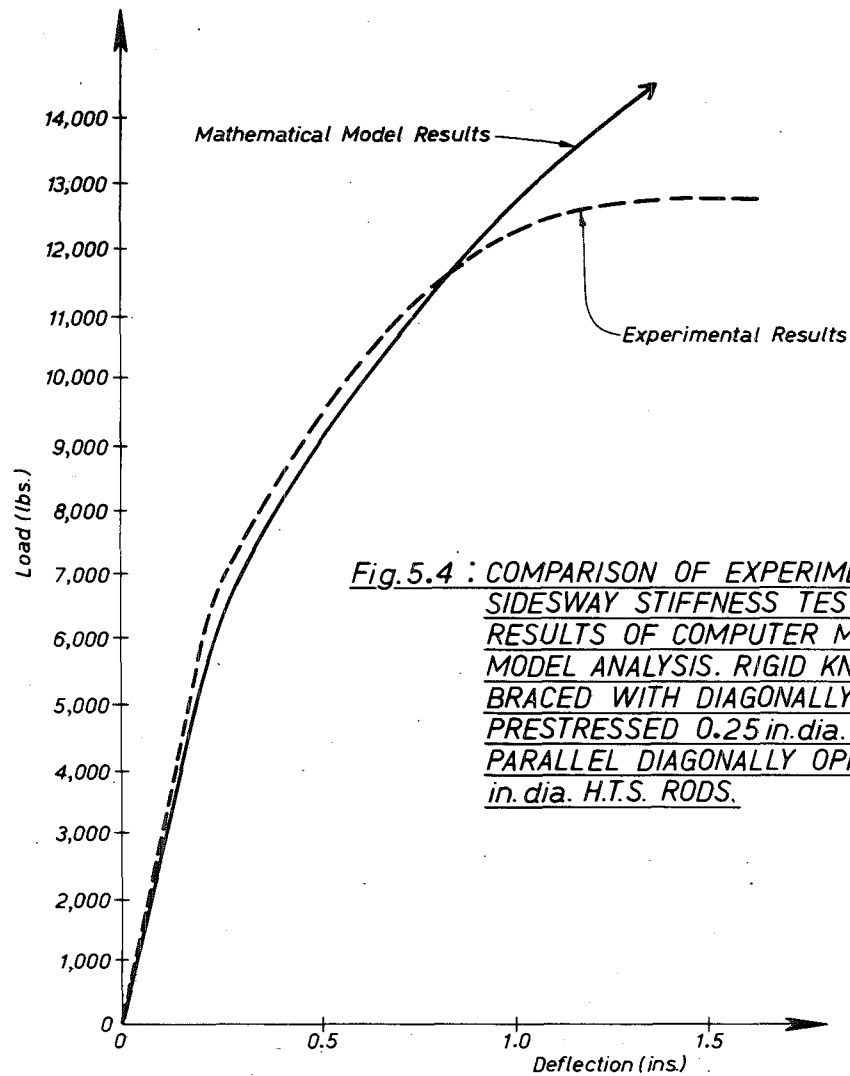


Fig.5.4 : COMPARISON OF EXPERIMENTAL SIDESWAY STIFFNESS TEST WITH RESULTS OF COMPUTER MATHEMATICAL MODEL ANALYSIS. RIGID KNEE PORTAL BRACED WITH DIAGONALLY OPPOSED PRESTRESSED 0.25 in.dia. M.S. RODS & PARALLEL DIAGONALLY OPPOSED 0.205 in.dia. H.T.S. RODS.

appropriate modification to the program was not considered necessary although this upper limit to the validity of the mathematical model clearly exists.

V.6 (iii) Main program XBFRME

A flow chart for program XBFRME is presented in Figure 5.2 and a complete listing is given in LIST 4.

In writing this program considerable effort was expended in an attempt to make it easy to follow, specifically by the generous use of comment cards, but an outline of the main features is included in the following stages of this section of this thesis.

After setting the DIMENSIONS and specifying DOUBLE PRECISION for the variables occurring in the numerical integration portion a control card, which also contains the damping coefficients, is read. Next, details of the mass and stiffness of the unbraced tower are read. After computation of the damping matrix the program essentially duplicates KLAT (LIST 3) until the lateral stiffness matrix of the braced frame has been determined.

The subsequent section contains the numerical integration process which is based on the solution of equation 4(15) by the stepwise process presented at the end of section IV.4. Provision is made for diversion past unnecessary steps in the solution process where these are avoidable, specifically by checking whether the stiffness has changed since the previous cycle and acting accordingly.

The final section of the main program XBFRME enables both written and punched card output to be produced, the selection being made by

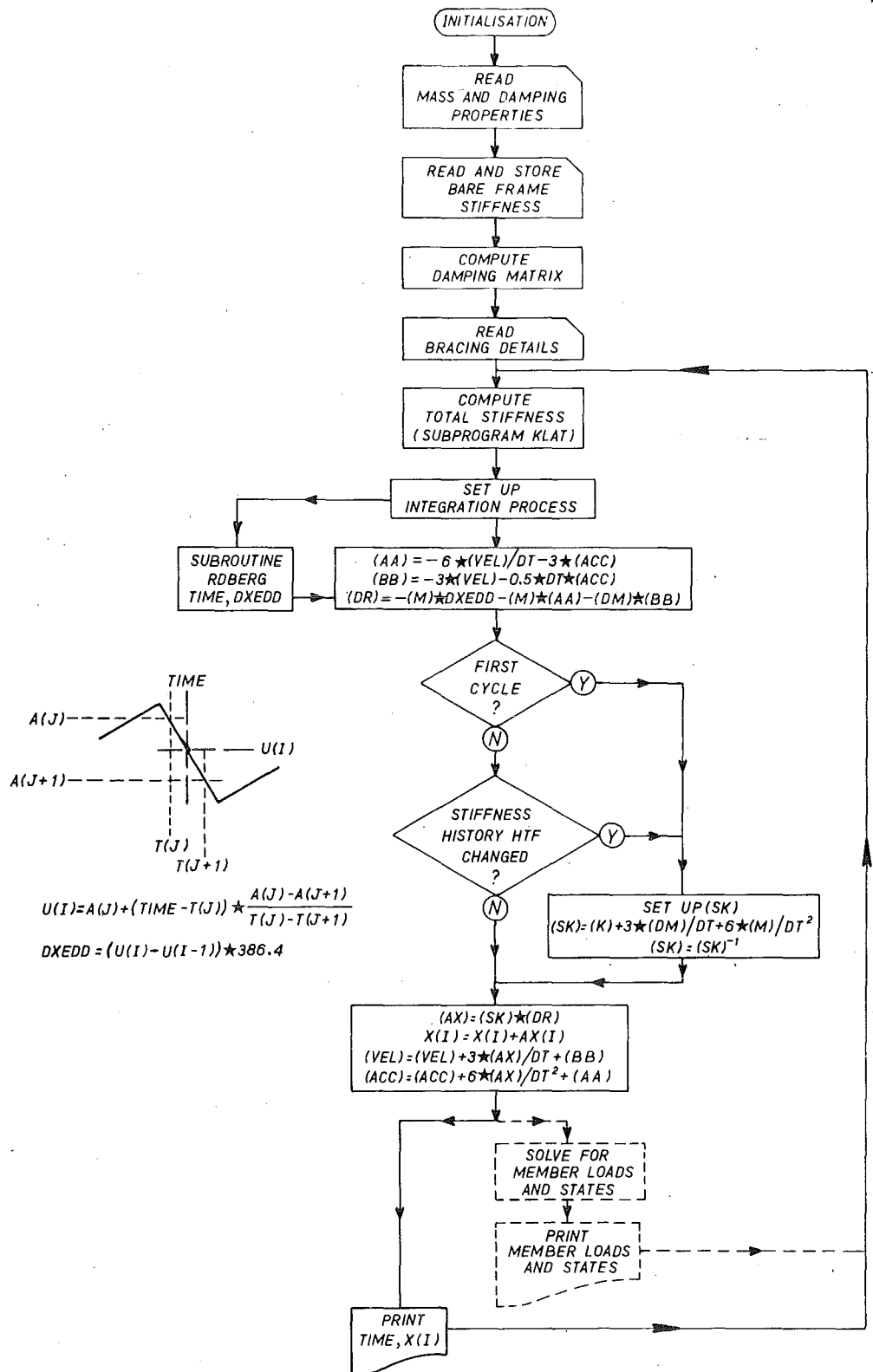


Fig. 5.5 : FLOW CHART FOR COMPUTER PROGRAM XBFRME


```

C   BRACING HIGH TENSILE STEEL TWC ( TOP LEFT TO BOTTOM RIGHT )   RS
   READ(5,220) A,ZL,HTS1P(I),HTS1U(I),ANG,EHT                   RS
   WRITE(6,220) A,ZL,HTS1P(I),HTS1U(I),ANG,EHT                   RS
   ANG=ANG*3.1415926/180.                                         RS
   HTS1K(I)=EHT*A/ZL*CCS(ANG)*CCS(ANG)                             RS
   READ(5,220) A,ZL,HTS2P(I),HTS2U(I),ANG,EHT                   RS
   WRITE(6,220) A,ZL,HTS2P(I),HTS2U(I),ANG,EHT                   RS
   ANG=ANG*3.1415926/180.                                         RS
   HTS2K(I)=EHT*A/ZL*CCS(ANG)*CCS(ANG)                             RS
   RS

C   ADJUST FOR LOSS OF PRESTRESS OR FOR YIELDING IF NECESSARY     RS
   AMS1D0(I)=-AMS1P(I)/AMS1K(I)                                     RS
   AMS2D0(I)=-AMS2P(I)/AMS2K(I)                                     RS
   HTS1D0(I)=-HTS1P(I)/HTS1K(I)                                     RS
   HTS2D0(I)=-HTS2P(I)/HTS2K(I)                                     RS
   AMS1DN(I)=AMS1D0(I)                                             RS
   AMS2DN(I)=AMS2D0(I)                                             RS
   FMS1K(I)=AMS1K(I)                                               RS
   FMS2K(I)=AMS2K(I)                                               RS
   FHTS1K(I)=HTS1K(I)                                              RS
   FHTS2K(I)=HTS2K(I)                                              RS
   RS
3   CCNTINUE                                                         RS
C   INITIALISE INTEGRATION PROCESS                                   RS
C   IF(DT.EQ.0.) DT=1.0/256.0                                       RS
   DC235 I=1,NM                                                    RS
   DR(I)=0.                                                         RS
   X(I)=0.                                                         RS
   VEL(I)=0.                                                         RS
235 ACC(I)=0.                                                       RS
C   ADJUST FOR LOSS OF PRESTRESS OR FOR YIELDING IN M.S. IF NECESSARY RS
C   ADJUST FOR LOSS OF PRESTRESS OR FOR FRACTURE IN M.T.S. DITTC  RS
C   SWAY OF TOP OF BRACED PANEL TO RIGHT RELATIVE TO BASE         RS
C   IS POSITIVE X                                                  RS
C   THE INTERSTOREY DRIFT EQUALS X(I) MINUS X(I-1)                RS
C   RS
C   MILD STEEL BRACING ONE                                          RS
C   FIRST, LOSS OF PRESTRESS DUE TO BRACING GOING SLACK          RS
240 DC 5 I=1,NM                                                    RS
   XIO=X(I-1)                                                       RS
   IF(I.EQ.1)XIO=0                                                  RS
   AMS1K(I)=FMS1K(I)                                               RS
   HMS1(I)=2                                                         RS
   B=X(I)-XIO-AMS1DN(I)                                             RS
   IF(B.GE.0.0) GC TC 10                                           RS
   AMS1K(I)=0.0                                                     RS
   HMS1(I)=1                                                         RS
10  CCNTINUE                                                         RS
C   SECOND QUERY IF YIELD HAS TAKEN PLACE                          RS
   AMS1DY(I)=(AMS1Y(I)/FMS1K(I))+AMS1DN(I)                         RS
   C=X(I)-XIO-AMS1DY(I)                                             RS
   IF(C.LT.0.0) GC TC 20                                           RS
   AMS1K(I)=AMS1PYK(I)                                              RS
   HMS1(I)=3                                                         RS
C   FOLLOWING YIELD ADJUSTMENT OF ELASTIC RANGE POSITION NECESSARY RS
   ADJ1(I)=X(I)-XIO-AMS1DY(I)                                       RS
   AMS1DN(I)=AMS1DN(I)+ADJ1(I)                                       RS
   TADJ1(I)=TADJ1(I)+ADJ1(I)                                       RS
   RS

```

```

20  CONTINUE                                                         RS
C   MILD STEEL BRACING TWO                                          RS
   AMS2K(I)=FMS2K(I)                                               RS
   HMS2(I)=2                                                         RS
   GG=X(I)-XIO-AMS2DN(I)                                           RS
   IF(GG.LE.0.0) GC TC 30                                         RS
   AMS2K(I)=0.0                                                     RS
   HMS2(I)=1                                                         RS
30  CONTINUE                                                         RS
   AMS2DY(I)=(-AMS2Y(I)/FMS2K(I))+AMS2DN(I)                       RS
   CC=X(I)-XIO-AMS2DY(I)                                           RS
   IF(CC.GT.0.0) GC TC 40                                         RS
   AMS2K(I)=MS2PYK(I)                                              RS
   HMS2(I)=3                                                         RS
   ADJ2(I)=X(I)-XIO-AMS2DY(I)                                       RS
   AMS2DN(I)=AMS2DN(I)+ADJ2(I)                                       RS
   TADJ2(I)=TADJ2(I)+ADJ2(I)                                       RS
40  CONTINUE                                                         RS
C   HIGH TENSILE STEEL BRACING CNE                                  RS
   IF(HTS1(I).GT.3) GC TC 60                                       RS
   HTS1K(I)=FHTS1K(I)                                              RS
   HHTS1(I)=2                                                         RS
   BBB=X(I)-XIO-HTS1D0(I)                                           RS
   IF(BBB.GE.0.0) GC TC 50                                         RS
   HTS1K(I)=0.0                                                     RS
   HHTS1(I)=1                                                         RS
50  CCNTINUE                                                         RS
   HTS1D0(I)=(HTS1U(I)/FHTS1K(I))+HTS1D0(I)                       RS
   CCC=X(I)-XIO-HTS1D0(I)                                           RS
   IF(CCC.LE.0.0) GC TC 60                                         RS
   HTS1K(I)=0.0                                                     RS
   HHTS1(I)=4                                                         RS
60  CCNTINUE                                                         RS
C   HIGH TENSILE STEEL BRACING TWC                                  RS
   IF(HTS2(I).GT.3) GC TC 80                                       RS
   HTS2K(I)=FHTS2K(I)                                              RS
   HHTS2(I)=2                                                         RS
   BBBB=X(I)-XIO-HTS2D0(I)                                           RS
   IF(BBBB.LE.0.0) GC TC 70                                         RS
   HTS2K(I)=0.0                                                     RS
   HHTS2(I)=1                                                         RS
70  CONTINUE                                                         RS
   HTS2D0(I)=(-HTS2U(I)/FHTS2K(I))+HTS2D0(I)                     RS
   CCCC=X(I)-XIO-HTS2D0(I)                                           RS
   IF(CCCC.GE.0.0) GC TC 80                                         RS
   HTS2K(I)=0.0                                                     RS
   HHTS2(I)=4                                                         RS
80  CONTINUE                                                         RS
C   FORM TOTAL STIFFNESS MATRIX                                     RS
C   DC 4 L=1,NM                                                    RS
   DC 4 J=1,NM                                                    RS
4   TK(L,J)=FK(L,J)                                                RS
   TK(1,1)=TK(1,1)+AMS1K(I)+AMS2K(I)+HTS1K(I)+HTS2K(I)          RS
   IF(NM.EQ.1) GC TC 5                                             RS
   DC 6 L=2,NM                                                    RS
   AK=AMS1K(L)+AMS2K(L)+HTS1K(L)+HTS2K(L)                         RS
   TK(L-1,L-1)=TK(L-1,L-1)+AK                                       RS
   TK(L-1,L)=TK(L-1,L)-AK                                           RS
   RS

```

[illegible]

56

RS
RS

RS
RS
RS
RS
RS
RS
RS
RS
RS

[illegible]

96

INPUT DATA ECHO CHECK

MASS MATRIX

0.1369E 05 C.1294E 05 0.6780E 06 C.2480E 06
UNBRACED FRAME LATERAL STIFFNESS MATRIX

0.134000E 05
0.131000E 05
0.451000E 04
0.104000E 01
0.131000E 05
0.221000E 03
0.127000E 05
0.655000E 01
0.444000E 04
0.127000E 05
0.992000E 04
0.257000E 03
0.559000E 02
0.489000E 02
0.238000E 03
0.235000E 03

DAMPING MATRIX

0.516396E 03
0.504481E 03
0.170984E 03
0.215271E 01
0.504481E 03
0.851413E 03
0.489077E 03
0.188314E 01
0.173690E 03
0.489077E 03
0.399969E 03
0.216538E 01
0.400504E 01
0.252240E 00
0.989707E 01
0.156157E 02

BRACING DETAILS

4.82 566. 0.0 C.298E 06 0.110E 05 49.7 0.312E 08
4.82 566. 0.0 C.298E 06 0.110E 05 49.7 0.312E 08
786 566. 0.0 0.0 49.7 0.289E 08
786 566. 0.0 0.0 49.7 0.289E 08

BRACING DETAILS

7.10 530. 0.0 C.425E 06 0.160E 05 52.3 0.312E 08
7.10 530. 0.0 C.425E 06 0.160E 05 52.3 0.312E 08
786 530. 0.0 0.0 52.3 0.289E 08
786 530. 0.0 0.0 52.3 0.289E 08

BRACING DETAILS

4.66 509. 0.0 0.519E 06 0.190E 05 53.4 0.312E 08
4.66 509. 0.0 0.519E 06 0.190E 05 53.4 0.312E 08
786 509. 0.0 0.0 53.4 0.289E 08
786 509. 0.0 0.0 53.4 0.289E 08

DETAILS OF EARTHQUAKE BEING USED...

EARTHQUAKE BEING USED IS THE EL CENTO MAY 1940 ONE.(NCRTH-SCUTH)...

NUMBER OF EARTHQUAKE CARDS TO BE READ

= 125

IG E/G RECORD FACTOR

= 1.00

TIME STEP INTERVAL

= 0.00390625

TIME

DISPLACEMENT OF MASSES

HISTORY RECORD

0.1563E-01 -0.3398E-03 -0.3739E-03 -0.3700E-03 -0.3700E-03 1214 1214 2141
0.1412E-01 -0.1149E-02 -0.1459E-02 -0.1437E-02 -0.1437E-02 1214 1214 1244
0.4688E-01 -0.1825E-02 -0.2686E-02 -0.3027E-02 -0.3030E-02 1214 1214 1244
0.6250E-01 -0.2268E-02 -0.3756E-02 -0.4786E-02 -0.4803E-02 1214 1214 1244
0.7813E-01 -0.3056E-02 -0.5246E-02 -0.7047E-02 -0.7197E-02 1214 1214 1244
0.9375E-01 -0.4667E-02 -0.7801E-02 -0.1018E-01 -0.1034E-01 1214 1214 1244
0.1094E 00 -0.7237E-02 -0.1158E-01 -0.1455E-01 -0.1487E-01 1214 1214 1244
0.1250E 00 -0.1008E-01 -0.1610E-01 -0.2012E-01 -0.2069E-01 1214 1214 1244
0.1406E 00 -0.1254E-01 -0.2069E-01 -0.2795E-01 -0.2743E-01 1214 1214 1244
0.1563E 00 -0.1465E-01 -0.2517E-01 -0.3329E-01 -0.3473E-01 1214 1214 1244
0.1719E 00 -0.1693E-01 -0.3072E-01 -0.4000E-01 -0.4232E-01 1214 1214 1244

0.1430E 02 0.3837E 01 C.4916E 01 0.5598E 01 -0.2324E 01 3144 2144 2144
0.1431E 02 0.3768E 01 C.5083E 01 0.6088E 01 -0.2310E 01 3144 2144 2144
0.1432E 02 0.3735E 01 C.5258E 01 0.6595E 01 -0.2297E 01 3144 2144 2144
0.1433E 02 0.3699E 01 C.5433E 01 0.6959E 01 -0.2284E 01 3144 2144 2144
0.1434E 02 0.4397E 01 C.5605E 01 0.7340E 01 -0.2269E 01 3144 2144 2144
0.1435E 02 0.4558E 01 C.5777E 01 0.7688E 01 -0.2250E 01 3144 2144 2144
0.1436E 02 0.4719E 01 C.5949E 01 0.8036E 01 -0.2231E 01 3144 2144 2144
0.1437E 02 0.4880E 01 C.6121E 01 0.8385E 01 -0.2212E 01 3144 2144 2144
0.1438E 02 0.5041E 01 C.6293E 01 0.8734E 01 -0.2193E 01 3144 2144 2144
0.1439E 02 0.5202E 01 C.6465E 01 0.9083E 01 -0.2174E 01 3144 2144 2144
0.1440E 02 0.5363E 01 C.6637E 01 0.9432E 01 -0.2155E 01 3144 2144 2144
0.1441E 02 0.5524E 01 C.6809E 01 0.9781E 01 -0.2136E 01 3144 2144 2144
0.1442E 02 0.5685E 01 C.6981E 01 1.0130E 01 -0.2117E 01 3144 2144 2144
0.1443E 02 0.5846E 01 C.7153E 01 1.0479E 01 -0.2098E 01 3144 2144 2144
0.1444E 02 0.6007E 01 C.7325E 01 1.0828E 01 -0.2079E 01 3144 2144 2144
0.1445E 02 0.6168E 01 C.7497E 01 1.1177E 01 -0.2060E 01 3144 2144 2144
0.1446E 02 0.6329E 01 C.7669E 01 1.1526E 01 -0.2041E 01 3144 2144 2144
0.1447E 02 0.6490E 01 C.7841E 01 1.1875E 01 -0.2022E 01 3144 2144 2144
0.1448E 02 0.6651E 01 C.8013E 01 1.2224E 01 -0.2003E 01 3144 2144 2144
0.1449E 02 0.6812E 01 C.8185E 01 1.2573E 01 -0.1984E 01 3144 2144 2144
0.1450E 02 0.6973E 01 C.8357E 01 1.2922E 01 -0.1965E 01 3144 2144 2144
0.1451E 02 0.7134E 01 C.8529E 01 1.3271E 01 -0.1946E 01 3144 2144 2144
0.1452E 02 0.7295E 01 C.8701E 01 1.3620E 01 -0.1927E 01 3144 2144 2144
0.1453E 02 0.7456E 01 C.8873E 01 1.3969E 01 -0.1908E 01 3144 2144 2144
0.1454E 02 0.7617E 01 C.9045E 01 1.4318E 01 -0.1889E 01 3144 2144 2144
0.1455E 02 0.7778E 01 C.9217E 01 1.4667E 01 -0.1870E 01 3144 2144 2144
0.1456E 02 0.7939E 01 C.9389E 01 1.5016E 01 -0.1851E 01 3144 2144 2144
0.1457E 02 0.8100E 01 C.9561E 01 1.5365E 01 -0.1832E 01 3144 2144 2144
0.1458E 02 0.8261E 01 C.9733E 01 1.5714E 01 -0.1813E 01 3144 2144 2144
0.1459E 02 0.8422E 01 C.9905E 01 1.6063E 01 -0.1794E 01 3144 2144 2144
0.1460E 02 0.8583E 01 C.1007E 01 1.6412E 01 -0.1775E 01 3144 2144 2144
0.1461E 02 0.8744E 01 C.1029E 01 1.6761E 01 -0.1756E 01 3144 2144 2144
0.1462E 02 0.8905E 01 C.1041E 01 1.7110E 01 -0.1737E 01 3144 2144 2144
0.1463E 02 0.9066E 01 C.1063E 01 1.7459E 01 -0.1718E 01 3144 2144 2144
0.1464E 02 0.9227E 01 C.1085E 01 1.7808E 01 -0.1699E 01 3144 2144 2144
0.1465E 02 0.9388E 01 C.1107E 01 1.8157E 01 -0.1680E 01 3144 2144 2144
0.1466E 02 0.9549E 01 C.1129E 01 1.8506E 01 -0.1661E 01 3144 2144 2144
0.1467E 02 0.9710E 01 C.1151E 01 1.8855E 01 -0.1642E 01 3144 2144 2144
0.1468E 02 0.9871E 01 C.1173E 01 1.9204E 01 -0.1623E 01 3144 2144 2144
0.1469E 02 1.0032E 01 C.1195E 01 1.9553E 01 -0.1604E 01 3144 2144 2144
0.1470E 02 1.0193E 01 C.1217E 01 1.9902E 01 -0.1585E 01 3144 2144 2144
0.1471E 02 1.0354E 01 C.1239E 01 2.0251E 01 -0.1566E 01 3144 2144 2144
0.1472E 02 1.0515E 01 C.1261E 01 2.0600E 01 -0.1547E 01 3144 2144 2144
0.1473E 02 1.0676E 01 C.1283E 01 2.0949E 01 -0.1528E 01 3144 2144 2144
0.1474E 02 1.0837E 01 C.1305E 01 2.1298E 01 -0.1509E 01 3144 2144 2144
0.1475E 02 1.1000E 01 C.1327E 01 2.1647E 01 -0.1490E 01 3144 2144 2144

MAXIMUM VALUES

0.1452E 02 0.4600E 01
0.1452E 02 0.8243E 01
0.1453E 02 0.7423E 01
0.2562E 01 0.1029E 02

TOTAL YIELD DISPLACEMENT OF MS FRACES.

0.400511E 01 0.0 0.0
0.0 -0.163373E 01 0.0
0.0 0.0

LIST 4 OUTPUT

the appropriate insertion on the control card at the start of the program. Typical line printer output is shown at the end of LIST 4 and the results of using the punched output to activate the X-Y plotter on line to the University of Canterbury's IBM 1620 computer are shown in the displacement/time plots presented in Chapter Six.

The subroutine RDBERG is used to produce a set of exciting accelerations at selected times for use in the numerical integration section of XBFRME, by suitable modification of Berg type⁽⁷⁰⁾ digitised accelerograms. In their original state these accelerograms exist in digitised form with four successive peak values of acceleration, together with the time of each event, listed on each card. It is assumed that the accelerograms are fully defined by these points, a series of straight lines drawn between the points being sufficient to complete the traces. For the purpose of numerical integration it is necessary to convert the Berg digitised records to a set of acceleration values at equal (preselected) time intervals. The principle used in RDBERG is that of establishing the gradient of the accelerogram between two consecutive time points and then determining the value of acceleration at the time interval chosen by calculating the product of the gradient and the time elapsed since the last peak on the accelerogram. (See Figure 5.2). The procedure adopted has the effect of cutting off the peaks of the original accelerogram in all cases other than when the exact multiple of the selected integration time step coincides with the time at which the peak occurs, but this is considered to be satisfactory providing the step interval is small enough to reduce the neglected peaks to an insignificant proportion

of the whole accelerogram.

V.6 (iv) Input data XBFRME program

1. First Card, NM, NPS, TR, DT, CG, CR, NPLOT, NWRTE

Format (2I5, 4G 10.0, 2I5)

N = Number of Masses (one per storey)
 NPS = Number of time steps before printing
 TR = Length of earthquake record (seconds)
 DT = Step interval (seconds)
 CG = Damping Coefficient
 CR = Damping Coefficient
 NPLOT = 0 for no plotter output, 1 for plotter output
 NWRTE = 0 for no printed output, 1 for printed output

2. Mass Card(s). (Actually in lb. weight units) From bottom up.

Format (8E10.4)

3. Unbraced Frame Lateral Stiffness Matrix Card(s).

Format (8G10.3)

4. Bracing Detail Cards (4 Cards necessary for each bay).

For each bay, Two Mild Steel Cards (Format 8G10.3)

Containing: (N.B. ? represents digit 1 or digit 2).

A = Bracing Rod Area (in^2)
 ZL = Bracing Rod Length (in)
 AMS?P = Prestressing Force in Bracing Rod (lbs)
 AMS?Y = Axial Force at which Bracing Rod will Yield (lbs)
 MS?PYK = Post yield axial stiffness of Bracing Rod (lb/in)
 ANG = Angle to horizontal of Bracing Rod (degrees)
 EMS = Elastic Modulus (lb/in^2)

and, for each bay, a second pair of cards, for the high tensile steel containing:

A = Bracing Rod Area (in^2)
 ZL = Bracing Rod Length (in)
 HTS?P = Prestressing Force in Bracing Rod (lbs)
 HTS?U = Axial Force at which Bracing Rod will break (lbs)
 ANG = Angle to horizontal of Bracing Rod (degrees)
 EHT = Elastic Modulus (lbs/in^2)

(N.B. for a three storey frame there will be a total of twelve bracing cards, read in storey by storey, MS1, MS2, HTS1, HTS2 from the ground up).

5. A Control Card NCARD, SF

Format (I5, G10.0)

NCARD = Number of Earthquake Record Cards to be read
(consistent with TR in first card).

SF = Scale factor by which earthquake accelerations may
be multiplied.

6. Digitised Earthquake Record Cards.

First one Title Card - Format (20A4)

Remainder, in numerical sequence up to NCARD,

Berg type Format I3, 4 (F8.4, F9.6), I4

ISC = Sequence Number

T(I), G(I), I-2, 5 = four co-ordinate points - time (seconds),
acceleration (fraction of g) for each point

NR = Earthquake Record Number

OUTPUT DATA XBFRME PROGRAM

1. Input Data Echo Check - Unbraced Frame Lateral Stiffness Matrix
- Computed Damping Matrix - Input Bracing
Details - Earthquake Record Details.
2. Written Output - Time, Displacement of Masses and Bracing
History Record.
3. Plotter Output - Time and Mass Displacement values for
Plotting on off-line X-Y plotter.

V.6 (v) Symbol table XBFRME program

A(main program)	- Bracing Cross Section Area
A(subroutine)	- Ground Acceleration, (proportion of gravity)
AA	- Vector used in the integration process
ACC	- Vector used in the integration process
ANG	- Angle of Bracing rod to horizontal
ADJ1	- Adjustment to Bracing Rod 1 elastic range after yield
ADJ2	- Adjustment to Bracing Rod 2 elastic range after yield
AK	- Incremental Lateral Stiffness due to Bracing
AMS1DN	- Position of zero load in M.S. Bracing Rod 1
AMS1DO	- Original zero load position for M.S. Bracing Rod 1
AMS1DY	- Position at which M.S. Bracing Rod 1 just yields
AMS1K	- Axial Stiffness of M.S. Bracing Rod 1
AMS1P	- Prestressing force in M.S. Bracing Rod 1
AMS1Y	- Elastic limit force in M.S. Bracing Rod 1
AMS2DN	- Position of zero load in M.S. Bracing Rod 2
AMS2DO	- Original zero load position for M.S. Bracing Rod 2
AMS2DY	- Position at which M.S. Bracing Rod 2 just yields
AMS2K	- Axial Stiffness of M.S. Bracing Rod 2
AMS2P	- Prestressing Force in M.S. Bracing Rod 2
AX	- Incremental deflection
BB	- Vector used in the integration process
BC	- Vector used in the integration process
BX	- Maximum displacement
CG	- Damping Coefficient
CR	- Damping Coefficient
DXEDD	- Exciting acceleration
DXGDD (subroutine)	- Exciting acceleration
DM	- Damping Matrix
DR	- Vector used in the integration process
DT	- Time step
EHT	- Elastic Modulus H.T.S. Bracing
EMS	- Elastic Modulus M.S. Bracing
FHTS1K	- Initial axial stiffness of H.T.S. Bracing Rod 1
FHTS2K	- Initial axial stiffness of H.T.S. Bracing Rod 2
FK	- Unbraced frame lateral stiffness matrix
FMS1K	- Initial axial stiffness of M.S. Bracing Rod 1
FMS2K	- Initial axial stiffness of M.S. Bracing Rod 2
HTF	- Bracing Rod load state record
HHTS1	- History indicator H.T.S. Bracing Rod 1
HHTS2	- History indicator H.T.S. Bracing Rod 2
HMS1	- History indicator M.S. Bracing Rod 1
HMS2	- History indicator M.S. Bracing Rod 2
HTS1DO	- Original zero load position for H.T.S. Bracing Rod 1
HTS1DU	- Ultimate load position for H.T.S. Bracing Rod 1
HTS1K	- Axial Stiffness of H.T.S. Bracing Rod 1
HTS1P	- Prestressing force in H.T.S. Bracing Rod 1
HTS1U	- Ultimate load in H.T.S. Bracing Rod 1
HTS2DO	- Original zero load position for H.T.S. Bracing Rod 2

HTS2DU	- Ultimate load position for H.T.S. Bracing Rod 2
HTS2K	- Axial Stiffness of H.T.S. Bracing Rod 2
HTS2P	- Prestressing force in H.T.S. Bracing Rod 2
HTS2U	- Ultimate load in H.T.S. Bracing Rod 2
MS1PYK	- Post yield axial stiffness of M.S. Bracing Rod 1
MS2PYK	- Post yield axial stiffness of M.S. Bracing Rod 2
NM	- Number of masses in system
NPLOT	- Punched Card output control
NPS	- Number of time steps per write step
NWRTE	- Line Printer output control
PHTF	- Bracing Rod load state record in previous cycle
PX	- Deflection in previous cycle
SK	- Vector used in integration process
TADJ1	- Total yield displacement of M.S. Bracing Rod 1
TADJ2	- Total yield displacement of M.S. Bracing Rod 2
T (subroutine)	- Time
TR	- Total length of accelerogram record
TX	- Time at which maximum deflection occurs
VEL	- Vector used in the integration process
W	- Weight
X	- Displacement
XP1	- Displacement arrays used in Plotter output
XP2	- Displacement arrays used in Plotter output
XP3	- Displacement arrays used in Plotter output
ZM	- Mass vector
ZL	- Length of Bracing Rods

V.6 (vi) Checks on XBFRME program

Because of the novelty of the XBFRME analysis it was not possible, in the case of multiphase bracing response, to check it out against results obtained from a completely independent procedure. However it was confirmed that the integration, RDBERG and output routines do function correctly. This was done both by reading in bracing details which resulted in the frame being effectively unbraced (readily achieved by setting the bracing elastic modulus at 30×10^{-6} instead of $30 \times 10^{+6}$) and subsequently by selecting a sufficiently high level of yield load in the braces (10^8 lbs for the frame analysed in Chapter Six) to ensure that the bracing always responded in the extended elastic range throughout the full analysis.

Independent analyses were made of the resulting two sets of fully elastic systems using the library program ELRES (LIST LP4) which, as stated earlier, is based on a numerical integration solution of equation 4(1). Virtually identical displacement/time plots to those obtained from ELRES were determined using XBFRME providing that the time step interval was set to be sufficiently small. Evidence of non-agreement was obtained at XBFRME time step intervals down to less than $1/100$ second but no difference was evident when a time step of $1/256$ second was used. This result is entirely consistent with that of an earlier investigation⁽⁶³⁾ of the use of the IBM 360/44 for this type of numerical analysis and consequently all subsequent analyses using XBFRME were carried out with the integration time step set at $1/256$ second. This also ensured that the displacement step interval would be small enough to make negligible the error introduced by projecting across the step interval at a gradient defined by the last value of stiffness (referred to in section V.6 (ii) above).

Comparisons between ELRES and XBFRME were made for both undamped and damped elastic systems. Virtually identical results were obtained from the two analysis procedures, as is illustrated by the results for the elevated water tank tower discussed in Chapter Six.

Since verification that KLAT functions satisfactorily had been previously made (section V.6 (ii) above) it was concluded that no other validity checks on XBFRME could be made with advantage.

V.7 Summary of the Use of Digital Computer Programs in the Determination of the Seismic Response of Elevated Water Tanks

Subsequent to the idealisation of the supporting structure to a discrete mass system with specified geometric and mass characteristics, the following steps are followed to determine the seismic response of an elevated water tank supported on a cross braced frame tower.

- A. The elastic stiffness characteristics of the unbraced tower framework are computed. (Program '2-D STRUCTURE', LIST LP1, Appendix IV).
- B. The post yield characteristics of the mild steel bracing members are calculated (Program 'TRUEFORCE', Chapter Three).
- C. The convective effect of the water in the tank (i.e. the two mass representation of the tank and contents) is determined. (Program 'MODANAL', Chapter Two).
- D. Using the results of steps A and C, the normal mode frequencies of lateral vibration of the undamped tower supporting the two mass representation of the tank and contents is computed. (Program 'NORMOD', LIST LP2, Appendix IV).
- E. Using the normal mode frequencies determined in step D, the damping characteristics are established. (Program 'DAMPING MATRIX', LIST LP2A, Appendix IV).
- F. Using the results of steps A, B, C and E the seismic response of the elevated water tower is determined. (Program 'XBFRME', Chapter Five, Section 6).

C H A P T E R S I X

SEISMIC RESPONSE ANALYSESVI.1 Introduction

To illustrate the analysis procedures presented in previous sections of this thesis the water tank described by Moran and Cheney⁽²¹⁾ was used as the basis of a prototype system and the analyses carried out on this structure are described below.

VI.2 The Structure Examined

The structure used for the verification and sensitivity analyses presented in this chapter is shown diagrammatically in Figure 6.1. The tower has welded tubular columns and circular section bracing rods. The columns are 22 in. inside diameter and of $5/16$ in. thickness in the upper section, of $3/8$ in. thickness in the centre section, and of $7/16$ in. thickness in the lower section. The bracing rods are of $2\frac{3}{8}$ in. diameter for the upper section, $2\frac{1}{8}$ in. diameter for the centre section and $1\frac{3}{4}$ in. for the lower section. The horizontal strut members are each fabricated from two channels (see the detail on Figure 6.1). Between the centre and upper sections the channel with the horizontal web is of 8 in. web dimension and weighs 11.5 lb/ft. whereas the channel having horizontal flanges is of 9 in. web dimensions and weighs 13.4 lb/ft. Between the lower and centre sections the channel

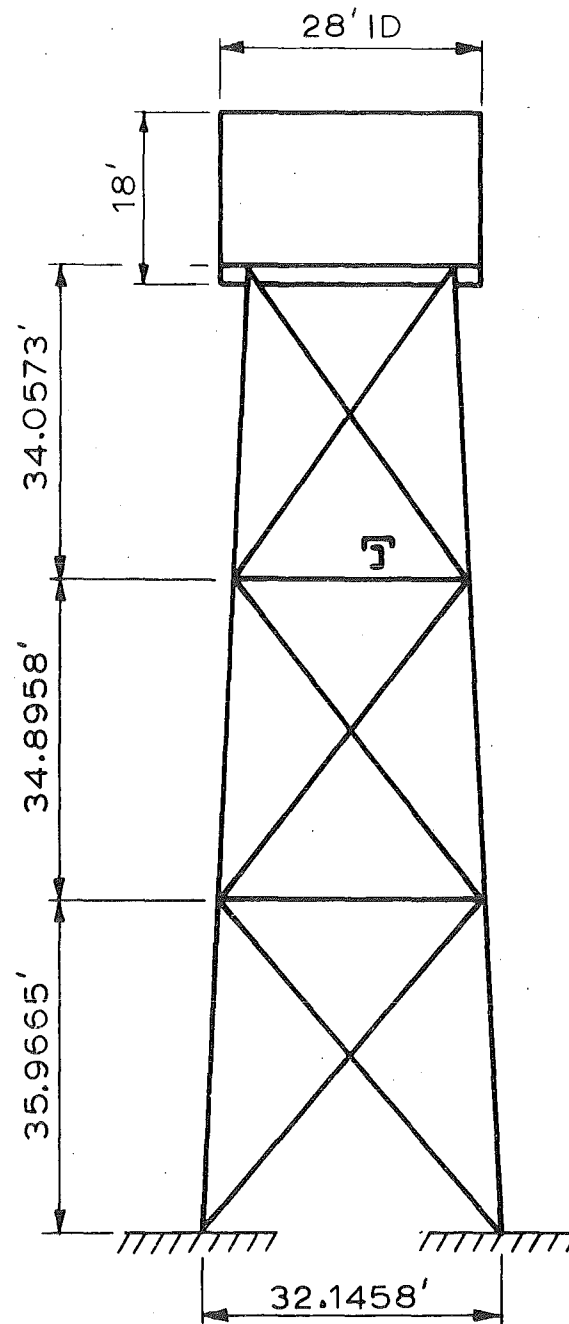


Fig.6.1 : Elevated Water Tank Analysed
(After Moran & Cheney)

with the horizontal web is of 8 in. web size and weighs 11.5 lb/ft. whereas the channel with the horizontal flanges is of 10 in. web dimension and weighs 15.3 lb/ft. Moran and Cheney give the weight of the tank and its contents as 926,000 lb.

For the purpose of this study a cylindrical tank is used in place of the original one which had a domed top and bottom.

A summary of the calculations undertaken in modelling the three storey tower frame is presented in Appendix V. Since the capacity of the tank is given as 100,000 (U.S.) gallons when full the contents were assumed to weigh 832,000 lbs hence the tank structure weight was deduced to be 94,000 lbs.

The self-weight mass distribution when the tank is empty, is

$$\begin{array}{ll} 13,688 \text{ lbs} & M_1 \\ 12,942 \text{ lbs} & M_2 \\ 99,110 \text{ lbs} & M_3 + m_s \end{array} \quad (\text{See Figure 4.2})$$

and these values are used in the following analyses. (Note the computer programs accept weights rather than masses and factor accordingly in the computational procedure).

VI.3 Digital Computer Analyses With No Convective Action of the Water

(Note: All numerical values in lb.in. units)

Step A. The unbraced frame flexibility matrix for the three mass system may be determined using the '2-D STRUCTURE' Program and has form:

$$10^{-4} \times \begin{bmatrix} 5.642 & 7.513 & 7.236 \\ 7.513 & 11.86 & 12.07 \\ 7.236 & 12.07 & 13.50 \end{bmatrix}$$

This, when inverted, using the matrix inversion program (LIST, LP3), gives the lateral stiffness matrix for the unbraced frame which has form

$$10^4 \times \begin{bmatrix} 1.34 & -1.31 & 0.453 \\ -1.31 & 2.22 & -1.28 \\ 0.453 & -1.28 & 0.975 \end{bmatrix}$$

- Step B. The post yield axial stiffness characteristics of the bracing rods, determined using program 'TRUEFORCE', are presented in Figure 6.2, from these results values of 5,500 lb/in., 8,000 lb/in. and 9,500 lb/in. may be deduced for the effective post yield stiffnesses of each bracing rod in the lower, middle and upper braced bays.
- Step D. When the mass and stiffness properties previously established are used as input to the normal mode analysis program, natural frequencies of 0.2716 cps and 5.774 cps may be determined for the first and second modes of the unbraced tower supporting an empty tank.
- Step E. Since it is generally accepted that elevated water tank structures exhibit relatively low percentage critical damping characteristics, 2% critical was selected for each

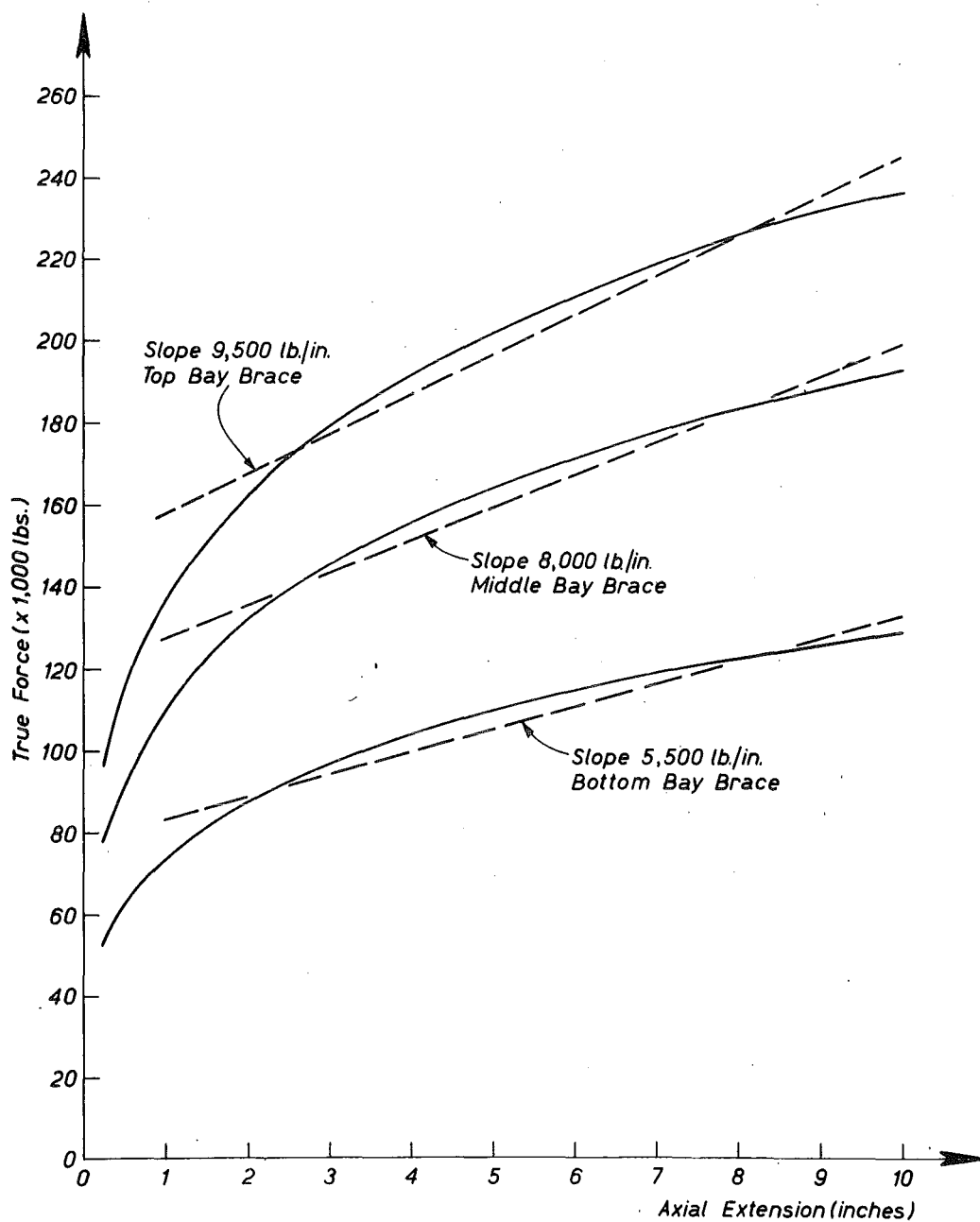


Fig. 6.2 : TRUE FORCE / TRUE DEFLECTION CURVES FOR BRACING RODS.

of the first two modes of vibration and, when used as input to the library program 'DAMPING MATRIX', damping coefficients of $CG = 0.00105$ and $CR = 0.0652$ may be determined, also the damping matrix

$$10^2 \times \begin{bmatrix} 0.164 & -0.138 & 0.048 \\ -0.138 & 0.256 & -0.135 \\ 0.048 & -0.135 & 0.270 \end{bmatrix}$$

may be derived.

Step F. The input data determined as described above was used in the program XBFRME together with the digitised North/South accelerations of the 1940 El Centro earthquake, to determine a series of displacement/time histories as shown in the accompanying figures.

The displacement response of each of the three masses of the system to the El Centro accelerogram factored by 1.0, when no damping is allowed for in the unbraced frame supporting an empty tank, is shown in Figure 6.3. The result of this essentially elastic analysis is identical to that obtained by the use of the library program ELRES to undertake the same response calculation.

Maximum displacements were determined as follows

Mass 1 :	10.73 ins	at 5.449 secs
Mass 2 :	15.99 ins	at 5.402 secs
Mass 3 :	17.87 ins	at 5.250 secs

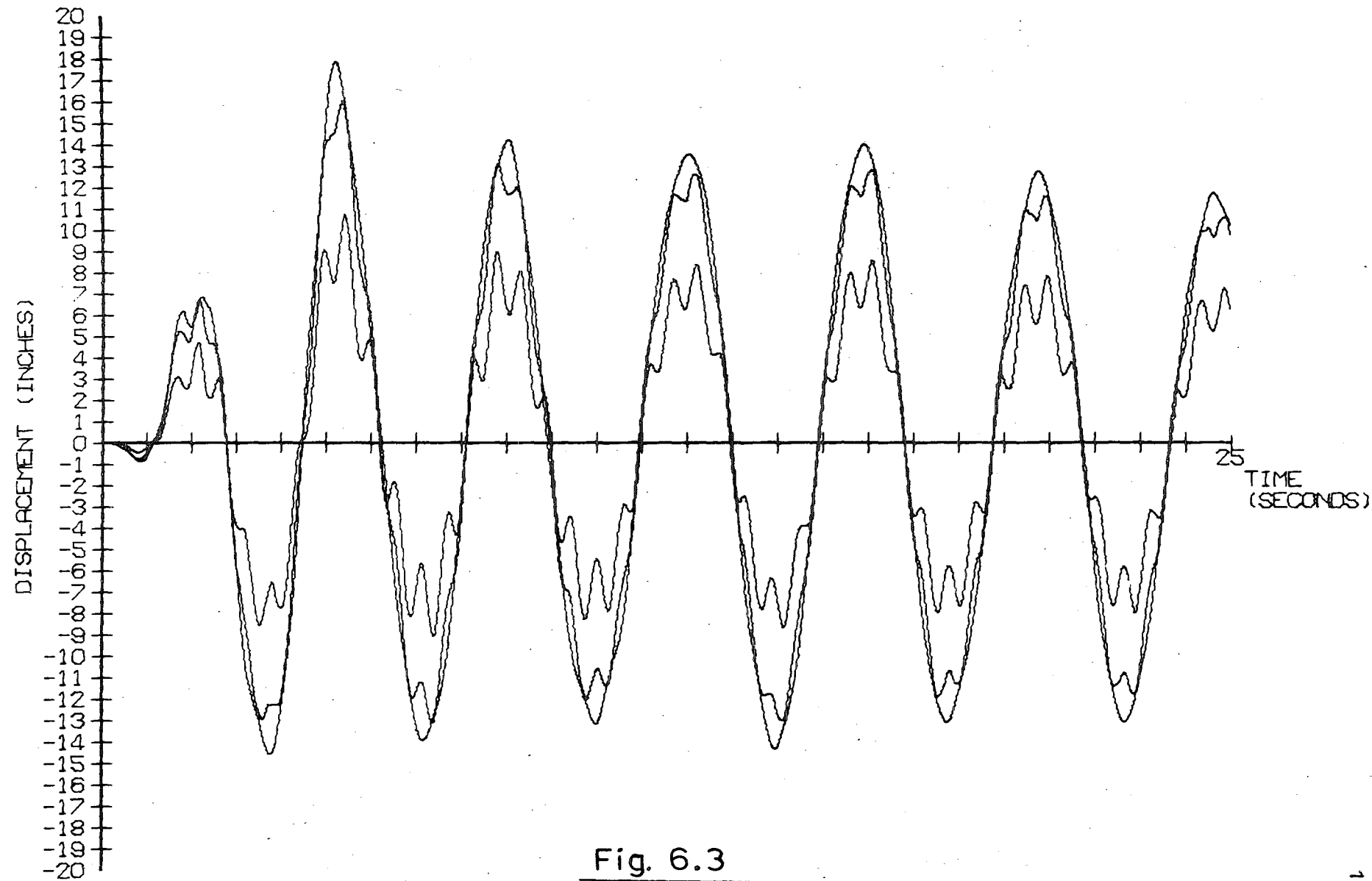


Fig. 6.3

A second analysis, similar to the first one except that the 2% damping coefficients were read in to the XBFRME program, resulted in the displacement/time history shown in Figure 6.4 being produced.

Maximum displacements in this case are

Mass 1 :	9.364 ins	at 5.441 secs
Mass 2 :	14.35 ins	at 5.391 secs
Mass 3 :	16.53 ins	at 5.234 secs

Once again this result is identical to that given by an ELRES analysis.

When the Moran and Cheney bracing with no prestress was incorporated and allowed to act in an extended elastic manner the undamped response of the frame, supporting the full tank with no convective action of the water, to the El Centro N/S accelerogram factored by 1.0, as presented in Figure 6.5 was determined.

In this case the maximum displacements are

Mass 1 :	3.934 ins	at 23.58 secs
Mass 2 :	6.717 ins	at 23.57 secs
Mass 3 :	8.901 ins	at 24.26 secs

Inclusion of 2% damping in this analysis was next undertaken. In the first place the damping matrix was calculated using the effective total lateral stiffness characteristics of the braced frame and was then overwritten into the program XBFRME. The resulting response is shown in Figure 6.6.

Maximum displacements in this case are:-

Mass 1 :	1.978 ins	at 14.58 secs
Mass 2 :	3.391 ins	at 14.58 secs
Mass 3 :	4.504 ins	at 14.58 secs

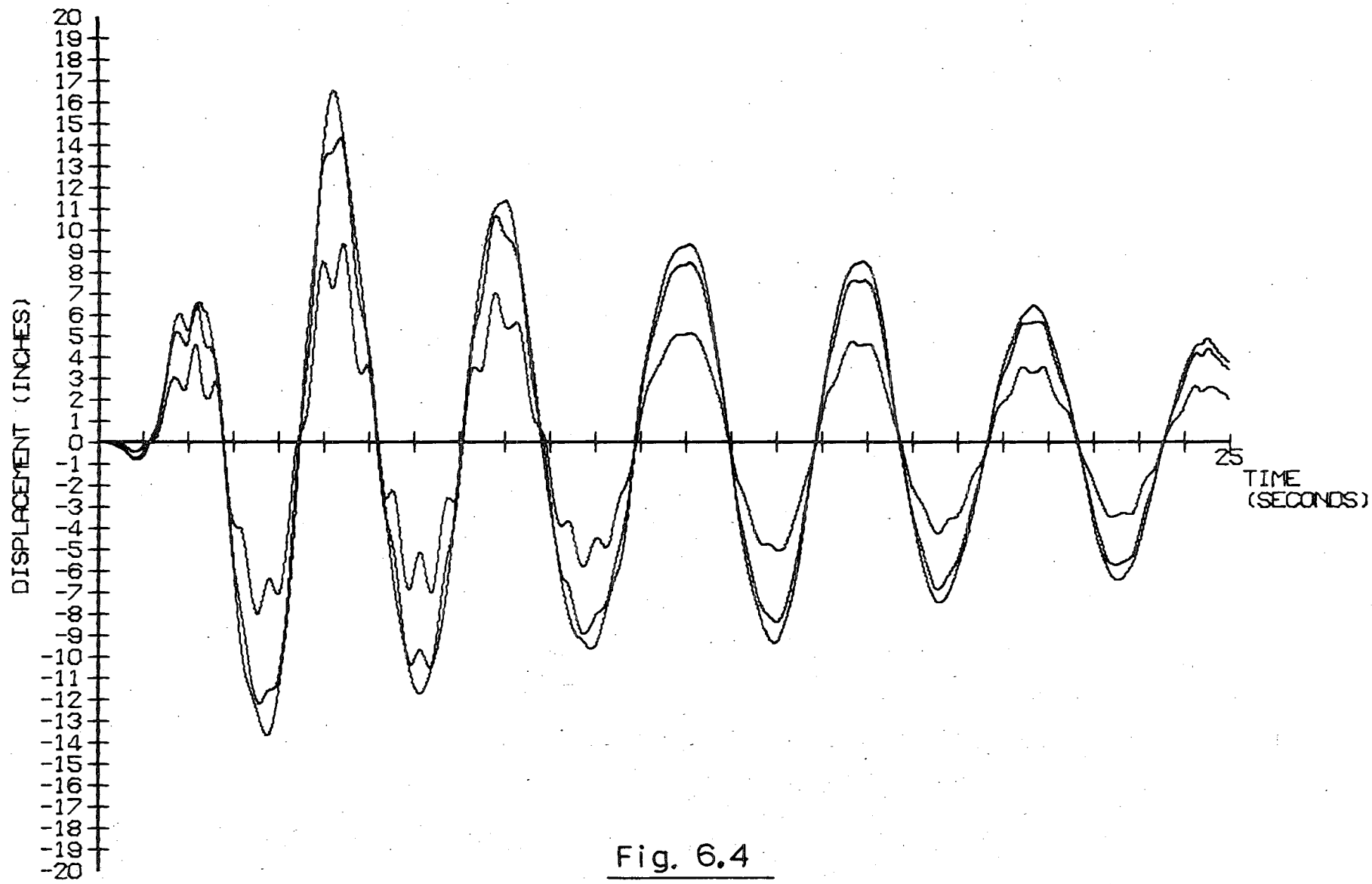


Fig. 6.4

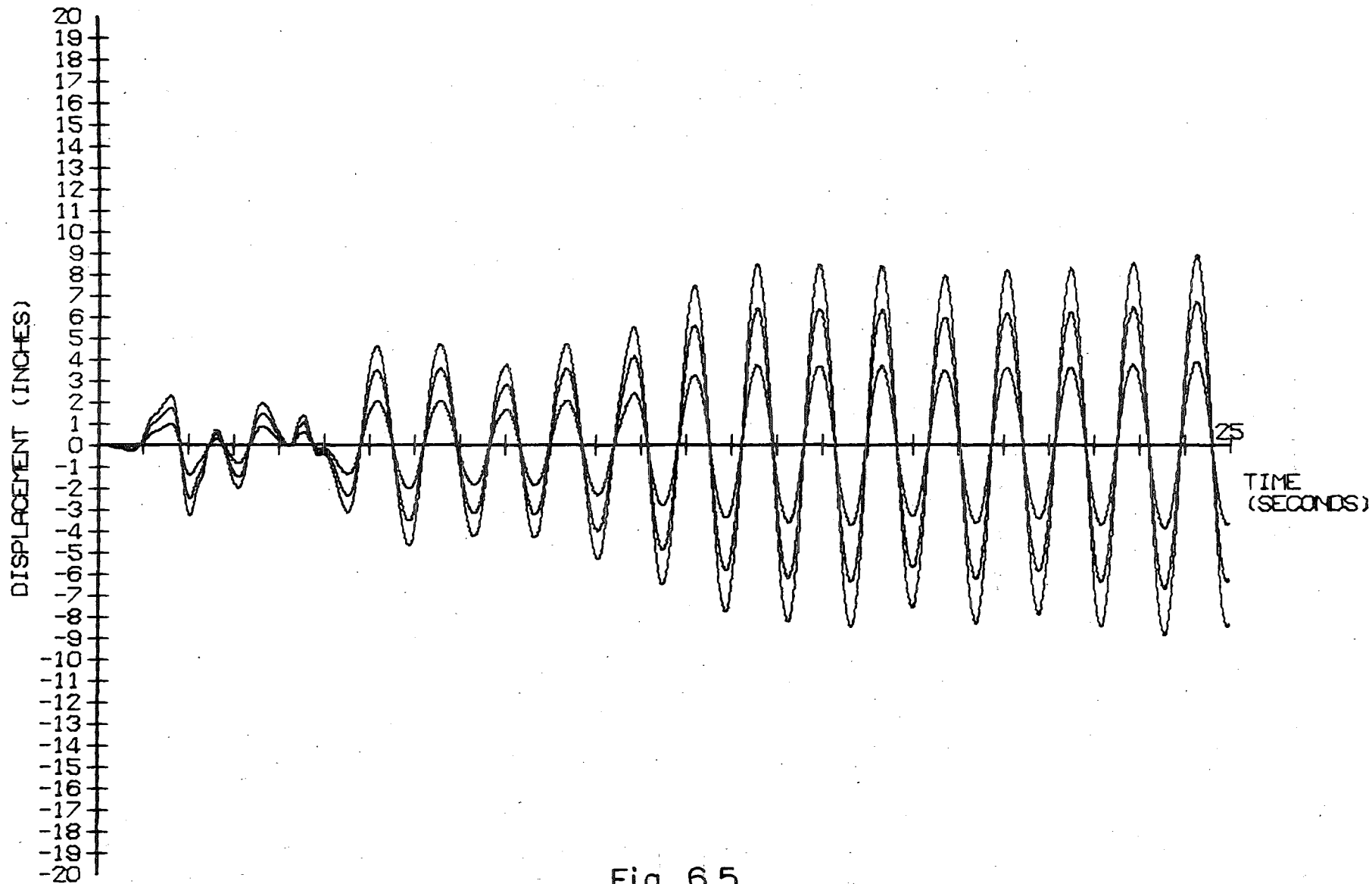


Fig. 6.5

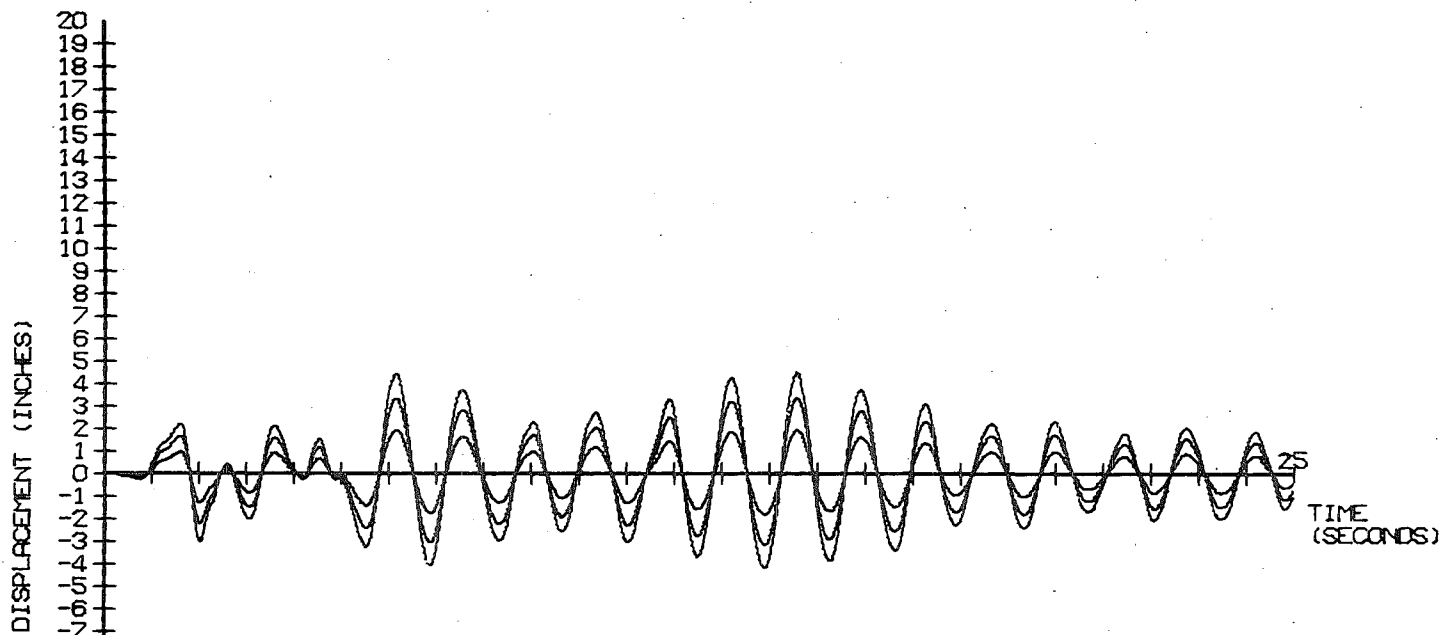


Fig. 6.6

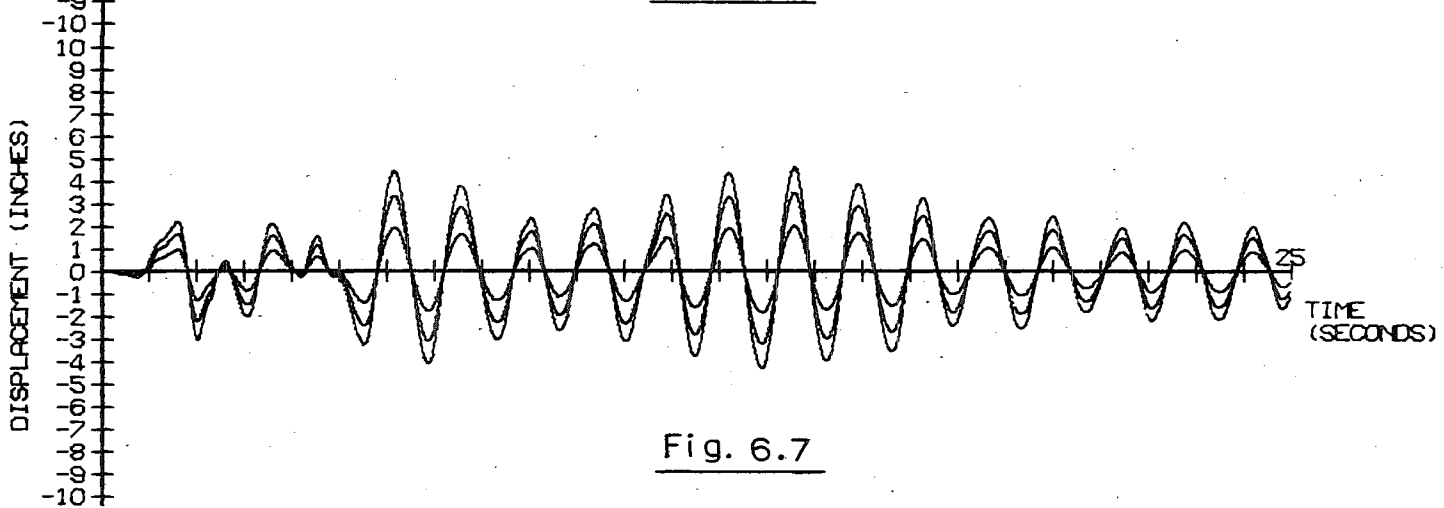


Fig. 6.7

A further analysis, similar to the previous one except that the 2% damping matrix was determined internally in the XBFRME program (and therefore based on the unbraced frame lateral stiffness matrix) after the damping coefficients had been read in, resulted in the displacement/time plot shown in Figure 6.7.

Maximum displacements in this case are:-

Mass 1 : 2.047 ins at 14.57 secs
 Mass 2 : 3.500 ins at 14.57 secs
 Mass 3 : 4.644 ins at 14.58 secs

The responses of Figures 6.5 and 6.6 were again confirmed by an independent ELRES analysis of the system.

The effect of sealing the El Centro accelerogram by 1.5 instead of 1.0 was examined by applying this excitation to the 2% damped extended elastic braced frame supporting a full tank (with no allowance for the convective action of the water) and the response shown in Figure 6.8 was obtained.

The maximum displacements are 50% greater than in the previous analysis viz:

Mass 1 : 3.07 ins at 14.57 secs
 Mass 2 : 5.25 ins at 14.57 secs
 Mass 3 : 6.96 ins at 14.58 secs

The 2% damped extended elastic response, to the El Centro N/S accelerogram factored by 1.0, of the Moran and Cheney braced frame supporting half a tank full of water acting as a solid mass, is shown in Figure 6.9. The maximum displacements are:-

Mass 1 : 2.744 ins at 4.418 secs
 Mass 2 : 4.686 ins at 4.418 secs
 Mass 3 : 6.198 ins at 4.418 secs

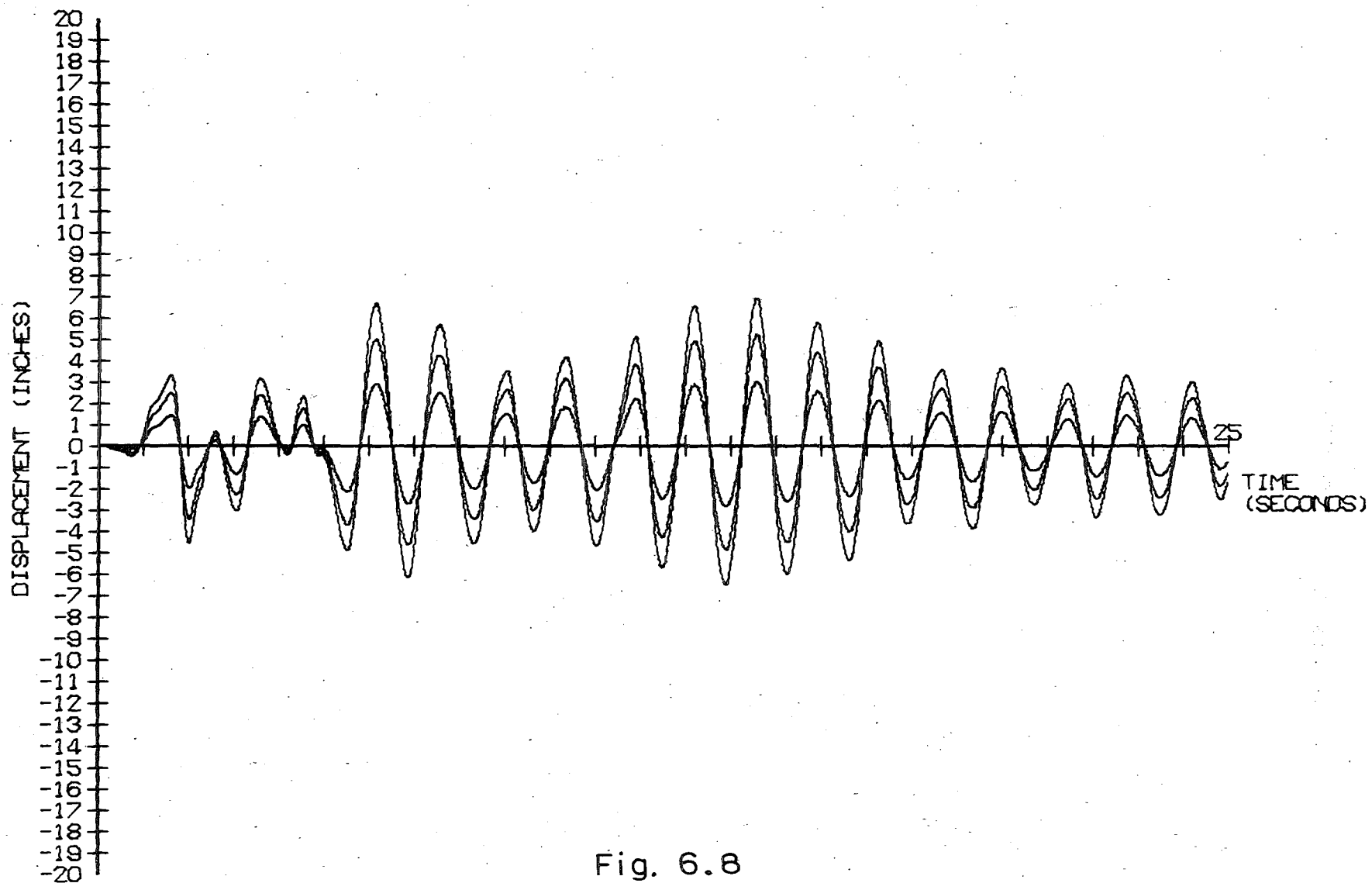


Fig. 6.8

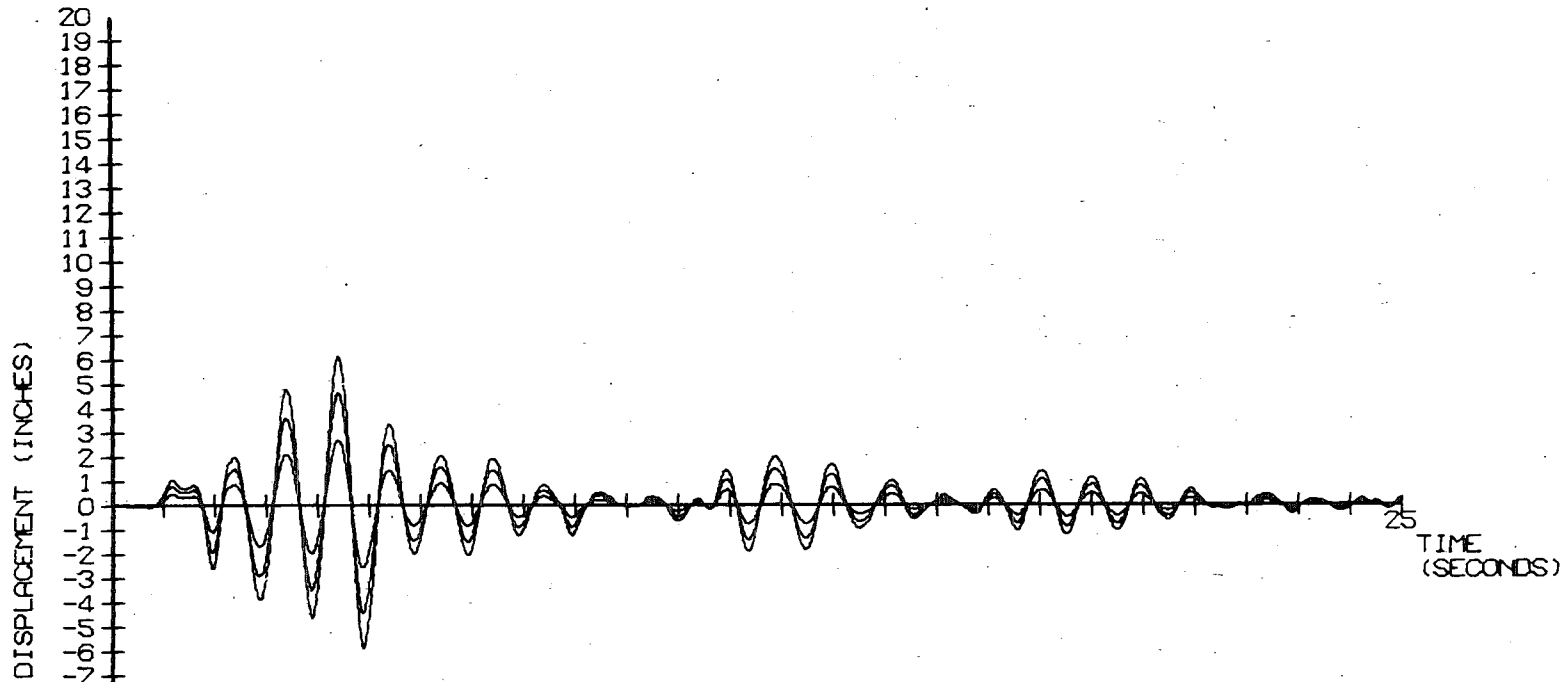


Fig. 6.9

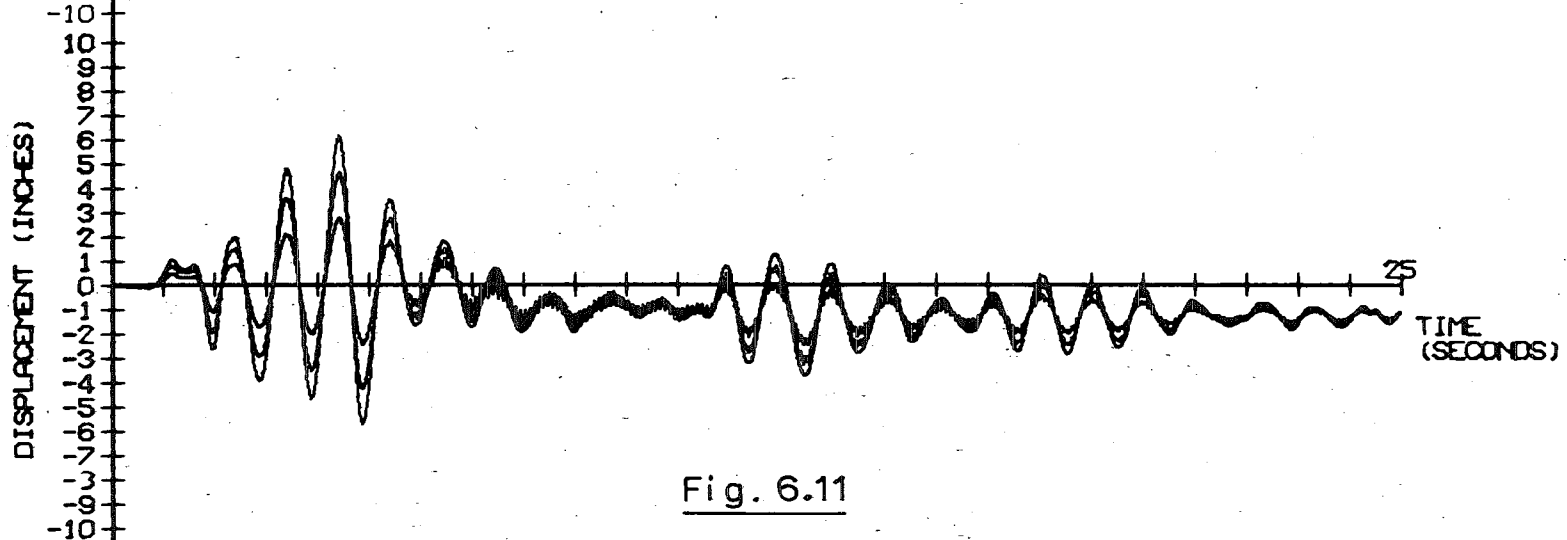


Fig. 6.11

The 2% damped response to the same excitation when the Moran and Cheney frame, having the mild steel bracing rods pretensioned to one quarter of their yield value and the previously established post yield axial stiffness incorporated, supports a full tank acting as a rigid mass is presented in Figure 6.10. The maximum displacements are:-

Mass 1 : 8.004 ins at 6.215 secs
 Mass 2 : 9.252 ins at 6.199 secs
 Mass 3 : 9.835 ins at 6.180 secs

and the total yield displacements suffered by the bottom bay braces are 6.058 ins and 4.931 ins respectively.

In Figure 6.11 the response of half a tank of water acting as a rigid mass in an otherwise similar system subject to the same excitation, is shown. The maximum displacements are:-

Mass 1 : 2.818 ins at 4.437 secs
 Mass 2 : 4.704 ins at 4.430 secs
 Mass 3 : 6.198 ins at 4.418 secs

Total yield displacements of 0.223 ins and 0.027 ins occur in the bottom bay braces.

VI.4 Digital Computer Analyses Including Convective Action of the Water

When the fluid in the elevated tank is represented by a two mass system, the incorporation of Step C (section V.7) is necessary in the analysis procedure. In the case of the tank used in this study the results of a MODANAL analysis, for various water depths, is presented in Table 4.

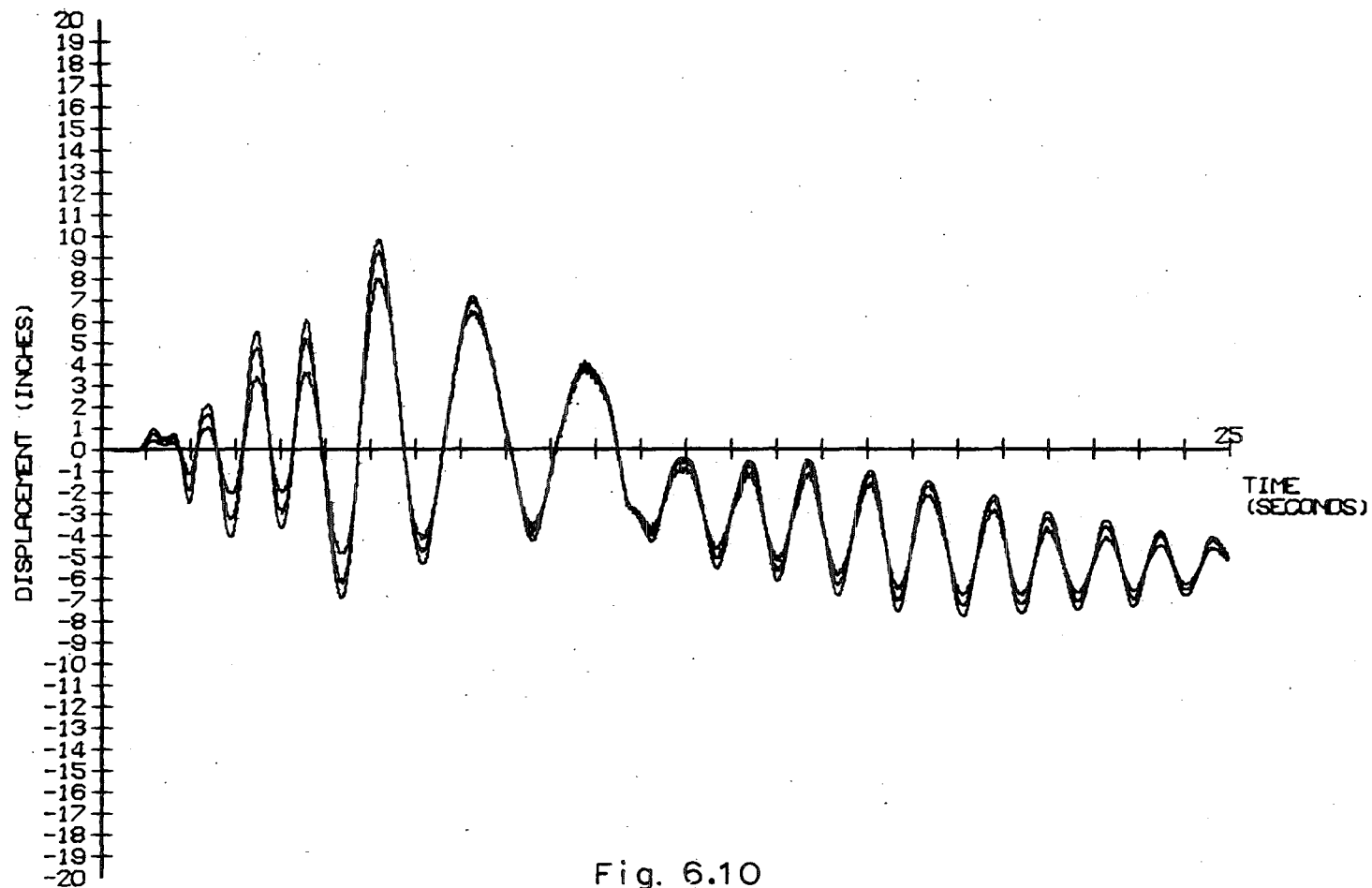


Fig. 6.10

Water Depth (ft)	m_{so} (lb.wt)	m_1 (lb.wt)	k_1 (lb.wt/ft)
18.0	640,000	246,000	36,310
13.5	256,000	238,000	33,530
9.0	250,000	210,000	25,810
4.5	145,000	134,000	10,600

Table 4

Using these results the equivalent four mass system (Figure 4.2) for each depth of water may be set up. The use of the '2D-Structure' program (Appendix IV) then enables a flexibility matrix for each system to be determined. For the full tank case this has the form

$$10^{-4} \times \begin{bmatrix} 5.773 & 7.731 & 7.480 & 7.971 \\ 7.731 & 12.219 & 12.472 & 13.301 \\ 7.480 & 12.472 & 13.957 & 14.913 \\ 7.971 & 13.301 & 14.913 & 58.433 \end{bmatrix}$$

Use of the matrix inversion program (LIST LP3, Appendix IV) enables the corresponding lateral stiffness matrix to be calculated, viz:-

$$10^4 \times \begin{bmatrix} 1.34 & -1.31 & 0.451 & -0.0001 \\ -1.31 & 2.21 & 1.27 & 0.0006 \\ 0.444 & -1.27 & 0.99 & -0.026 \\ 0.0056 & -0.0049 & -0.023 & 0.024 \end{bmatrix}$$

and subsequently the normal mode analysis (LIST LP2) and damping matrix formation (LIST LP 2A) programs may be used to determine the damping coefficients corresponding to 2% critical damping required as input for the XBFRME program

viz: CG = 0.03851

and CR = 0.01023 for the full tank case.

Similar necessary input data can be prepared for other depths of water in the tank to enable the XBFRME program to be used to determine the seismic response of alternative four mass systems.

The 2% damped response of Moran and Cheney's tower, acting in the extended elastic range and supporting a full tank of water free to act convectively, to the El Centro digitised accelerogram factored by 1.0 is shown in Figure 6.12. The maximum displacement values are:-

	Figure 6.12	whereas in	Figure 6.7
Mass 1 :	3.776 ins at 17.91 secs		2.047 ins at 14.57 secs
Mass 2 :	6.458 ins at 17.91 secs		3.500 ins at 14.57 secs
Mass 3 :	8.561 ins at 17.91 secs		4.644 ins at 14.58 secs

the displacements of Figure 6.7 being those of an identical structural system but with no allowance for the convective action of the water (i.e. a three mass model instead of the four mass one). The half full tank response, in an otherwise identical analysis is shown in Figure 6.13. The maximum displacements are:-

Mass 1 :	2.441 ins at 13.65 secs
Mass 2 :	4.161 ins at 13.65 secs
Mass 3 :	5.477 ins at 13.66 secs

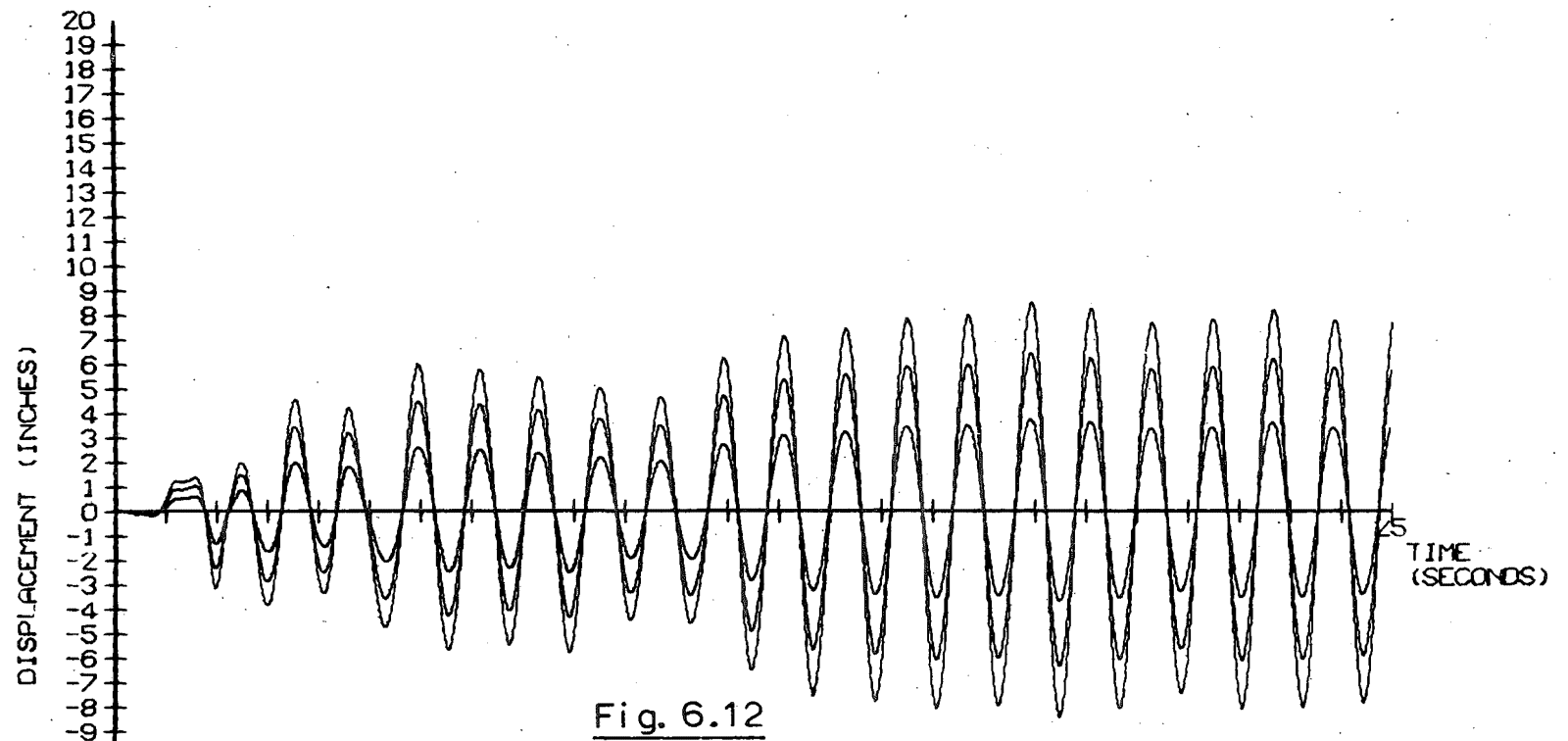


Fig. 6.12

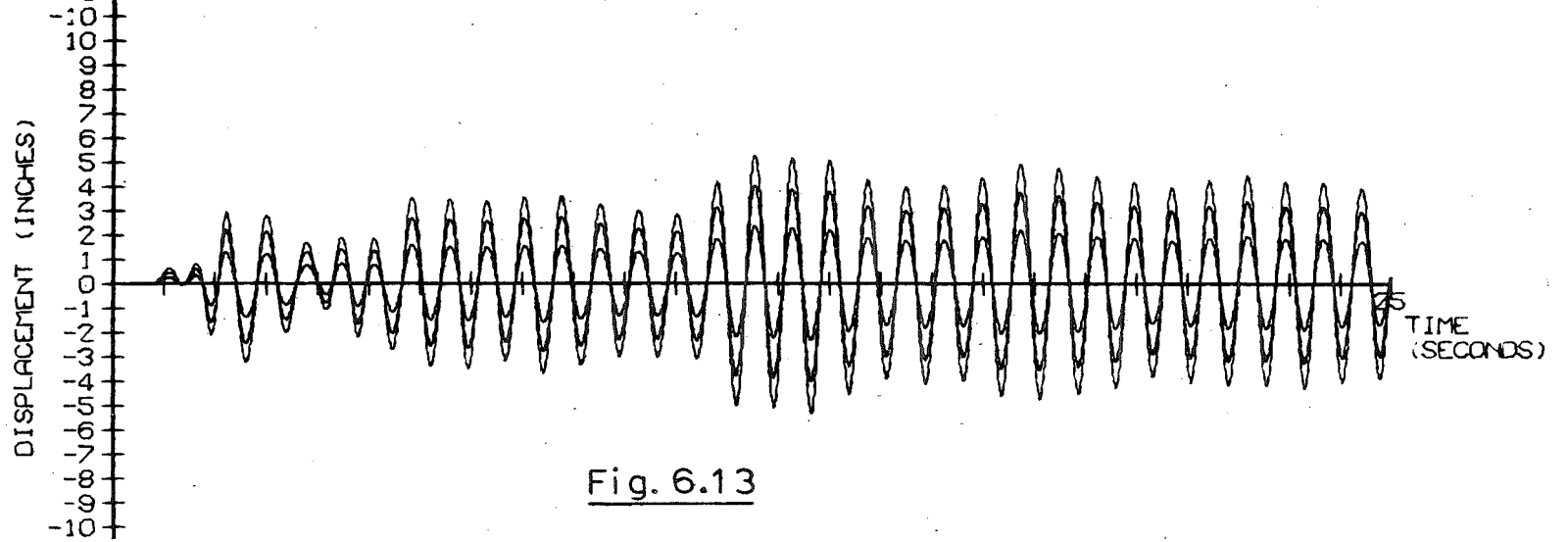


Fig. 6.13

When the full water tank is represented by a two mass system, and the Moran and Cheney braced tower has the mild steel bracing rods prestressed to one quarter of their yield level and their post yield axial stiffnesses set at the values determined earlier using the TRUEFORCE program, the 2% damped responses to the El Centro accelerogram, factored by 1.0 and 0.6 respectively, are shown in Figures 6.14 and 6.15. The maximum displacements are:-

Figure 6.14

Figure 6.15

Mass 1 :	5.042 ins at 4.422 secs	and	3.508 ins at 7.254 secs
Mass 2 :	6.549 ins at 4.414 secs		4.510 ins at 7.250 secs
Mass 3 :	7.729 ins at 4.398 secs		5.169 ins at 7.230 secs

The total yield displacements suffered by the bottom bay braces are 3.096 ins and 2.697 ins in the first case and 1.562 ins and 1.200 ins in the second one.

In Figure 6.16 the 2% damped convective response of a full water tank system to a similar excitation, when the Moran and Cheney braced tower has no prestress in the diagonal members, is presented. The maximum displacements are:-

Mass 1 :	6.600 ins at 14.52 secs
Mass 2 :	8.243 ins at 14.52 secs
Mass 3 :	9.425 ins at 14.53 secs

and total yield displacement of 4.005 ins and 1.433 ins are experienced by the bottom bay braces.

In Figures 6.17 and 6.18 the responses are shown of systems in which the structural bracing has been selected to exhibit multiphase characteristics, including fracturing of high tensile steel members. In both cases the bracing was similar to that of the Moran and Cheney frame, but prestress forces equal to one quarter of the yield loads

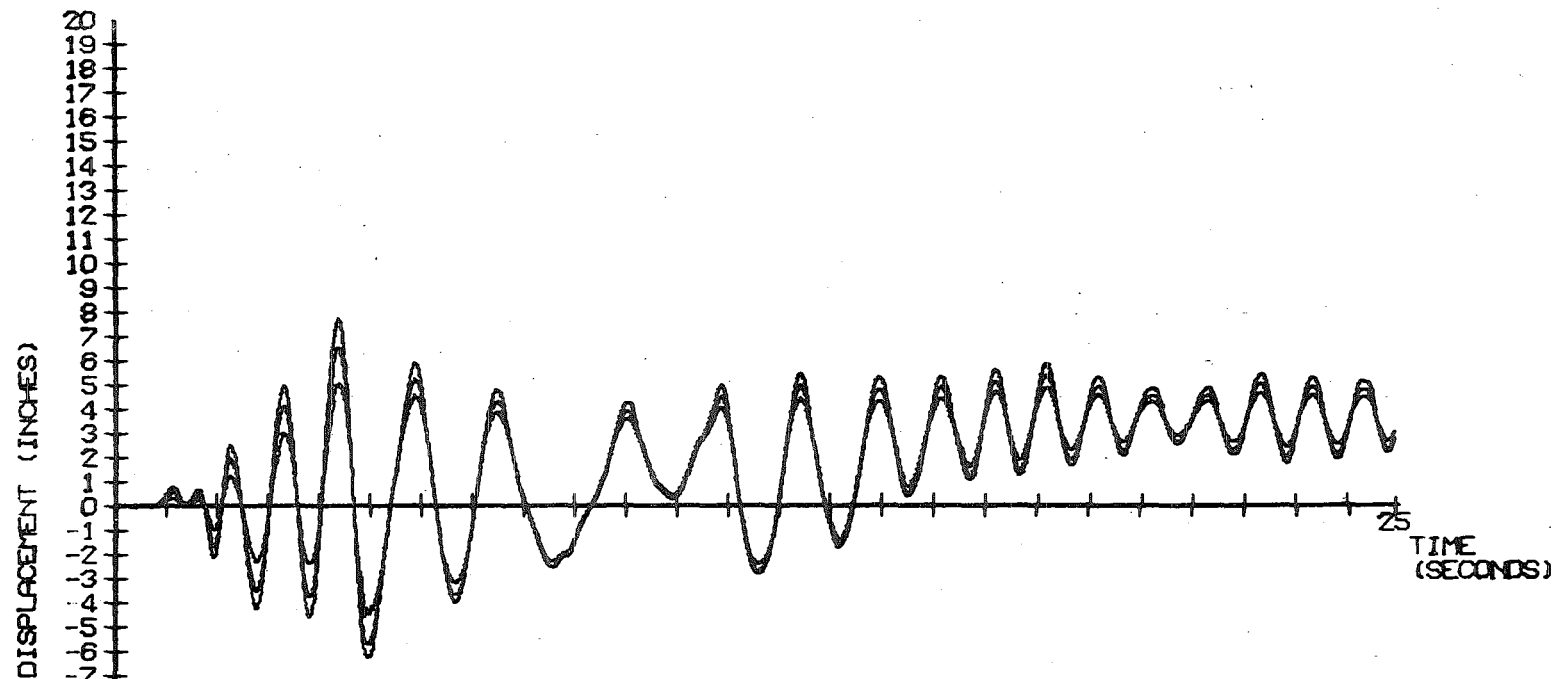


Fig. 6.14

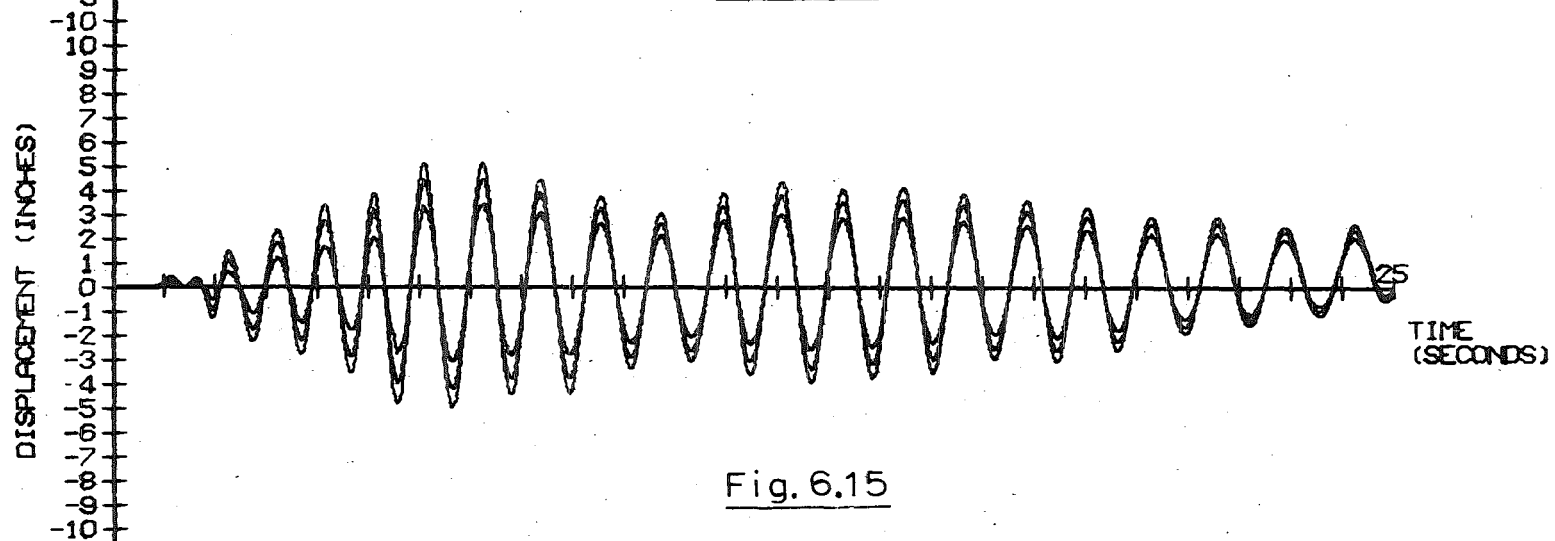


Fig. 6.15

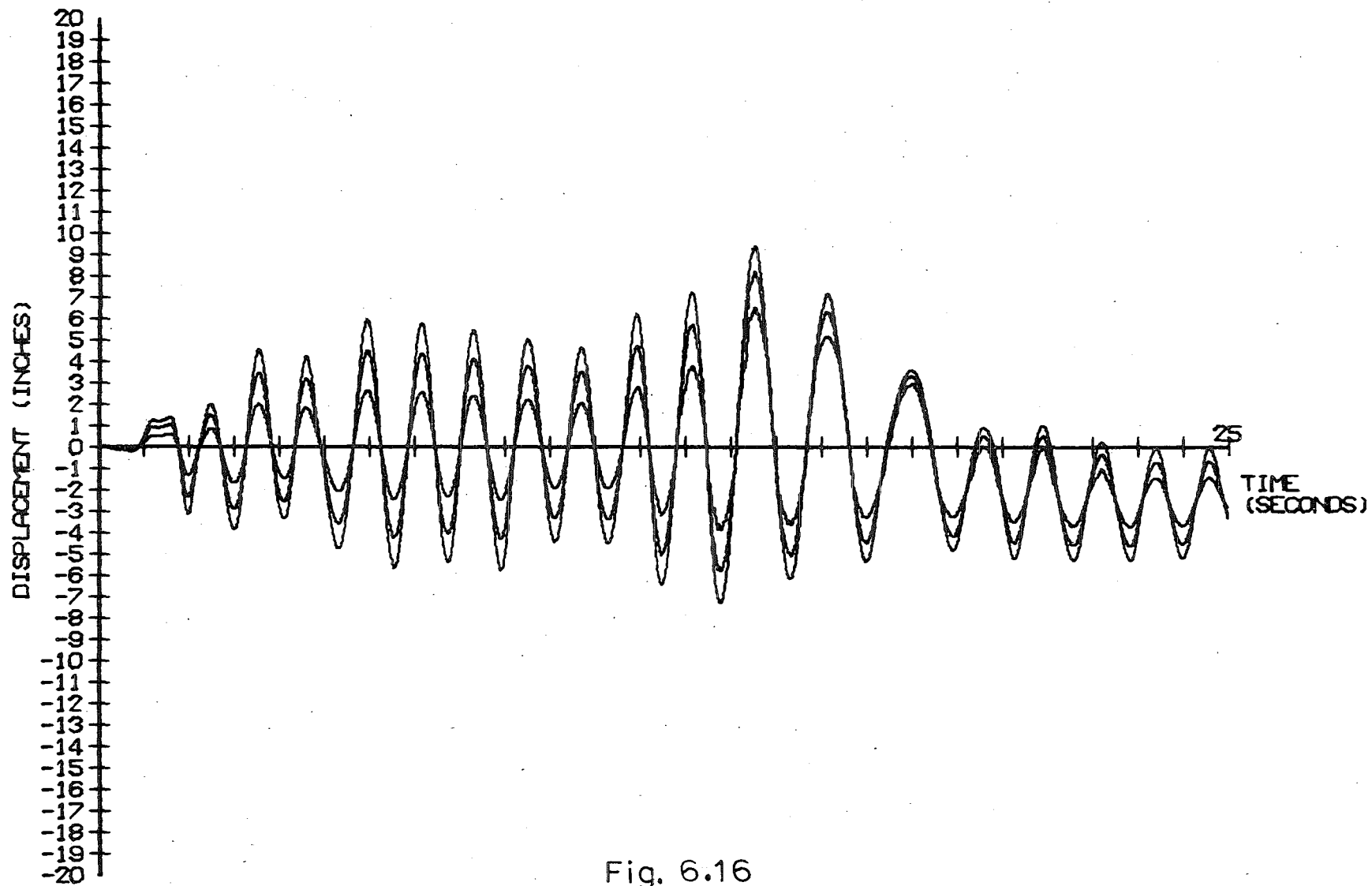


Fig. 6.16

were incorporated. However, the bottom bay bracing was considered to be composed of the equivalent of 2 in² high tensile steel and 2.82 in² mild steel diagonals instead of the original total of 4.82 in² of mild steel bracing. As the high tensile steel fractured at about three seconds after the commencement of the accelerogram the effect was to produce a flexible lower bay for the remainder of the response. Figures 6.17 presents the displacement/time history for the full tank case and that of the half full tank case is shown in Figure 6.18. In both cases convective action of the water is taken into account. The maximum displacements are:-

Figure 6.17

Figure 6.18

Mass 1 :	7.438 ins at 22.89 secs	and	7.791 ins at 15.14 secs
Mass 2 :	7.753 ins at 22.88 secs		8.115 ins at 15.14 secs
Mass 3 :	7.954 ins at 20.29 secs		8.311 ins at 15.16 secs

Total yield displacements in the bottom bay braces were calculated to be 4.475 ins and 5.500 ins in the first case and 5.853 ins and 2.565 ins in the second one.

When half the Moran and Cheney (prestressed) mild steel bracing was combined, in parallel, with selected high tensile steel bracing in the basic frame the 2% damped responses of the system, allowing for a full tank of water which acts convectively, to the El Centro accelerogram are presented in Figures 6.19, 6.20, 6.21 and 6.22.

The system responding as shown in Figure 6.19 has the equivalent of two 0.25 in. diameter high tensile steel rods in each bay, pre-stressed to one quarter of their ultimate strength, whereas the system corresponding to the response shown in Figure 6.20 has 0.5 in. diameter high tensile steel rods in place of the 0.25 in. diameter

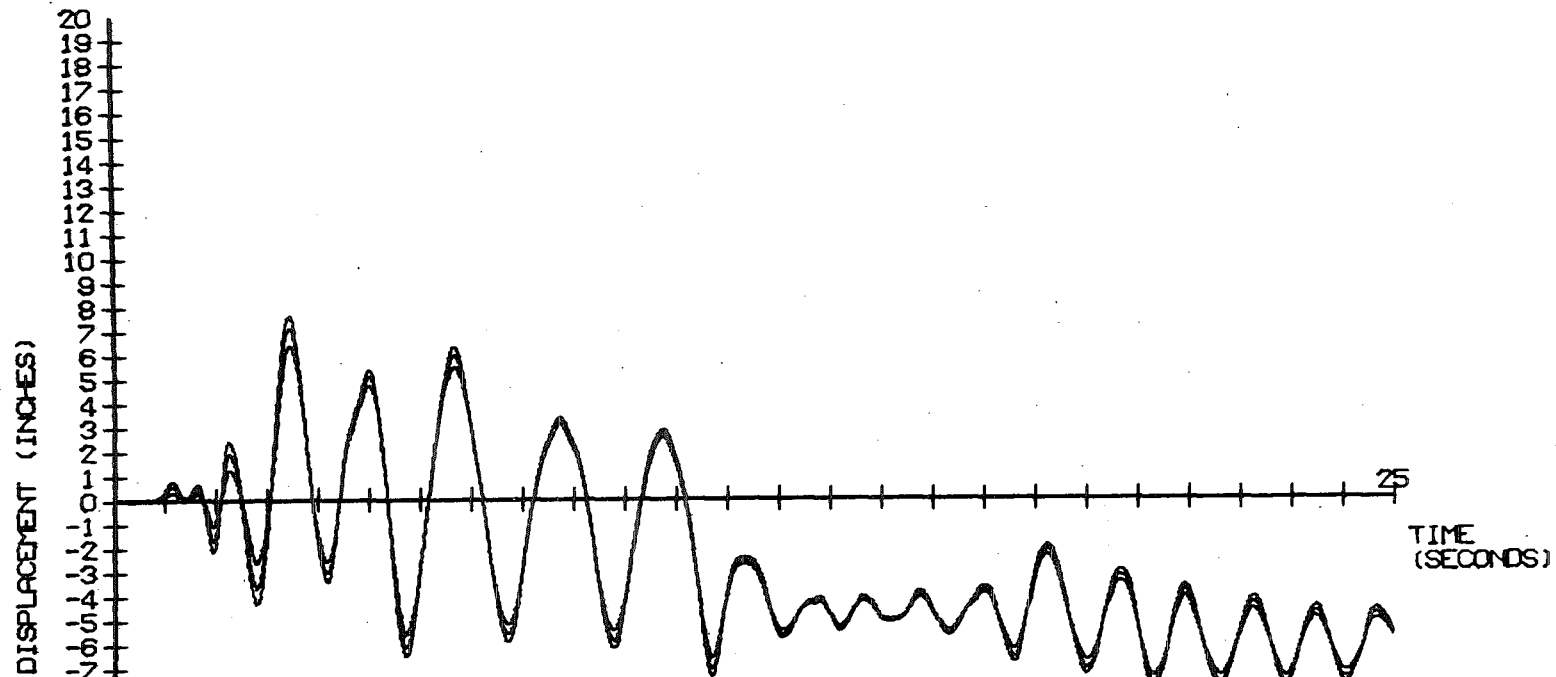


Fig. 6.17

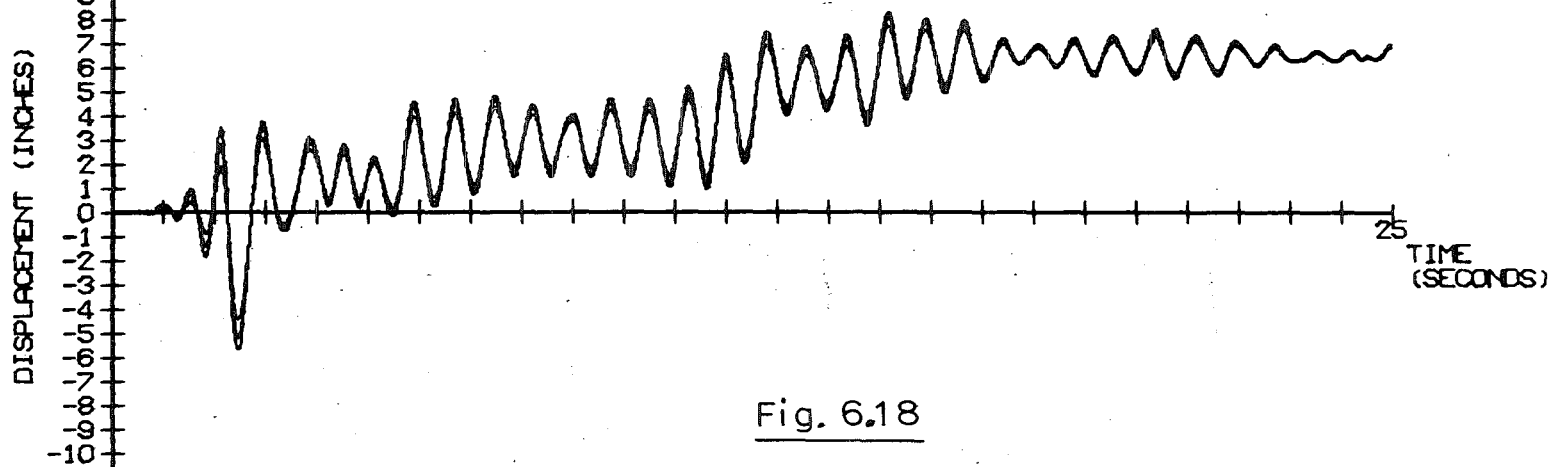


Fig. 6.18

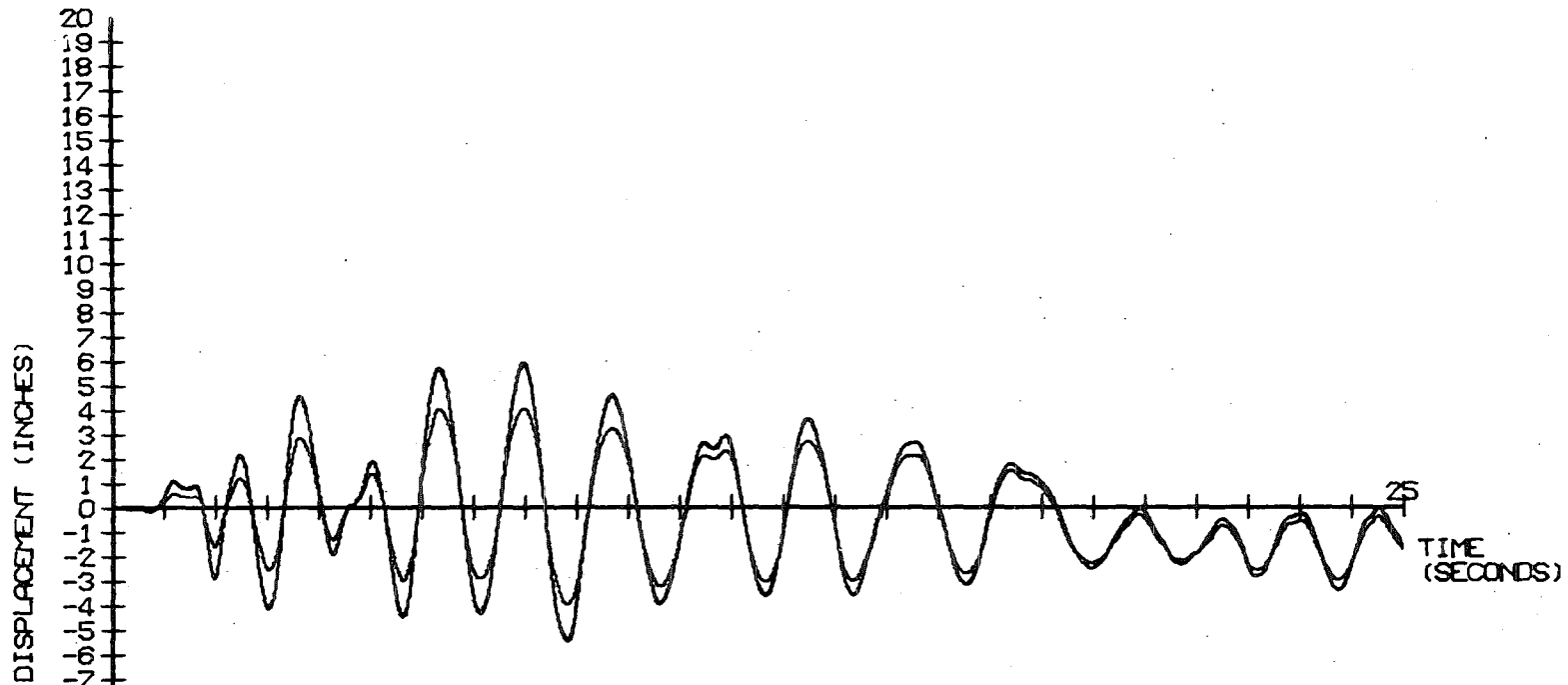


Fig. 6.19

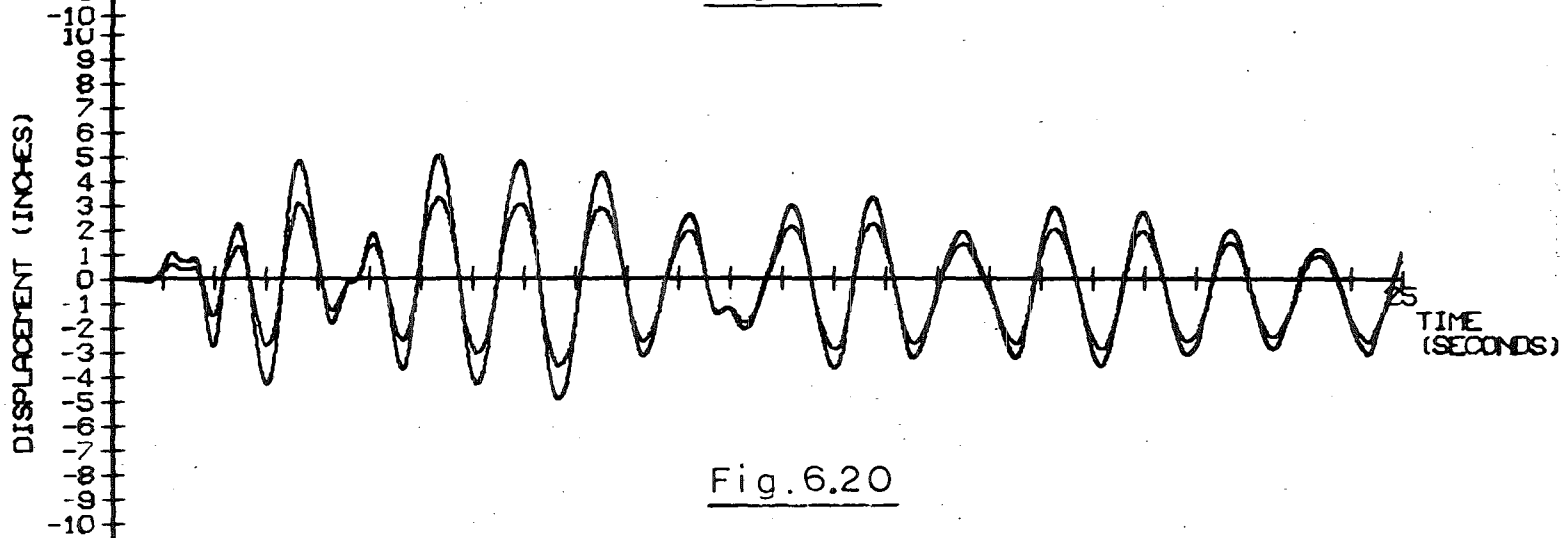


Fig. 6.20

ones. The maximum displacements are:-

Figure 6.19

Mass 1 : 4.070 ins at 7.977 secs
 Mass 2 : 5.875 ins at 7.988 secs
 Mass 3 : 5.964 ins at 7.988 secs

Figure 6.20

and 3.650 ins at 8.664 secs
 5.022 ins at 6.344 secs
 5.102 ins at 6.340 secs

with bottom bay bracing yield extensions of 2.127 in. and 2.072 in. respectively in the first case and 1.413 in. and 1.706 in. in the second one.

The responses of two similar systems but with 0.75 in. diameter and 1.0 in. diameter high tensile steel rods respectively replacing the 0.5 in. diameter ones of the last system are presented in Figures 6.21 and 6.22. The maximum displacements are:-

Figure 6.21

Mass 1 : 3.759 ins at 3.684 secs
 Mass 2 : 5.193 ins at 3.672 secs
 Mass 3 : 5.265 ins at 3.672 secs

Figure 6.22

and 4.969 ins at 24.61 secs
 5.645 ins at 13.39 secs
 5.714 ins at 13.39 secs

with bottom bay bracing yield extensions of 1.816 in. and 1.214 in. in the first case and 3.026 in. and 1.899 in. in the second one.

In all of the last four systems at least two of the high tensile steel rods fractured during the response.

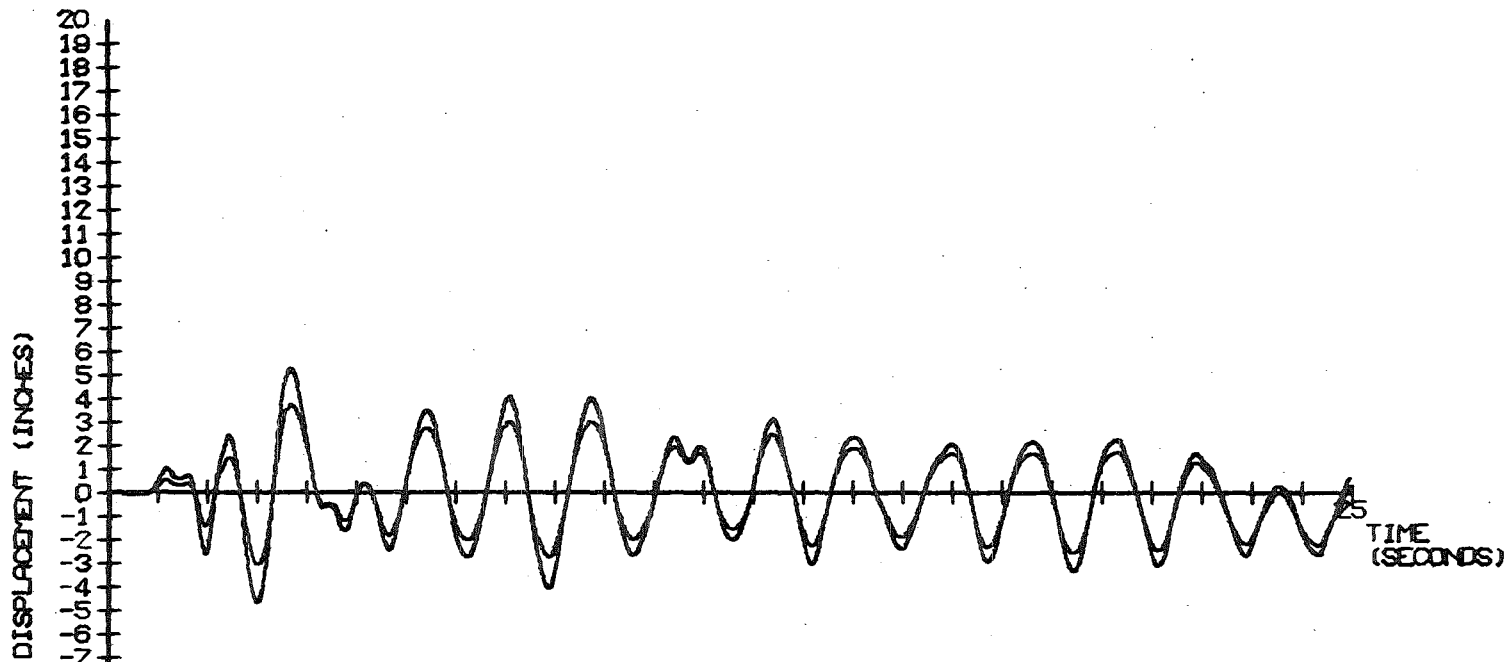


Fig. 6.21

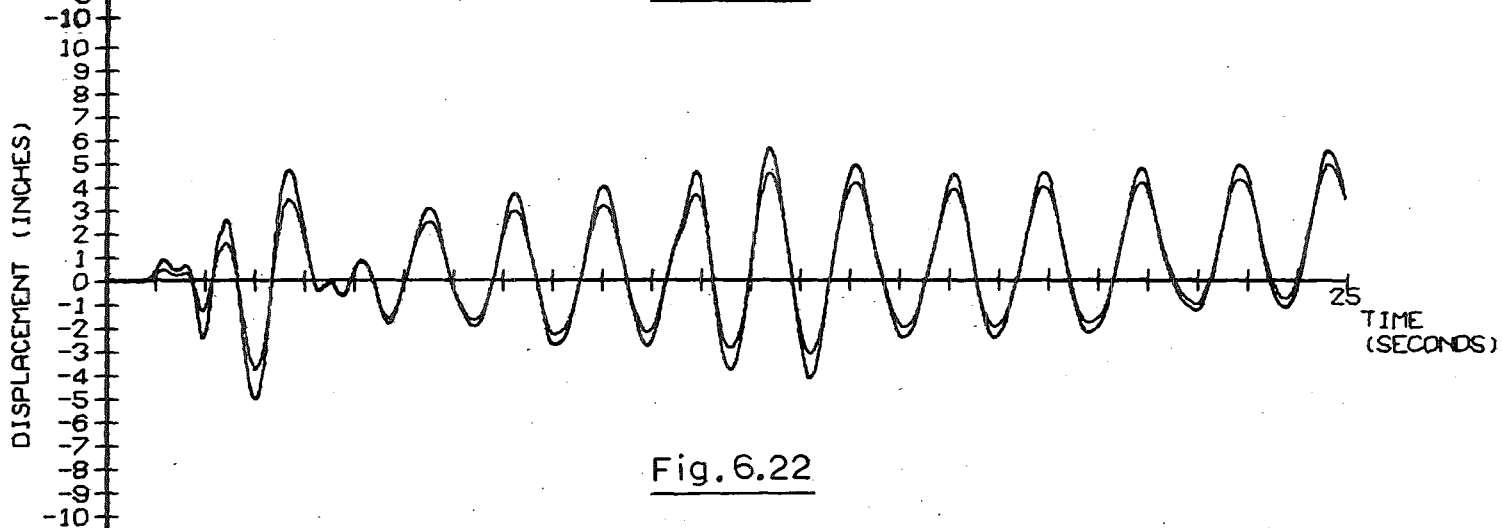


Fig. 6.22

C H A P T E R S E V E N

REVIEW OF ANALYSES UNDERTAKEN AND COMMENTS ON
APPLICABILITY OF THE PROPOSED ANALYSIS METHODVII.1 Review of the Analyses Described in Chapter Six

The undamped extended elastic response shown in Figure 6.3 of an empty tank on the unbraced Moran and Cheney frame, to the El Centro N/S accelerogram, is itself of limited interest apart from serving as a confirmation of the correct functioning of the integration process in the XBFRME program by virtue of the response being identical to that derived using the ELRES program. Some evidence of beating of the first and second masses is evident in the plot. However when Figure 6.4 is compared with Figure 6.3 the effect of the inclusion of 2% of critical viscous damping in the response calculation is apparent. Since it would be unrealistic to take no account of damping in seismic response calculations, some small allowance is normally included and on the basis of previous tests⁽²¹⁾ and of the result presented in Chapter Two, 2% appears to be a reasonable figure to use for the elevated water tower type of structure. Independent determination of the displacement/time response using the ELRES program confirmed that the damping section of XBFRME functions correctly.

The extended elastic responses to the same excitation of a full tank (with no allowance for the convective action of the

contents) on a Moran and Cheney frame braced as in the original structure⁽²¹⁾ are presented in Figure 6.5 for the undamped situation and in Figure 6.6 for the 2% damping case. The necessity to include some damping if the prototype system is to be accurately modelled is even more evident as a result of this comparison. The continued build-up of displacements with time beyond 20 seconds in the undamped case does not correlate with the recorded motion of structures in earthquakes whereas the plot in Figure 6.6 does represent the observed movements more reasonably. However a problem does arise in the formation of the damping matrix referred to in Chapter Four (equation 4(7)) when the stiffness of the system is not constant throughout the response calculation. The results presented in Figure 6.6 were calculated using a damping matrix formed with equation 4(7), the total initial frame stiffness (i.e. including the bracing contribution) being used as the term $[K]$. The damping matrix was overwritten into the program XBFRME for this particular analysis whereas in its normal operation the program XBFRME calculates the damping matrix on the basis of the unbraced frame stiffness. When the normal procedure was followed, that is the 2% damping matrix was assembled by the XBFRME provision based on FK rather than TK in the notation of the program - the response plot shown in Figure 6.7 was obtained. The top mass displacement is 3% greater in the second case and this reflects the effectively lower damping allowance made. The true response of a system having its stiffness varying between the TK and FK values will lie somewhere between the plots of Figure 6.6 and 6.7. Provision to calculate the damping matrix at each change of stiffness could have been

incorporated in the XBFRME program but in view of the small differences in response which were determined in the checks on the two extreme cases this provision was considered to be unnecessary. In fact all subsequent analyses were carried out using the XBFRME damping matrix determination based on the unbraced frame stiffness.

In Figure 6.8 the displacement/time plot is shown of an identical system to that having the response presented in Figure 6.7, but on this occasion the exciting accelerogram was factored by 1.5. The plot confirms that the factoring of the amplitude of the excitation merely affects the displacement of the response of the elastic system in a linear manner.

The response of an identical structural system supporting half a tank full of water (with no allowance for convective action) instead of a full tank is shown in Figure 6.9. The accelerogram was factored by 1.0 to produce this plot and so the response is directly comparable with that of Figure 6.7, the full tank case. The larger, and earlier, response of the lighter system to the particular excitation used is evident from a comparison between these figures.

The first multiphase response plot is that presented in Figure 6.10, being the 2% damped response to the El Centro N/S accelerogram of a full tank (with no allowance for convective water action) supported on a Moran and Cheney frame having the original mild steel bracing prestressed to one quarter of the yield level and having the post yield axial stiffness of the braces set at the values determined using the TRUEFORCE program (Chapter Three), assuming that the material

exhibits similar properties to the mild steel of the rods used in the tests described in Chapter Three. The plot is limited to 25 seconds from the commencement of the excitation, but it is evident that this does include the maximum amplitude. From the typed output of the XBFRME program it may be determined that substantial yielding in the bottom bay braces occurs in the 3 to 6 seconds section of the response and that the motion in the subsequent 5 seconds is essentially that of a frame unbraced in the bottom bay - with consequent lengthened period - whereas from about twelve seconds onwards the response corresponds to that of a frame cross-braced elastically in the upper bays but with one elastic brace active for part of the time in the bottom bay. The bracing extensions in the post elastic range correspond to ductility requirements of 5.7 and 4.6 respectively (where ductility is defined as the ratio of the total displacement to the yield displacement). Values of this magnitude can be achieved readily by mild steel components in tension. The loading state of the frame when the bottom mass displacements are of the order of 8 ins can conveniently be determined using the '2-D STRUCTURE' program (Appendix IV, L.P.1) and confirmation that the residual members in the bottom bay are still within the elastic range may be obtained. Based on a yield stress of 19.4 T/in^2 (Appendix III) the combined bending and axial stresses in the bottom columns (the critical members) will not exceed the elastic range until a lateral displacement of the bottom mass of 10.2 inches is reached.

Although the displacement/time plot of Figure 6.10 and other subsequent figures indicate that some shift of the zero amplitude

point of the elastic vibrations occurs towards the end of the plot, it does not follow that the water tank has developed a permanent set to one side. Providing that the stresses in the columns and horizontal struts do not exceed the elastic limits, the residual elastic system will ensure that the structure resumes its original position when the effects of the seismic disturbance have decayed away. An exception to this behaviour would occur if the initial balance between the prestressed members in any one bay is disturbed during the shaking so that the residual prestressing loads do not counterbalance each other. In such circumstances some permanent sway displacement would be expected after the movements resulting from the earthquake excitation have ceased.

The multiphase response of a half full tank (without any allowance for the convective action of the water) in similar conditions to the situation giving the results presented in Figure 6.9, is shown in Figure 6.11. Since the system barely exceeds the elastic range (confirmed by the very small calculated yield displacements) the maximum mass displacements are very similar in magnitude and time of occurrence to those determined for the extended elastic case (Figure 6.9).

In Figures 6.12 and 6.13 the full and half full tank extended elastic 2% damped responses - allowing for convective water action - of the elevated Moran and Cheney water tower, braced with rods of the sizes used in the original structure with no prestress and excited by the El Centro N/S accelerogram, are shown. The comparisons between the extended elastic displacements determined both neglecting

the convective action and including it, are summarised in Table 5.

Water State	Tank Full or Half full	Max. Tower Top Displacement (ins)	Time at Maximum Displacement (secs)
STATIC	1.0	4.644	14.58
STATIC	0.5	6.198	4.42
CONVECTIVE	1.0	8.561	17.91
CONVECTIVE	0.5	5.477	13.66

Table 5.

The full tank comparison emphasizes the possible amplification of the response which the shaking of the liquid may cause and supports the requirement⁽⁷⁾ of a substantially increased seismic design coefficient for elevated fluid containers relative to the basic value specified for normal building structures.

Since the hypothetical extended elastic bracing invoked in the computations leading to the plots of Figures 6.5, 6.6, 6.7, 6.8, 6.9, 6.12, and 6.13 cannot, in fact, be achieved by typical mild steel braces of the dimensions specified, the actual displacement/time history of the Moran and Cheney frame - having prestressed braces and supporting a full water tank acting convectively - is of the form presented in Figure 6.14 in which the system responds in much the same manner as that described above when commenting on plot 6.10, namely it passes through a phase of acting as if there is no

effective bracing in the bottom bay between 6 seconds and 12 seconds, followed by a pattern of behaviour consistent with only one brace being active intermittently in the bottom bay. The ductility requirements of 2.9 and 2.5 are lower than those necessary for the non-convective water case and are well within the range available from typical mild steel elements.

The response of an identical system to the El Centro record factored by 0.60, serves to confirm that whereas in the extended elastic cases factoring of the excitation produces a direct linear variation in the responses (Figures 6.7 and 6.8) this relationship is not valid for the yielding systems. An increase from 0.60 to 1.0 in the excitation accelerogram amplitude only increases the displacement response amplitudes by about 30% at the critical lower mass level.

The introduction of bracing prestress in the earlier analyses was made in recognition of the fact that many tank structures do have the cross bracing pretensioned to ensure that it is effective in contributing to the lateral stiffness, in fact doubling it at low amplitudes of vibration until the prestress is cancelled by the effect of the lateral displacement. The extreme sensitivity of the system to the presence of pretension in the bracing is clearly indicated by a comparison of Figure 6.14 with Figure 6.16, which corresponds to the identical situation to that used to produce 6.14 except that no prestress was introduced into the braces. The absence of prestress results in the initially more flexible system taking longer to build up its maximum response (14.53 seconds instead

of 4.398 seconds) and the plot follows the extended elastic pattern of Figure 6.12 for the first 13 seconds after which, during the following 6 or 7 seconds, the effectively unbraced bottom bay breaks up the regular form of oscillation and brings about a substantial reduction in the vibrational amplitude in the later part of the plot. In this phase the bottom bay once more responds as a partially braced panel for some of the time. The bottom bay bracing ductility requirements are actually higher in the pretensioned case, having values of 3.8 and 1.4 in the system corresponding to the plot of Figure 6.16.

When a deliberate attempt is made to promote the development of multiphase response with the consequent break-up of the regular oscillatory pattern of the seismically excited structural system, plots of the form of those shown in Figures 6.17 and 6.18 may be obtained. In these the El Centro N/S accelerogram is used as the excitation applied to a Moran and Cheney frame with original (but prestressed) bracing in the top two bays and with modified prestressed bracing in the bottom bay. Cross bracing with each member having the equivalent of 2 ins^2 of high tensile steel in parallel with 2.82 ins^2 of mild steel is included in the bottom bay so that the total bracing steel area is equivalent to that originally provided. The 2% damped response of a full tank is shown in Figure 6.17 and that of a half full tank in Figure 6.18, in both cases provision for the convective action of the water is made. For each tank condition typed output from the XBFRME program confirms that the yielding of the mild steel and early fracturing of the sacrificial high tensile steel occurs within the first 3 seconds and the irregular pattern of the subsequent

response may be followed conveniently from the figures. The maximum ductilities of 4.7 and 5.5 can be readily provided by mild steel braces of the configuration envisaged and the maximum frame displacements are within the elastic range so that no yielding of the column or strut members would be expected to occur as a result of the seismic loading.

The analyses leading to the displacement/time plots presented in Figures 6.19, 6.20, 6.21 and 6.22 were undertaken to indicate the type of optimisation of the choice of bracing which may be undertaken using the XBFRME program. On the assumption that the design condition is selected as being the response to the El Centro N/S accelerogram of a full tank system (allowing for the convective action of the water) and that owing to the necessity to resist wind and other service loads satisfactorily, an initial value of lateral stiffness close to that provided by the Moran and Cheney frame with the original unstressed bracing is required, several combinations of mild steel and high tensile steel braces were investigated. The multiphase responses presented in Figures 6.19, 6.20, 6.21 and 6.22 all involve the progressive yielding or fracturing of sacrificial prestressed braces. In each case the bottom bay mild steel braces yield and the corresponding high tensile steel braces fracture and in the cases corresponding to Figures 6.19, 6.20 and 6.21 the middle bay high tensile steel breaks also. Of the particular systems checked that corresponding to Figure 6.20 has both the smallest lateral displacement response and minimum ductility requirement and so could be selected in preference to the others. This example comprises a very

limited use of the bracing selection procedure made possible by the use of the XBFRME program but should be sufficient to illustrate the range of possible application.

VII.2 Considerations of Dissipated Energy as a Proportion of the Total Seismic Input Energy

Housner has suggested⁽²⁴⁾ that the maximum energy E attained by an oscillator subject to seismic excitation may be estimated using the expression

$$E = \frac{1}{2} m S_{v,n}^2$$

where m is the mass of the oscillator and $S_{v,n}$ is the velocity spectrum ordinate for damping n , assuming the velocity spectrum to consist of a straight horizontal line.

For the El Centro N/S component, at 2% critical damping $S_{v,0.02}$ may be taken to be equal to 2.05 ft/second⁽²⁴⁾ and hence the total energy input to the Moran and Cheney frame, supporting a full tank of water, resulting from this excitation will be approximately equal to

$$\frac{1}{2} \frac{952,600}{32.2} (2.05)^2 = 62,000 \text{ ft.lbs}$$

If this energy was entirely in the form of strain energy, the stress state in the members of the frame would correspond to a lateral load of

$$\frac{2\pi}{T} \cdot S_{v,n} = \frac{2\pi}{1.4} \cdot \frac{2.05}{32.2} \cdot g = 0.28g$$

where T , the period of oscillation, is taken as 1.4 second.

Moran and Cheney's estimate of 0.20g loading corresponding to the elastic limit of the frame would involve an elastic strain energy

in the structure of

$$\left(\frac{20}{28}\right)^2 64,000 = 33,000 \text{ ft.lbs}$$

If a total energy input of 64,000 ft.lbs is to be absorbed, then that portion dissipated in plastic deformation may be estimated to be

$$62,000 - 33,000 = \underline{29,000} \text{ ft.lbs}$$

In the system giving rise to the displacement/time response shown in Figure 6.10, bottom bay bracing yields of 6.058 ins and 4.931 ins were calculated. The dissipated work corresponding to these plastic distortions may be calculated viz.-

$$\begin{aligned} \frac{1}{2} \times \frac{11,000}{12} \times 6.058^2 &= 16,700 \\ \frac{1}{2} \times \frac{11,000}{12} \times 4.931^2 &= \underline{11,100} \\ &\underline{27,800 \text{ ft.lb}} \end{aligned}$$

Allowing for the assumptions made by Housner, (which tend to over-estimate the plastic energy absorption requirement) and the replacement of the actual post yield axial stiffness curve of the bracing rods by a straight line (Figure 6.2) for the purpose of establishing a value for use in the XBFRME program (which procedure underestimates the plastic energy dissipation for small yield displacements) the correlation between the 29,000 ft.lbs and 27,800 ft.lbs is satisfactory.

In the case of allowance for convective water action being made - in the system having the response presented in Figure 6.14 - the dissipated work corresponding to the plastic displacements of 3.096 ins and 2.697 ins is only 7,700 ft.lb and the correlation

between the estimate of the requirement based on Housner's method and the value computed from the XBFRME results is much less close. However this result is consistent with the assumptions used in the Housner and XBFRME approaches.

If only that part of the water mass which moves with the tower is included in the total energy input calculation, the value becomes

$$\frac{1}{2} \frac{710,600}{32.2} (2.05)^2 = 46,000 \text{ ft.lbs}$$

Hence the dissipated energy requirement estimated using Housner's method is

$$46,000 - 33,000 = 13,000 \text{ ft.lb}$$

which correlates more satisfactorily with the value based on the XBFRME plastic deformations i.e. 7,700 ft.lb.

Certainly a calculation following the Housner approach will serve as a valuable check on the XBFRME yield distortion predictions, particularly in the non-convective water situations.

VII.3 The Choice of Accelerogram

Since the El Centro 1940 N/S accelerogram represented, until quite recently, the largest strong motion seismic excitation reliably recorded it has been used in almost all of the numerical integration studies made of seismic response. Justifiable criticism of the application of a particular earthquake record to a general response prediction procedure have been made and these have become more frequent as appreciation has grown of the sensitivity of a structure's response to the characteristics of the excitation used and, more recently, of the significant effects which local site conditions may have in

modifying the base rock seismic disturbance and consequently producing an excitation peculiar to the particular site on which a projected structure is to be built.

The El Centro 1940 N/S accelerogram was used exclusively in the analyses reported in Chapter Six in order to provide a common basis for comparison with previous studies and to eliminate a further variable in the sensitivity analyses. However the XBFRME program can equally well accept input from any of the Berg type records⁽⁷⁰⁾, six of which are available, representing a range of natural earthquakes differing in their spectral properties according to the characteristics of the shaking at the recording site.

In an attempt to overcome the problem of lack of generality posed by the use of a particular accelerogram record from a past earthquake Jennings et al⁽⁷¹⁾ have produced simulated earthquake motions suitable for use in numerical integration analyses and these are freely available on request from the originators.

The Jennings type synthetic digitised records are designed to represent four types of earthquakes; the shaking near the causative fault in a large (Richter Magnitude > 8) earthquake, the shaking close to the fault in a Magnitude 7 earthquake, the motion expected in the epicentral region of a Magnitude 5.5 to 6 shock and the shaking close to the fault in a very small Magnitude 4.5 to 5.5 earthquake. In their original form these records do not conform to the Berg type format but suitable modifications have been made to produce card decks containing the digitised card decks in similar configuration to the Berg records. Consequently the XBFRME program can be run using any of

these synthetic earthquake records as the exciting accelerogram.

General acceptance of these synthetic accelerograms as the basis of seismic design analyses may have to wait until suitable techniques for allowing for the particular site conditions are more widely appreciated and for a better understanding of the dynamic properties of soils to be developed. In the meantime the use of records such as the El Centro accelerogram in numerical integration analyses is likely to continue. It can be no less valid as a design aid than the response curves included in current design codes⁽⁹⁾ which are, in many cases, based on the El Centro and other natural earthquake records.

VII.4 Torsional Response Consideration

When a vertical axis through the centre of mass does not coincide with a similar vertical axis through the centre of resistance at each mass level, lateral seismic excitations at the base of a structure necessarily induce torsional oscillations in addition to the lateral vibration. That torsional displacements have occurred in elevated water towers has been reported^(3, 20), consequently the possibility of torsional response must be considered at the design stage of elevated water tanks.

Because of the inherent simplicity of a cross braced elevated water tower it should be possible for the designer to maintain sufficient control of the structural configuration to ensure that the representation of the system as a plane frame is sufficiently realistic for design purposes, in which case the XBFRME program is applicable to the prediction of the response. However there may be

circumstances in which, due to the necessity to introduce off-centre inlet and outlet pipes or to link with adjacent structures, it does not prove possible to retain the symmetry of the system and in these circumstances the analysis technique must take account of the possible contribution of torsional displacement to the overall response. In principle the allowance may be made readily. In practice, because of the problems of accurately determining the mass and torsional stiffness distributions, it may be difficult to generate a sufficiently valid representation of the system to justify a substantial measure of confidence in the predictions made and it is suggested that a designer should make the avoidance of torsional response of prime importance when selecting the configuration of an elevated water tank structure. However, in those cases where this cannot be achieved, the response prediction technique presented in this thesis may be extended to the torsional response problem in the following manner.

An expression of the form of equation 4(1) can be written viz:-

$$\begin{bmatrix}
 M_1 & \cdot & \cdot & \cdot & \cdot & \cdot & \cdot & \cdot & \cdot & \cdot \\
 \cdot & \cdot & \cdot & \cdot & \cdot & \cdot & \cdot & \cdot & \cdot & \cdot \\
 \cdot & \cdot & M_N & \cdot & \cdot & \cdot & \cdot & \cdot & \cdot & \cdot \\
 \cdot & \cdot & \cdot & M_1 & \cdot & \cdot & \cdot & \cdot & \cdot & \cdot \\
 \cdot & \cdot & \cdot & \cdot & \cdot & \cdot & \cdot & \cdot & \cdot & \cdot \\
 \cdot & \cdot & \cdot & \cdot & \cdot & M_N & \cdot & \cdot & \cdot & \cdot \\
 \cdot & \cdot & \cdot & \cdot & \cdot & \cdot & I_1 & \cdot & \cdot & \cdot \\
 \cdot & \cdot & \cdot & \cdot & \cdot & \cdot & \cdot & \cdot & \cdot & \cdot \\
 \cdot & \cdot & \cdot & \cdot & \cdot & \cdot & \cdot & \cdot & \cdot & I_N
 \end{bmatrix}
 \begin{Bmatrix}
 \ddot{x}_1 \\
 \cdot \\
 \ddot{x}_N \\
 \ddot{y}_1 \\
 \cdot \\
 \ddot{y}_N \\
 \ddot{\theta}_1 \\
 \cdot \\
 \ddot{\theta}_N
 \end{Bmatrix}
 + [C]_T
 \begin{Bmatrix}
 \dot{x}_1 \\
 \cdot \\
 \dot{x}_N \\
 \dot{y}_1 \\
 \cdot \\
 \dot{y}_N \\
 \dot{\theta}_1 \\
 \cdot \\
 \dot{\theta}_N
 \end{Bmatrix}
 + [K]_T
 \begin{Bmatrix}
 x_1 \\
 \cdot \\
 x_N \\
 y_1 \\
 \cdot \\
 y_N \\
 \theta_1 \\
 \cdot \\
 \theta_N
 \end{Bmatrix}
 = -[M] \ddot{x}_g$$

in which x , y and θ are the two translational and the rotational displacements of each mass M

I_1 to I_N are the rotational inertias of the masses

M_1 to M_N about the centre of gravity

and $\begin{bmatrix} C \end{bmatrix}_T$ and $\begin{bmatrix} K \end{bmatrix}_T$ are respectively the damping and stiffness matrix⁽⁷³⁾ for coupled translational and rotational response.

The techniques described in Chapter Four could be applied to the solution of multiphase response, suitable modifications being made to the coupled stiffness matrix as the bracing rods slacken, yield or fracture. In a situation in which the analysis would not be restricted by the limitations of the digital computer on which the study described in this thesis was undertaken there appears to be no obstacle to the concepts used in the XBFRME program being extended to torsional response prediction.

VII.5 Conclusion

Because of the interactive nature of the problem, seismic design procedures necessarily involve a cyclic approach to the determination of an acceptable structure. Until the configuration of the system is known the response cannot be predicted, but a knowledge of the response is needed if an adequate structural system is to be selected. The designer normally tackles the problem by basing an initial selection of structural configuration and member sizes on an equivalent static load, applying perhaps 0.1g or 0.2g lateral acceleration to all the masses, and then providing a structure which will satisfactorily

resist the combined dead and equivalent seismic loads without exceeding the elastic behaviour range. The determination of the response of this system by a dynamic analysis subsequently enables the expected deformations and member loads arising from the selected design earthquake to be calculated. If the stresses are below the acceptable limits and consistent with an economic use of material, the design is considered to be satisfactory. If these conditions are not met, a modified structure is selected and a further response prediction is undertaken. This cycle is repeated as often as required to achieve an acceptable design.

Techniques suitable for the prediction of the dynamic response in both the elastic⁽⁶⁾ and post-yield^(53,54) ranges of beam and column frame structures have been published previously although to date the post-yield analyses have been restricted to ideal elasto-plastic considerations. Attempts are currently being made⁽⁷⁴⁾ to extend the numerical integration approach to the more general case of degrading stiffness systems to represent more accurately the observed behaviour of reinforced and prestressed concrete frameworks in particular.

The method which is presented in this thesis of determining the seismic response of braced water tower structures in the yield range of the bracing has not been advanced previously. If it is to be of practical value a designer requires reassurance that specific multi-phase response can be achieved reliably, without recourse to techniques which would prove impracticable with respect to detailing, fabrication or erection. It is submitted that the testing described in Chapter Three indicates that the provision of multiphase bracing is a

practicable proposition and that preselected behaviour can be achieved satisfactorily.

In so far as it has been possible to verify the mathematical modelling of an elevated fluid container by the small amplitude shaking tests described in Chapter Two and by correlation with both observed behaviour⁽²¹⁾ and other predictions⁽²⁴⁾ this has been done. Further tests on prototype structures or large scale models, preferably involving excitation of the system beyond the elastic range of the bracing rods, are highly desirable and will undoubtedly be undertaken when facilities such as the earthquake simulator shaking table planned for the Richmond field station at the University of California at Berkeley become available.

In its present form the XBFRME program allows for the inclusion of one mild steel rod in each diagonal brace of a moment resistant frame. The program may be applied equally conveniently to pin jointed tower frameworks such as it would be required to analyse if a bolted or riveted non-moment-resistant frame was used to support a water tank. In such a situation if any residual elastic resistance was to be incorporated in the structure it would be essential to provide a bracing member, which would remain elastic, in parallel with the sacrificial one, in each case. Relatively little programming effort would be needed to extend the XBFRME program to allow for more than two parallel braces if this should be required. The number of storeys which may be catered for by the XBFRME program in the form presented in Chapter Five is limited by the output statements. For convenience these specifically apply to the three and four mass systems

analysed as described in Chapter Six. Minor modifications to the output prescriptions would allow extension to as many masses as may be required for a particular analysis, subject only to the storage limitations of the computer used.

If the design of elevated water tank structures is to be placed on a more rational basis than hitherto, it is evident that the operating conditions and the level of seismic resistance sought will each have to be specified more accurately than has been the case in the past. For instance, if a tank is to be used to provide a constant head supply it is most unlikely that it will be in any state other than either full or completely empty when excited by an earthquake. Hence it would not be necessary to check the response of a series of partially full conditions, as would be the case for a supply tank which could well be at any stage of draw down when an earthquake occurs. Where the possibility exists of the tank contents being frozen the situation in which the non-convective response could prove to be critical must be examined. The statistical probability of ground shaking of a particular magnitude being experienced at a chosen site should be taken into account in selecting a suitable exciting accelerogram and, wherever possible, the characteristics of this record should reflect the site properties. An assessment of the acceptability of sacrificial bracing elements must be made and, when such response is anticipated, suitable remedial action must be arranged to ensure speedy restoration of the structure after a major shock has occurred. Generally a more sophisticated approach than that used up to now will be necessary. The use of a

torsion spanner to set bracing prestress levels may appear to be an unfamiliar technique in civil engineering but the example set by the Japanese, who have showed their willingness to adopt elaborate detailing and to include ingenious devices in seismic resistant structures⁽⁷⁵⁾, could well be followed by others.

It is submitted that the method of predicting the seismic response of cross braced elevated water tower structures which is presented in this thesis is valid and that the use of this approach will enable designers to achieve earthquake resistance in this type of structure with greater confidence.

APPENDIX ICALCULATIONS UNDERTAKEN IN MODELLING OF ILAM WATER TOWER(a) Determination of Lateral Stiffness $\frac{3EI}{L^3}$

Second Moment of Area I for main column

$$\frac{\pi}{64} (d_1^4 - d_2^4) = \frac{\pi}{64} (57^4 - 54^4) = 101,000 \text{ in}^4$$

and for inner tubes

$$\frac{\pi}{64} (39^4 - 36^4) = 31,100 \text{ in}^4$$

$$\frac{\pi}{64} (25.5^4 - 23^4) = 7,500 \text{ in}^4$$

$$\text{Hence, Total I} = 140,000 \text{ in}^4$$

Taking Elastic Modulus $E = 6 \times 10^6 \text{ psi}$ and Length $L = 360 \text{ inches}$ Lateral Stiffness $k_{so} = 54,000 \text{ lb/in or } 650,000 \text{ lb/ft.}$ (b) Determination of Masses m and m_s Bowl Contents m

$$\text{Tank Capacity} \quad \pi \times 4^2 \times 6.5 = 328 \text{ ft}^3$$

$$\text{Contents' Weight} = 328 \times 62.4 = 20,500 \text{ lbs}$$

$$\text{and } m = \frac{20,500}{g} = \frac{20,500}{32.2} = \underline{\underline{638}} \text{ lbs/g}$$

Structure m_s

$$\text{Bowl Concrete Volume} \quad \frac{8 \times \pi \times 6.5}{4} \approx 40 \text{ ft}^3$$

$$\text{Bowl Weight} \quad 40 \times 150 = 6,000 \text{ lbs}$$

$$\text{Insert Weight} = 1530 \text{ lbs}$$

$$\therefore \text{Total Weight} = \underline{\underline{7,530 \text{ lbs}}}$$

Pipe Weights

$$4.5 \text{ ft I.D. pipe} \quad \frac{\pi \times 4.5 \times 150}{4} \quad \approx \quad 500 \text{ lb/ft run}$$

$$3.0 \text{ ft I.D. pipe} \quad \frac{\pi \times 3 \times 5 \times 150}{24} \quad \approx \quad 300 \text{ lb/ft run}$$

$$2.0 \text{ ft I.D. pipe} \quad \approx \quad 200 \text{ lb/ft run}$$

$$\text{Total} \quad \underline{\underline{1000 \text{ lb/ft run}}}$$

$$\begin{aligned} \text{Thus Bowl Weight} + \frac{1}{3} \text{ Tower Weight} &= 7,530 + 10,000 \\ &= 17,530 \text{ lbs} \end{aligned}$$

$$\text{in which case } m_s = \frac{17,530}{32.2} = \underline{\underline{545 \text{ lbs/g}}}$$

or, considering all pipes to be full of water,

$$\text{Weight of Water} = \pi \times 2^2 \times 30 \times 62.4 = 24,500 \text{ lbs}$$

$$\text{in which case } m_s = (17,530 + \frac{24,500}{3}) = \underline{\underline{800 \text{ lbs/g}}}$$

Input to MODANAL Program, therefore,

$$k_{so} = 650,000$$

$$m = 0 \rightarrow 638 \text{ since, when water height, } m$$

$$0 \quad 0$$

$$2.0 \quad 196$$

$$3.5 \quad 340$$

$$5.0 \quad 490$$

$$6.5 \quad 638$$

$$\text{and } m_s = 545 \rightarrow 800$$

APPENDIX IIPOST YIELD AXIAL STIFFNESS OF BRACING RODS

True stress is the ratio of the load to the cross-sectional area at any instant.

$$\begin{aligned} \text{and true strain} &= \int_{L_0}^L \frac{\sigma L}{L} \quad \text{where } \sigma L \text{ is change in length} \\ &\quad \text{and } L \text{ is specimen length} \\ &= \log_e \left(\frac{L}{L_0} \right) \quad \text{where } L_0 \text{ is original specimen length} \\ &= \log_e (1+s) \quad \text{where } s \text{ is the normal engineering strain.} \end{aligned}$$

Now the relation between true stress σ_i and true strain ϵ_i may be expressed

$$\sigma_i = K_0 (\epsilon_i)^n$$

where K_0 is a constant known as the strength coefficient and n is a constant known as the strain hardening coefficient.

The true force/true deflection curve may be determined using the true stress/true strain relationship for a bracing rod, in the following manner.

$$\begin{aligned} \text{The true force} &= \sigma_i \times \frac{A_0 L_0}{L_i} \quad \text{where } A_0 \text{ is original rod cross-sectional area} \\ &\quad \text{and } L_i \text{ is rod length when true force is determined.} \end{aligned}$$

$$= \frac{A_0 L_0}{L_i} \cdot K_0 (\epsilon_i)^n$$

Using this expression, the post yield true force, true deflection curves may be determined for the range of bracing rods used.

APPENDIX III

GEOMETRICAL AND STRUCTURAL PROPERTIES OF TEST FRAME

Centreline dimensions of frame 45 in x 36 in
 Hence diagonal length 57.63 in
 and angle with horizontal $38^{\circ} 37'$

Thus, horizontal component of bracing force $F = 0.782 F$
 and vertical component of bracing force $F = 0.624 F$

Cross Bracing Stiffness Considerations

(neglecting second order effects)

$$\text{Lateral Load} = 0.782 F = 0.782 EA \frac{\delta L}{L}$$

where E is elastic modulus of bracing

A is cross sectional area of bracing

δL is change in length of bracing

L is original length of bracing.

$$\text{Thus Lateral Load} = \frac{0.782^2 EA}{L} \times \text{lateral deflection}$$

$$\text{and Lateral Stiffness} = \frac{0.782^2 EA}{L}$$

In the case of initial pretensioning of diametrically opposed diagonal braces, this stiffness is doubled.

Where pairs of braces are used the stiffness becomes

$$0.782^2 \Sigma \frac{EA}{L}$$

Elastic Limit Sway (d_{yb}) of Bracing

$$d_{yb} = 0.782 \frac{L}{E} \times \text{bracing yield stress}$$

Unbraced Portal Stiffness Considerations

Analysing half of the rigid knee portal

From diagram A III.1

$$M_{BA} + P \cdot L_{AB} = 0$$

$$M_{AB} = 0$$

$$M_{CB} = 0$$

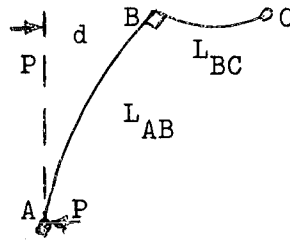


Fig. A III.1

Slope Deflection equations may be written

$$M_{AB} = \frac{2EI}{L_{AB}} \left(2\theta_A + \theta_B - \frac{3d}{L_{AB}} \right)$$

$$M_{BA} = \frac{2EI}{L_{AB}} \left(2\theta_B + \theta_A - \frac{3d}{L_{AB}} \right)$$

$$M_{BC} = \frac{2EI}{L_{BC}} (2\theta_B + \theta_C)$$

$$M_{CB} = \frac{2EI}{L_{BC}} (2\theta_C + \theta_B)$$

Since hinges exist at A and C

$$\theta_A = \frac{1}{2} \left(\frac{3d}{L_{AB}} - \theta_B \right)$$

$$\theta_C = -\frac{\theta_B}{2}$$

$$\text{Equilibrium at B implies } M_{BA} + M_{BC} = 0$$

$$\therefore L_{BC} \left(2\theta_B + \theta_A - \frac{3d}{L_{AB}} \right) + L_{AB} (2\theta_B + \theta_C) = 0$$

$$L_{BC} \left(2\theta_B + \frac{3d}{2L_{AB}} - \frac{\theta_B}{2} - \frac{3d}{L_{AB}} \right) + L_{AB} \left(2\theta_B - \frac{\theta_B}{2} \right) = 0$$

$$L_{BC} \left(\frac{3}{2} \theta_B - \frac{3}{2} \frac{d}{L_{AB}} \right) + L_{AB} \left(\frac{3}{2} \theta_B \right) = 0$$

$$\therefore \theta_B = \frac{d}{L_{AB}} \frac{L_{BC}}{(L_{BC} + L_{AB})}$$

Hence

$$\frac{2EI}{L_{AB}} \left(\frac{3}{2} \frac{d}{L_{AB}} \frac{L_{BC}}{(L_{BC} + L_{AB})} - \frac{3}{2} \frac{d}{L_{AB}} \right) + P \cdot L_{AB} = 0$$

and

$$\frac{P}{d} = \frac{-2EI}{L_{AB}^2} \left(\frac{3}{2} \cdot \frac{1}{L_{AB}} \cdot \frac{L_{BC}}{(L_{BC} + L_{AB})} - \frac{3}{2} \cdot \frac{1}{L_{AB}} \right)$$

Therefore Lateral Stiffness of Half of Rigid Knee Portal

$$= \frac{-2 \times 13,000 \times 2}{36^2} \left(\frac{3}{2} \frac{22.5}{36 \times 58.5} - \frac{3}{2} \frac{1}{36} \right)$$

$$= \frac{13,000}{18^2} (0.0417 - 0.0163) = \frac{13,000 \times 0.0254}{18^2}$$

$$= 1.02 \text{ Ton/in.}$$

Or, Lateral Stiffness of Unbraced Rigid Knee Test Portal

$$= 2.04 \text{ Ton/in.}$$

Elastic Limit Sway (d_{yp}) of Portal

Taking the yield stress to be 20 Ton/in². (Experimental value 19.4 Ton/in² - section III.3)

$$d_{yp} = \frac{M_{BA}}{1.02 \times 36} = \frac{20 \times 2}{1.02 \times 36 \times 1.5} = 0.76 \text{ in.}$$

APPENDIX IV

LISTINGS OF UNIVERSITY OF CANTERBURY
CIVIL ENGINEERING DEPARTMENT'S LIBRARY PROGRAMS
USED IN THE ANALYSES OF CROSS BRACED FRAMEWORKS

CCCCCCCCCCCCCCCC

```
*****
*
*      CIVIL ENGINEERING PROGRAM LIBRARY
*
*PROGRAM FOR STRUCTURAL ANALYSIS BY DIRECT STIFFNESS METHOD USING
*      FINITE ELEMENT CONCEPTS IN PLANE PROBLEMS
*
*****
```

```
COMMON/PARA/NA,MM,NUMEL,NUMNP,NFP,NSTOP,NFIX(99),R(198)
DATA FLAX/4HSTCP/
DATA FLAG/4HRUNS/
NSTOP=0
```

```

READ10,CHECK
FORMAT(A4)
IF(CHECK.EC.FLAX) GO TO 20
IF(CHECK.NE.FLAG) GO TO 5
NCH=KLOCK(AT)
CALL LOAD('PHASEA')
CALL SETUP
IF(NSTOP.NE.C) GC TO 15
CALL LOAD('PHASER')
CALL DRSTIF
CALL LOAD('PHASEC')
CALL FORCE
NEXT=KLOCK(NTT)
NETT=NETT-NCH
PRINT17,NETT
FORMAT(//23H TOTAL TIME IN SECCNDS=I5 )
GO TO 5
PRINT 30
FORMAT(1H1)
RETURN
END

```

```

0001 SUBROUTINE SETUP
C
C *****
C SUBROUTINE TO READ,CHECK DATA,FORM ELEMENT PROPERTIES,READ LCADS
C *****
C
0002 COMMON/PARA/NN,MM,NLMEL,NUMAP,NFP,NSTOP,NFIX(99),R(198)
0003 DIMENSION XCRC(99),YCRD(99),HEAD(20),NP(160,3),AR(16C),SI(16C), IP
IERM(3),A(3),R(3),RR(3)
0004 EQUIVALENCE (XCRC,R), (R(100),YCRD), (HEAD,NP)
0005 DATA IPERM/2,3,1/
C
0006 REWIND 1
0007 NSTOP=0
0008 READ10,HEAD
0009 1C FORMAT(2CA4)
0010 PRINT12,HEAD
0011 12 FORMAT(1H1,2CA4)
0012 DO 5 I=1,99
0013 XCRC(I)=0.0
0014 YCRD(I)=0.0
0015 5 NFIX(I)=0
0016 DO 6 I=1,160
0017 SI(I)=0.0
0018 AR(I)=0.0
0019 CO6J=1,3
0020 6 NP(I,J)=0
C
0021 READ15,NUMAP,NLMEL,KP,EMCD,XU
0022 15 FORMAT(3I5,2F1C.3)
0023 NFP=3
0024 IF(KP,EQ.2) NFP=2
0025 PRINT 17,NUMAP,NLMEL,NFP,EMCD,XU
0026 17 FORMAT(//24H NUMBER OF NCELL PCINTS=,I4/
1 3 24H NUMBER OF ELEMENTS =,I4/
2 3 24H NUMBER OF ECNS/ECDE =,I4/
3 3 24H ELASTIC MODULUS =,E15.3/
4 3 24H PCISSONS RATIC =,E15.3)
0027 NN=NFP+NLMKP
0028 IF(NN.GT.198)NSTOP=1
0029 IF(NLMEL.GT.16C)NSTOP=1
0030 IF(NSTOP.NE.0) PRINT18
0031 18 FORMAT(31H INITIAL PARAMETER ERROR,CANCEL )
0032 IF(NSTOP.NE.0) RETURN
C
C READ STRUCTURAL DATA
C
0033 READ20,(I,XCRC(I),YCRD(I),YCRD(I),NFI(1),N=1,NUMAP)

```

```

C034      2C FORMAT(11G,2F10.3,15)
C035      PRINT21
C036      21 FORMAT(13H1NCCE      XORD      YORD NFIX )
C037      PRINT22,(1,XCRD(1),YCRD(1),NFIX(1),I=1,NUMNP)
C038      22 FORMAT(15,2F10.3,16)

C
C      FINITE MEMBERS

C039      25 READ 26,(L,NP(L,I),I=1,3),AR(L),SI(L),N=1,NUMEL)
C040      26 FORMAT(4I4,F9.3,F10.3)
C041      PRINT27
C042      27 FORMAT(46H1  A   I   J   K      AREA,TH      M CF I   )
C043      PRINT28,(L,(NP(L,I),I=1,3),AR(L),SI(L),L=1,NUMEL)
C044      28 FORMAT(4I4,2F15.3)

C
C      CHECK BAND WIDTH

C045      MAXDIF=30-NFP
C046      IFLAG=0
C047      MM=0
C048      DO50N=1,NUMEL
C049      IF(NP(N,3).NE.C) GO TO 45
C050      NFF=NP(N,1)-NP(N,2)
C051      NFF=NFF*NFP
C052      NDIF=ABS(NFF)
C053      IF(NDIF.EQ.0.CR.NDIF.GT.MAXDIF) IFLAG=1
C054      IF(NDIF.GT.MM) MM=NDIF
C055      GO TO 49
C056      45 DO47I=1,3
C057      J=IPERM(I)
C058      NFF=NP(N,I)-NP(N,J)
C059      NFF=NFF*NFP
C060      NDIF=ABS(NFF)
C061      IF(NDIF.EQ.0.CR.NDIF.GT.MAXDIF) IFLAG=1
C062      47 IF(NDIF.GT.MM) MM=NDIF
C063      48 IF(IFLAG.NE.0) NSTCP=1
C064      IF(IFLAG.NE.C) PRINT42,N
C065      42 FORMAT(26H NCDE ARRAY ERROR, MEMBER=,15)
C066      50 IFLAG=0
C067      MM=MM+NFP
C068      IF(NSTOP.NF.C) RETURN

C
C      FORM ELEMENT PROPERTIES

C069      DO 100 N=1,NUMEL
C070      IF(NP(N,3).NE.C) GO TO 61
C071      I=NP(N,1)
C072      J=NP(N,2)
C073      K=C

```

```

C074      AA=XORD(J)-XCRD(I)
C075      HH=YORD(J)-YCRD(I)
C076      AREA=AR(N)
C077      SII=SI(N)
C078      IF(NFP.EQ.2) SII=0.0
C079      CALL HEAM (AA,BB,AREA,SII,EMCC,I,J)
C080      GO TO 100
C081      61 DO 7C I=1,3
C082      J=IPERM(I)
C083      K=IPERM(J)
C084      L=NP(N,J)
C085      M=NP(N,K)
C086      A(I)=XORD(M)-XCRD(L)
C087      7C R(I)=YORD(L)-YCRD(M)
C088      I=NP(N,1)
C089      J=NP(N,2)
C090      K=NP(N,3)
C091      THICK=AR(N)
C092      CALL SCST(A,B,THICK,I,J,K,EMCC,XU)
C093      8C CONTINUE
C094      10C CONTINUE

C
C      READ LOADS

C095      PRINT105
C096      105 FORMAT(35H1NCDE      XLNAC      YLCAC      PCMENT )
C097      DO 110 N=1,139
C098      11C R(N)=0.C
C099      DO200N=1,NUMNP
C100      READ120,M,(RR(I),I=1,NFP)
C101      IF(M.EQ.C) GO TO 201
C102      12C FORMAT(15,3F10.3)
C103      PRINT120,M,(RR(I),I=1,NFP)
C104      L=(M-1)*NFP
C105      DO130K=1,NFP
C106      J=L+K
C107      13C R(J)=R(J)+RR(K)
C108      20C CONTINUE
C109      201 CONTINUE

C
C      REWIND 1
C110      RETURN
C111
C112      END

```

```

0001      SUBROUTINE BEAM (XLX,XLY,AREA,SII,EMOD,II,JJ)
      C
      C *****
      C BEAM MEMBER, PRISMATIC
      C *****
0002      DIMENSION ST(6,6),TM(3,6),A(3,6)
      C
0003      KK=0
0004      CDF=0.5
0005      XL=SQRT(XLX**2+XLY**2)
0006      S2=-XLY/XL
0007      C2=XLX/XL
0008      TEMP=4.0/XL*EMCD
0009      DO160I=1,3
0010      DO160J=1,3
0011      ST(I,J)=0.0
0012      SC ST(1,1)=AREA/4.0*TEMP
0013      ST(2,2)=SII*TEMP
0014      ST(3,3)=ST(2,2)
0015      ST(2,3)=ST(2,2)*COF
0016      ST(3,2)=ST(2,3)
0017      TM(1,1)=-C2
0018      TM(1,2)=+S2
0019      TM(1,3)=0.0
0020      TM(2,1)=-S2/XL
0021      TM(3,1)=TM(2,1)
0022      TM(2,2)=-C2/XL
0023      TM(3,2)=TM(2,2)
0024      TM(2,3)=-1.0
0025      TM(3,3)=0.0
0026      DO 180 I=1,3
0027      TM(1,I+3)=-TM(1,I)
0028      TM(3,I+3)=-TM(2,I)
0029      180 TM(2,I+3)=-TM(3,I)
0030      TM(2,6)=0.0
0031      TM(3,6)=-1.0
0032      DO220I=1,3
0033      DO220J=1,6
0034      A(I,J)=0.0
0035      DO220K=1,3
0036      220 A(I,J)=A(I,J)+ST(I,K)*TM(K,J)
0037      DO240I=1,6
0038      DO240J=1,6
0039      ST(I,J)=0.0
0040      DO240K=1,3
0041      240 ST(I,J)=ST(I,J)+TM(K,I)*A(K,J)
0042      WRITE (1) II,JJ,KK,ST,A
0043      RETURN

```

```

0001      SUBROUTINE SCST (A,B,THICK,II,JJ,KK,EMCD,XU)
      C
      C *****
      C CONSTANT STRAIN TRIANGLE
      C *****
0002      DIMENSION A(3),B(3),ST(6,6),S(3,6)
      C
0003      AREA=A(3)*B(2)-A(2)*B(3)
0004      C1=EMOD*THICK/(2.0*AREA*(1.0-XU**2))
0005      C2=C1*XU
0006      C3=0.5*C1*(1.0-XU)
0007      DO200I=1,3
0008      K=I+I
0009      DO200J=1,3
0010      L=J+J
0011      AA=A(I)*A(J)
0012      AB=B(I)*B(J)
0013      BA=A(I)*B(J)
0014      BA=B(I)*A(J)
0015      ST(K-1,L-1)=C1*BB+C3*AA
0016      ST(K,L)=C1*AA+C3*BB
0017      ST(K-1,L)=C2*BA+C3*AB
0018      200 ST(K,L-1)=C2*AB+C3*BA
0019      DO300I=2,6
0020      DO300J=1,I
0021      300 ST(I,J)=ST(J,I)
0022      C1=C1*2.0
0023      C2=C2*2.0
0024      C3=C3*2.0
0025      DO400I=1,3
0026      K=I+I-1
0027      J=I+I
0028      S(1,K)=B(I)*C1
0029      S(1,J)=A(I)*C2
0030      S(2,K)=B(I)*C2
0031      S(2,J)=A(I)*C1
0032      S(3,K)=A(I)*C3
0033      400 S(3,J)=B(I)*C3
0034      WRITE (1) II,JJ,KK,ST,S
0035      RETURN
0036      END

```


C001

SUBROUTINE DRSTIF

C
C
C
C
C
C

 SUBROUTINE TO FORM TOTAL STIFFNESS MATRIX BY THE DIRECT STIFFNESS
 METHOD

C002
C003
C004

COMMON/PARA/NN,MM,NEL,NPT,NFP,ASTOP,NFIX(99),B(198)
 DIMENSION A(198,3C),R(198),ST(6,6),NP(3),S(3,6)
 EQUIVALENCE (R,B)

C005
C006
C007
C008

C
 REWIND 1
 DO10I=1,NN
 DO10J=1,MM
 1C A(I,J)=0.0

C
C
C

SET UP TOTAL STIFFNESS MATRIX

C009
C010
C011
C012
C013

DO100N=1,NEL
 READ(1) II,JJ,KK,ST,S
 NP(1)=II
 NP(2)=JJ
 NP(3)=KK

C

C014
C015
C016
C017
C018
C019
C020
C021
C022
C023
C024
C025
C026
C027
C028
C029
C030
C031
C032
C033
C034
C035
C036
C037
C038

NNF=2
 NNE=3
 NFF=NFP
 IF(NP(3).EQ.0) NNE=2
 IF(NP(3).EQ.0) NNF=3
 IF(NP(3).NE.0) NFF=2
 DO90I=1,NNE
 K=NP(I)
 KK=NNF*(I-1)
 IK=NFP*(K-1)
 DO90J=1,NNE
 L=NP(J)
 IF(K.GT.L) GO TO 90
 LL=NNF*(J-1)
 JK=NFP*(L-K)+1
 DO 80 II=1,NFF
 IS=KK+II
 IA=IK+II
 JA=JK-II
 DO 80 JJ=1,NFF
 JS=LL+JJ
 JA=JA+1
 IF(JA.LE.0) GO TO 80
 A(IA,JA)=A(IA,JA)+ST(IS,JS)
 8C CONTINUE

FORTRAN IV

MODEL 44 PS

VERSION 3, LEVEL 3 DATE 7104E

C039
C040

90 CONTINUE
 1C0 CONTINUE

C
C
C

APPLY BOUNDARY CONDITIONS

C041
C042
C043
C044
C045
C046
C047
C048
C049
C050
C051
C052
C053
C054
C055
C056
C057
C058
C059

DO240N=1,NPT
 M=(N-1)*NFP
 IF(NFIX(N).EQ.C) GO TO 240
 I=100
 IF(NFP.EQ.2) I=10
 DO235J=1,NFP
 IF(NFIX(N).LT.I) GO TO 235
 L=M+J
 DO 230 K=1,MM
 LI=L+I-K
 A(L,K)=0.0
 IF(LI.LE.0) GO TO 230
 A(LI,K)=0.0
 230 CONTINUE
 A(L,I)=1.0
 R(L)=0.0
 NFIX(N)=NFIX(N)-I
 235 I=I/10
 240 CONTINUE

C
C
C

SOLVE SYSTEM FOR DISPLACEMENTS

C060
C061
C062
C063

C064
C065
C066

NA=NN
 NB=MM
 CALL SYMSOL(NA,NB,1,A,R)
 CALL SYMSCL(NA,NB,2,A,R)
 C
 REWIND 1
 RETURN
 END

```

C001 SUBROUTINE FORCE
C
C *****
C FORCE OUTPLT
C *****
C
C002 COMMON/ PARA/ NN, MM, NUMEL, NUMNP, NFP, NSTCP, AFIX(99), R(198)
C003 DIMENSION ST(3,6), SS(6,6), RB(6), S(3)
C004 DATA PCNE/ 4HBEAM/
C005 DATA PTWO/ 4H CST/
C
C006 REWIND 1
C
C PRINT DISPLACEMENTS
C
C007 IF(NFP.EQ.2) PRINT 260
C008 IF(NFP.EQ.3) PRINT 262
C009 260 FORMAT(35H1NCDE X-DISPLACEMENT Y-DISPLACEMENT )
C010 262 FORMAT(5CH1NCDE X-DISPLACEMENT Y-DISPLACEMENT THETA-ROTATION )
C011 DO280N=1,NUMNP
C012 I=(N-1)*NFP+1
C013 IF(NFP.EQ.2) PRINT 270,N,R(I),R(I+1)
C014 IF(NFP.EQ.3) PRINT 272,N,R(I),R(I+1),R(I+2)
C015 270 FORMAT(15,1PE15.4,1PE15.4)
C016 272 FORMAT(15,1PE15.4,1PE15.4,1PE15.4)
C017 280 CONTINUE
C
C PRINT ELEMENT FORCES.
C
C018 PRINT 290
C019 PRINT 291
C020 290 FORMAT( 67H1 N I J K BEAM AXIAL FORCE MOMENT AT I
C021 291 FORMAT( 67H CST X-STRESS Y-STRESS
C022 1 XY-STRESS )
C023 DO400N=1,NUMEL
C024 READ (1) II,JJ,KK,SS,ST
C025 IF(KK.EQ.0) GC TC 310
C026 K=(II-1)*NFP
C027 L=(JJ-1)*NFP
C028 DO 305 I=1,NFP
C029 J=K+I
C030 M=L+I
C031 RB(I)=R(JJ)
C032 305 RB(I+3)=R(JJ)
C033 IF(NFP.EQ.2)RB(3)=0.0
C034 IF(NFP.EQ.2)RB(6)=0.0
C035 CO 3C7 I=1,3
C036 S(I)=0.0

```

```

0036      DO 307 J=1,6
0037      307 S(I)=S(I)+ST(I,J)*RR(J)
0038      GO TO 320
0039      310 I=(I-1)*NFP+1
0040      J=(J-1)*NFP+1
0041      K=(K-1)*NFP+1
0042      R8(I)=R(I)
0043      R8(2)=R(I+1)
0044      R8(3)=R(J)
0045      R8(4)=R(J+1)
0046      R8(5)=R(K)
0047      R8(6)=R(K+1)
0048      D0350I=1,3
0049      S(I)=0.0
0050      D0350J=1,6
0051      350 S(I)=S(I)+ST(I,J)*R8(J)
0052      320 CONTINUE
0053      IF(KK.EQ.C) PRINT 360,N,II,JJ,KK,PCNE,(S(I),I=1,3)
0054      IF(KK.NE.C) PRINT 360,N,II,JJ,KK,PTWC,(S(I),I=1,3)
0055      360 FORMAT(4I4,2X,A4,1P3E15.5)
0056      400 CONTINUE
0057      REWIND 1
0058      RETURN
0059      END

```

INPUT DATA

ANALYSIS OF MORAN AND CHENG'S WATER TOWER (WITH SYM BRACING)

```

NUMBER OF NODAL POINTS= 8
NUMBER OF ELEMENTS     = 15
NUMBER OF EQNS/NODE     = 3
ELASTIC MODULUS        = 0.29CE OR
POISSONS RATIO         = 0.0

```

NODE	XORD	YORD	NFIX
1	0.0	0.0	110
2	386.000	0.0	110
3	21.000	432.000	0
4	365.000	432.000	0
5	41.000	851.000	0
6	345.000	851.000	0
7	61.000	1260.000	0
8	325.000	1260.000	0

N	I	J	K	AREA, TH	M C+ I
1	1	3	0	30.600	1856.000
2	3	4	0	15.660	236.000
3	2	4	0	30.600	1856.000
4	3	5	0	26.800	1640.000
5	5	6	0	14.500	173.600
6	4	6	0	26.800	1640.000
7	5	7	0	22.000	1346.000
8	7	8	0	100.000	4000.000
9	6	8	0	22.000	1346.000
10	1	4	0	4.820	0.0
11	2	3	0	4.820	0.0
12	3	6	0	7.100	0.0
13	4	5	0	7.100	0.0
14	5	8	0	8.660	0.0
15	6	7	0	8.660	0.0

NODE	XLOAD	YLOAD	MOMENT
3	0.500	C.C	0.0
4	0.500	C.C	0.0

OUTPUT

NODE	X-DISPLACEMENT	Y-DISPLACEMENT	THETA-ROTATION
1	-0.0	-0.0	-1.3593E-08
2	-0.0	-0.0	-1.3593E-08
3	4.6024E-06	5.2914E-08	-4.6623E-09
4	4.6024E-06	-5.2913E-08	-4.6623E-09
5	4.7658E-06	4.6801E-08	7.1846E-10
6	4.7658E-06	-4.6801E-08	7.1847E-10
7	4.8840E-06	4.0669E-08	-3.6934E-10
8	4.8840E-06	-4.0669E-08	-3.6935E-10

N	I	J	K	BEAM	AXIAL FORCE	MOMENT AT I	MOMENT AT J
						XY-STRESS	XY-STRESS
1	1	3	0	BEAM	5.66729E-01	-9.53674E-07	-2.21775E-00
2	3	4	0	BEAM	2.86102E-06	5.22216E-01	5.22216E-01
3	2	4	0	BEAM	-5.66929E-01	-1.90735E-06	-2.21775E-00
4	3	5	0	BEAM	3.11613E-03	1.69552E-00	4.70449E-01
5	5	6	0	BEAM	2.86102E-06	-1.01983E-01	-1.01983E-01
6	4	6	0	BEAM	-3.11661E-03	1.69552E-00	4.70447E-01
7	5	7	0	BEAM	-5.46873E-04	-3.68874E-01	-1.61487E-01
8	7	8	0	BEAM	1.52588E-05	1.61475E-01	1.61481E-01
9	6	8	0	BEAM	5.46815E-04	-3.68875E-01	-1.61485E-01
10	1	4	0	BEAM	7.24150E-01	0.0	0.0
11	2	3	0	BEAM	-7.24149E-01	0.0	0.0
12	3	6	0	BEAM	4.18016E-03	0.0	0.0
13	4	5	0	BEAM	-8.17923E-03	0.0	0.0
14	5	8	0	BEAM	-2.22350E-03	0.0	0.0
15	6	7	0	BEAM	2.22350E-03	0.0	0.0

TOTAL TIME IN SECONDS= 20

LIST LP. 1 (CONTINUED)

```

0001
0002
0003
0004
0005
0006
0007
0008
0009
0010
0011
C
0012
0013
0014
0015
0016
0017
0018
0019
0020
0021
0022
0023
0024
0025
0026
0027
0028
0029
C
0030
0031
0032
0033

*****
*
*      CIVIL ENGINEERING PROGRAM LIBRARY
*
*      NORMAL MODES FROM F(LAT)
*
*****

IL=1,OMEGA PRINTED, IL=0, NOT PRINTED
IM=1 PUNCHES 16 DISPLACEMENTS, IM=0 SKIPS.
1 READ30,NS,NM,E,CONV,IDAMP,IL,IM
30 FORMAT(2I3,2E10.4,3I3)
PRINT97,NS,NM,E,CONV,IDAMP,IL,IM
97 FORMAT(1H 215,2E14.6,3I5)
IL=IL+1
IM=IM+1
DO21=1,NS
DO2J=1,NS,5
2 READ21,A(I,J),A(I,J+1),A(I,J+2),A(I,J+3),A(I,J+4)
31 FORMAT(5E14.8)
READ DIAGONAL MASS MATRIX AND FORM PRODUCT (F)(M)
DO291=1,NS,8
29 READ32,W(I),W(I+1),W(I+2),W(I+3),W(I+4),W(I+5),W(I+6),W(I+7)
32 FORMAT(8E10.4)
DO721=1,NS
S(I)=0
U(I)=0
72 J=(NS+4)*5/5
L=NS+1
DO901=L,J
90 X(I)=0
K=(NS+7)*8/8
DO911=L,K
91 X2(I)=0
DO28J=1,NS
28 W(J)=W(J)/386.4
DO251=1,NS
DO25J=1,NS
25 A(I,J)=A(I,J)*W(J)
DETERMINE LATENT VECTOR AND LATENT ROOT
M=1
7 DO26J=1,NS
031 X(J)=1.0
032 N=0
033

```

```

0034
0035
0036
0037
0038
0039
0040
0041
0042
0043
0044
0045
0046
0047
0048
0049
0050
0051
0052
0053
0054
0055
0056
0057
0058
0059
0060
0061
0062
0063
0064
0065
0066
0067
0068
0069
0070
0071
0072
0073
0074
0075
0076
0077
0078
0079
0080
0081
0082

P=C
46 DO271=1,NS
T=C
DO40J=1,NS
40 T=T+A(I,J)*X(J)
27 X2(I)=T
WEXP2=1.0/X2(NS)
DO41J=1,NS
41 X(I)=X2(J)*WEXP2
043 IF(P/WEXP2-1.0-CONV)42,42,43
044 IF(P/WEXP2-1.0+CCNV)43,44,44
045 P=WEXP2
N=N+1
GO TO 46
44 PRINT33,M,N
33 FORMAT('1MDC=',I3,20X,'NUMBER OF CYCLES=',I3)
T=C
DO91=1,NS
IF(ABS(T)-ABS(X(I)))8,9,9
8 T=X(I)
9 CONTINUE
DO101=1,NS
10 X(I)=X(I)/T
PRINT34,WEXP2,P
34 FORMAT('ANGULAR FREQUENCY SQUARED=',E14.8,5X,E14.8)
GO TO (77,78),IL
78 Q=SQRT(WEXP2)
WRITE(17,372) Q
372 FORMAT(1X,5E20.8)
77 P=SQRT(WEXP2)/6.2831853
Q=1.0/P
PRINT35,P,Q
35 FORMAT('FREQUENCY=',E14.4,9X,'PERIOD=',E14.4)
IF(IDAMP-2173,74,75)
73 P=2.12
T=2.10
GO TO 76
74 P=1.28
T=1.26
GO TO 76
75 I=(IDAMP-5)*(4C-IDAMP)/150
P=C*P**I
T=-0.07
76 IF(Q-0.5)66,67,67
66 AM=0.37*(T-0.37)/(C-1.43*C*Q)/0.175
GO TO 68
67 AM=P*0.44/Q
68 PRINT361,M
36 FORMAT('AMPLIFICATION FACTOR=',F8.2)

```

LIST L.P. 2

OUTPUT

```

0083 C DETERMINE 1G DISPL. AND SHEAR FORCES.
0084 CONV=CONV+CONV
0085 P=0.
0086 D0531=1. NS
0087 P=P+W(I)*X(I)
0088 T=0.
0089 D0541=1. NS
0090 T=T+W(I)*X(I)*X(I)
0091 Q=P/T
0092 D0551=1. NS
0093 X2(I)=386.4/WEXP2*Q*X(I)
0094 C11)=D0(I)*X2(I)*AM*X2(I)*AM
0095 D056J=1. NS
0096 X3(J)=386.4*Q*W(J)*X(J)
0097 S(J)=S(J)+AM*AM*X3(J)*X3(J)
0098 GO TO (81,82),IM
0099 D0831=1. NS
0100 PUNCH32,X2(I),X2(I+1),X2(I+2),X2(I+3),X2(I+4),X2(I+5),
0101 1X2(I+6),X2(I+7)
0102 R1 PRINT39
0103 39 FORMAT('3DISPLACEMENT RATIOS.',6X,'1G DISPLACEMENTS.',10X,'1G FORC
0104 ES.')
0105 J=NS
0106 59 PRINT38,X(J),X2(J),X3(J)
0107 38 FORMAT(7X,F8.4,14X,E10.4,14X,E10.4)
0108 IF(J-1)64,64,65
0109 65 J=J-1
0110 GO TO 59
0111 C MODIFY (F)(M) TO GIVE CONVERGENCE TO HIGHER MODES.
0112 64 D0581=1. NS
0113 X(I)=X(I)/SQRT(T)
0114 IF(M-NM)47,69,69
0115 47 D0601=1. NS
0116 D060J=1. NS
0117 A(I,J)=A(I,J)-X(I)*X(J)*W(J)/WEXP2
0118 GO TO 7
0119 69 PRINT37
0120 37 FORMAT('1',22X,'PREDICTED ELASTIC RESPONSE.','',' DISPLACEMENT.'
0121 1,13X,'SHEARS.',17X,'FORCES.')
0122 P=0.
0123 J=NS
0124 71 S(J)=SQRT(S(J))
0125 D(J)=SQRT(D(J))
0126 X(J)=S(J)*P
0127 PRINT371,D(J),X(J),S(J)
0128 371 FORMAT(6X,E10.4,13X,E10.4,14X,E10.4)
0129 P=X(J)
0130 IF(J-1)1,1,70
0131 70 J=J-1
0132 GO TO 71
0133 END

```

```

MODE= 1 NUMBER OF CYCLES= 3
ANGULAR FREQUENCY SQUARED=0.30278134E 00 0.30278134E 00
FREQUENCY= 0.8758E-01 PERIOD= 0.1142E 02
AMPLIFICATION FACTOR= 0.03
DISPLACEMENT RATIOS. 1G DISPLACEMENTS. 1G FORCES.
1.0000 0.1282E 04 0.9355E 06
0.8956 0.1149E 04 0.1169E 05
0.5380 0.6899E 03 0.7492E 04

```

```

MODE= 2 NUMBER OF CYCLES= 6
ANGULAR FREQUENCY SQUARED=0.11579932E 03 0.11579981E 03
FREQUENCY= 0.1713E 01 PERIOD= 0.5839E 00
AMPLIFICATION FACTOR= 0.60
DISPLACEMENT RATIOS. 1G DISPLACEMENTS. 1G FORCES.
-0.0167 -1.988E-01 -1.5547E 04
0.7055 0.8402E 03 0.3259E 04
1.0000 0.1191E 01 0.4886E 04

```

```

MODE= 3 NUMBER OF CYCLES= 4
ANGULAR FREQUENCY SQUARED=0.92898401E 03 0.92900562E 03
FREQUENCY= 0.4851E 01 PERIOD= 0.2061E 00
AMPLIFICATION FACTOR= 0.67
DISPLACEMENT RATIOS. 1G DISPLACEMENTS. 1G FORCES.
-0.0071 0.4517E-03 0.1011E 04
1.0000 -6.341E-01 -1.9773E 04
-0.6751 0.4281E-01 0.1404E 04

```

PREDICTED ELASTIC RESPONSE.

DISPLACEMENT.	SHEARS.	FORCES.
0.3953E 02	0.3904E 05	0.2904E 02
0.3541E 02	0.3143E 05	0.2394E 04
0.2128E 02	0.3454E 05	0.3101E 04
3 3 0.100000E 01	0.100000E-04	10 0 0

C	CE020 CIVIL ENGINEERING PROGRAM LIBRARY DAMPING MATRIX FORMATION	
C		
C	SIMPLIFIED CALC. OF (C) MATRIX	1
	DIMENSION S(30,30),C(30,30),W(30)	2
	INP=5	3
	LNP=6	4
	IPCH=7	5
C	READ NO. OF STOREYS, PER CENT DAMPING 1ST AND 2ND MODES	51
	READ(INP,33) NS,C1,C2	6
33	FORMAT(13,2F3.0)	7
C	READ ANGULAR FREQUENCY 1ST MODE (RADIAN)	71
	READ(INP,34) W1	8
34	FORMAT(5E14.8)	9
C	READ ANGULAR FREQUENCY 2ND MODE (RADIAN)	91
	READ(INP,34) W2	10
	CG=.02*(C2*W2-C1*W1)/(W2*W2-W1*W1)	11
	CT=.02*C1*W1-CG*W1*W1	12
	WRITE(6,7) CG,CT	
	7 FORMAT(2E14.7)	
C	READ LATERAL STIFFNESS MATRIX	131
	1 READ(INP,94)((S(I,J),J=1,NS),I=1,NS)	
94	FORMAT(8E10.3)	
C	READ LUMPED STOREY WEIGHTS.	141
	READ(INP,32) (W(I),I=1,NS)	15
32	FORMAT(8E10.4)	16
	DC 4 I=1,NS	17
	DC 3 J=1,NS	18
	3 C(I,J)=CG*S(I,J)	19
	4 C(I,I)=C(I,I)+CT*W(I)/386.4	20
	WRITE(LNP,35) NS,C1,C2,W1,W2	21
35	FORMAT(/1X,13,2F5.1,2E13.3//)	22
	DC 2 I=1,NS	23
	2 WRITE(LNP,36) (S(I,J),J=1,NS)	24
36	FORMAT(1X,5E13.3)	25
	WRITE(LNP,38)	
	WRITE(LNP,37) (W(I),I=1,NS)	26
37	FORMAT(1X,10E13.3)	27
38	FORMAT(/)	28
	WRITE(LNP,38)	29
	DC 6 I=1,NS	30
	WRITE(LNP,36) (C(I,J),J=1,NS)	31
	6 WRITE(IPCH,39) (C(I,J),J=1,NS)	32
39	FORMAT(5E14.7)	33
	WRITE(LNP,40)	34
40	FORMAT(1X,'PROCESSING COMPLETE')	35
	STOP	36
	END	37

LIST L.P. 2A

```

0001      DIMENSION A(100,C,100)
0002      1 READ(100,C,N
0003      100 FORMAT(15)
0004      READ(101,((A(I,J),I=1,N),J=1,N)
0005      101 FORMAT(8F10.0)
0006      CALL PRINTM(A,N,1)
0007      CALL MATINV(A,N)
0008      CALL PRINTM(A,N,2)
0009      GO TC 1
0010      END

```

```

0001          SUBROUTINE MATINV(A,NMAX)
      C      MATRIX INVERSION (A,NMAX)
0002          DIMENSION A(100,100)
0003          DO 200 N=1,NMAX
0004              D=A(N,N)
0005              DO 100 J=1,NMAX
0006                  A(N,J)=-A(N,J)/D
0007                  DO 150 I=1,NMAX
0008                      IF(I-N) 110,150,C,110
0009                      110 DO 140 J=1,NMAX
0010                          IF(N-J) 120,140,C,120
0011                          120 A(I,J)=A(I,J)+A(I,N)*A(N,J)
0012                          140 CONTINUE
0013                      150 A(I,N)=A(I,N)/D
0014                      A(N,N)=1.0/D
0015              200 CONTINUE
0016          RETURN
0017          END

```

LIST L.P. 3

FORTRAN IV MODEL 44 PS VERSION 3, LEVEL 3 DATE 71040

```

0001          SUBROUTINE PRINTM(A,N,L)
0002          DIMENSION A(100,100)
0003          WRITE(6,100) L
0004100    FORMAT('//MATRIX NUMBER'//14//
0005          1          '-----'//)
0006          IF(N.GT.10) GO TO C
0007          DO 1 I=1,N
00081          1    WRITE(6,1C1) (A(I,J),J=1,N)
0009101    FORMAT(' '10G13.3)
0010          GO TO 5
0011          2    DO 3 I=1,N
0012          3    WRITE(6,101) (A(I,J),J=1,10)
0013          WRITE(6,1C2)
0014102    FORMAT('//')
0015          DO 4 I=1,N
0016          4    WRITE(6,1C1) (A(I,J),J=11,N)
0017          5    RETURN
0018          ENC

```

OUTPUT

MATRIX NUMBER 1

```

0.246E 06   -0.163E 06   0.292E 05
-0.163E 06   0.306E 06   -0.144E 06
0.292E 05   -0.144E 06   0.120E 06

```

MATRIX NUMBER 2

0.879E-05	0.957E-05	0.819E-05
0.857E-05	0.160E-04	0.171E-04
0.819E-05	0.171E-04	0.270E-04

DA2171
/E

```

C
C *****
C *
C * CIVIL ENGINEERING PROGRAM LIBRARY * CCCCC1
C *
C * PROGRAM ELRES * CCCCC2
C *
C * THIS PROGRAM DETERMINES THE ELASTIC RESPONSE OF MULTI-MASS * CCCCC3
C * SYSTEMS TO BERG FORMAT EARTHQUAKE RECORDS. * CCCCC4
C *****
C
C001 CALL TITLE
C002 C MS=1 ENTER (K)LAT,MS=2 ENTER (F)LAT
C DIMENSION S(20,20),F(20,20),QM(20),AA(20),BB(20),X(20),
C IVEL(20),ACC(20),Y(20),Z(20),T(5),G(5),BX(20),TX(20),C(20,20)
C N=NO OF MASSES,KP=NC OF STEPS BEFORE PRINTING,DT=STEP INTERVAL
C TR=LENGTH OF RECORD
C003 28 READ29,N,MS,KP,DT,TR
C004 29 FORMAT(3I3,2E10.4)
C005 PRINT321,N,MS,KP,DT,TR
C006 321 FORMAT('1 INPUT DATA ECHO CHECK'/'0',3I5,2E13.4)
C007 32 FORMAT(3I4,2E13.4)
C008 PRINT34
C009 34 FORMAT(//)
C010 KC=0
C011 30 FORMAT(8E10.4)
C READ (X)LAT OR (F)LAT
C IF(MS.EQ.1)PRINT 51
C IF(MS.EQ.2)PRINT 52
C012 51 FORMAT('0',30X,'LATERAL STIFFNESS MATRIX'//)
C013 52 FORMAT('C',30X,'LATERAL FLEXIBILITY MATRIX'//)
C014 DO40I=1,N
C015 READ31,(S(I,J),J=1,N)
C016 40 PRINT143,(S(I,J),J=1,N)
C017 143 FORMAT(1X,10E13.4)
C018 PRINT34
C019 C READ DAMPING MATRIX
C020 WRITE(6,53)
C021 53 FORMAT('0',40X,'DAMPING MATRIX'//)
C022 DO41I=1,N
C023 READ31,(C(I,J),J=1,N)
C024 41 PRINT143,(C(I,J),J=1,N)
C025 PRINT34
C026 31 FORMAT(5E14.8)
C027 WRITE(6,54)
C028 54 FORMAT('C',50X,'MASSES'//)
C029 GO TO (2,3),MS
C030

```

```

0031 3 CALL MATINV(S,N)
C READ MASS MATRIX
0032 2 READ30,(QM(I),I=1,N)
0033 PRINT143,(QM(I),I=1,N)
0034 WRITE(6,55)
0035 55 FORMAT('0',25X,50('**')/'0 TIME',30X,'DISPLACEMENTS OF MASSES'//
1)
0036 DO5I=1,N
0037 X(I)=0.
0038 VEL(I)=0.
0039 BX(I)=0.
0040 QM(I)=QM(I)/386.4
0041 Z(I)=0.
0042 Y(I)=0.
0043 DO5J=1,N
0044 5 F(I,J)=0.
0045 IS=1
C READ EQU. RECCRD CARD
0046 READ33,ISC,(T(I),G(I),I=2,5)
0047 IF(IS=ISC)43,42,43
0048 33 FORMAT(I3,4(F8.4,F9.6))
0049 42 M2=2
0050 P=G(2)*386.4
0051 DG=DT*386.4*(G(3)-G(2))/(T(3)-T(2))
0052 DO6I=1,N
0053 6 F(I,I)=1.0/QM(I)
0054 TM=0.
0055 DO7I=1,N
0056 7 Y(I)=QM(I)*P-Z(I)-Y(I)
0057 CALL VECMTP(ACC,F,Y,N,N)
0058 DO8I=1,N
0059 F(I,I)=QM(I)
0060 DO8J=1,N
0061 8 F(I,J)=F(I,J)+0.5*DT*C(I,J)+.16666667*DT*DT*S(I,J)
0062 CALL MATINV(F,N)
0063 25 IF(TM-TR+.5*DT)26,27,27
0064 26 IF(TM+DT-T(M2+1))10,10,11
0065 10 TM=TM+DT
0066 P=P-DG
0067 GO TO 12
0068 11 IF(M2-4)13,14,14
0069 13 M2=M2+1
0070 GO TO 15
0071 14 M2=1
0072 G(1)=G(5)
0073 T(1)=T(5)
0074 IS=IS+1
0075 READ33,ISC,(T(I),G(I),I=2,5)
0076 IF(IS=ISC)43,15,43

```



```

0077 15 TT=TM+DT-T(M2)
0078 TS=T(M2+1)-T(M2)
0079 IF(TS)11,11,16
0080 16 GS=(G(M2+1)-G(M2))*386.4
0081 GG=GS*TT/TS
0082 DG=GS*DT/TS
0083 P=-G(M2)*386.4-GG
0084 TM=TM+DT
0085 12 DO17I=1,N
0086 AA(I)=VEL(I)+.5*DT*ACC(I)
0087 17 BB(I)=X(I)+DT*VEL(I)+.33333333*DT*DT*ACC(I)
0088 CALL VECMTP(Y,S,BB,N,N)
0089 CALL VECMTP(Z,C,AA,N,N)
0090 DO18I=1,N
0091 Y(I)=QM(I)*P-Z(I)-Y(I)
0092 CALL VECMTP(ACC,F,Y,N,N)
0093 DO19I=1,N
0094 VEL(I)=AA(I)+.5*DT*ACC(I)
0095 19 X(I)=BB(I)+.16666667*DT*DT*ACC(I)
0096 KC=KC+1
0097 IF(KC,LT,KP) GC TC 20
0098 PRINT143,TM,(X(I),I=1,N)
0099 KC=0
0100 20 DO22I=1,N
0101 IF(ABS(X(I))-ABS(BX(I)))22,22,23
0102 23 BX(I)=X(I)
0103 TX(I)=TM
0104 22 CONTINUE
0105 GO TO 25
0106 27 WRITE(6,34)
0107 WRITE(6,56) (I,BX(I),TX(I),I=1,N)
0108 56 FORMAT('0 MASS',I3,' MAX DISPLACEMENT=',E13.4,' AT TIME',E13.4)
0109 1)
0110 STCP
0111 43 PRINT35,IS
0112 35 FORMAT(' CARDS OUT OF ORDER',I5)
0113 STCP 3333
      END

```

```

CCCC081
CCCC082
CCCC083
CCCC084
CCCC085
CCCC086
CCCC087
CCCC088
CCCC089
CCCC090
CCCC091
CCCC092
CCCC093
CCCC094
CCCC095
CCCC096
CCCC097
CCCC098
CCCC099
CCCC100
CCCC101
CCCC102
CCCC103
CCCC104
CCCC105
CCCC106
CCCC107
CCCC108
CCCC109

```

```

CCC111
CCC112
CCC113
CCC114
CCC115

```

```

C
C001 SUBROUTINE VECMTP(B,A,Y,M,N)
C      (B)=(A)*(Y) (A) OF ORDER MXN
      DIMENSION A(20,20),Y(20),B(20)
      DO1I=1,M
      T=C.
      DO2J=1,N
      2 T=T+A(I,J)*Y(J)
      1 B(I)=T
      RETURN
      END

```

LIST L.P. 4 (CONTINUED)

```

COC1      SUBROUTINE MATINV(S,N)
C          *****
C          INVERT MATRIX (S) IN SITU. (ORDER N X N)
C          USING JORDAN ELIMINATION METHOD
C          *****
C002      DIMENSION S(20,20)
C003      DO 50 I=1,N
C004      DIAG=S(I,I)
C005      IF(DIAG.NE.0.0) GC TC 45
C006      WRITE(6,43)
C007      43 FORMAT(1H0,28HSTIFFNESS MATRIX IS SINGULAR//
C          11X,16HHARD LUCK,BUDDY.)
C008      STOP
C
C009      45 S(I,I)=1.0
C010      DO 46 J=1,N
C011      46 S(I,J)=S(I,J)/DIAG
C012      DO 50 K=1,N
C013      IF(K.EQ.I) GC TO 50
C014      DIAG=S(K,I)
C015      S(K,I)=0.0
C016      DO 47 J=1,N
C017      47 S(K,J)=S(K,J)-DIAG*S(I,J)
C018      50 CONTINUE
C019      RETURN
C020      END

```

```

COC1      C
C          SUBROUTINE TITLE
C          *****
C          SUBROUTINE TC PRINT TITLE IN ASTERISKS
C          TITLE DATA CARD MUST HAVE A NUMBER GREATER THAN ZERO IN THE LAST
C          COLUMN IF TITLE CONTINUES ON TO THE FOLLOWING DATA CARD
C          *****
C002      DIMENSION HEAD(19)
C003      WRITE(6,1)
C004      1 FORMAT(1H1,23X,82(1H*)/24X,1H*,80X,1H*)
C005      2 READ(5,3) HEAD,REST,KONT
C006      3 FORMAT(19A4,A3,I1)
C007      WRITE(6,4)(HEAD(I),I=1,19),REST
C008      4 FORMAT(1H ,23X,1H*,19A4,A3,1X,1H*/24X,1H*,80X,1H*)
C009      IF(KONT.GT.0) GO TC 2
C
C010      WRITE(6,5)
C011      5 FORMAT(1H ,23X,82(1H*)///)
C
C012      RETURN
C013      ENC

```

INPUT DATA ECHO CHECK

3 1 4 0.7813E-02 0.1500E 02

EARTHQUAKE BEING USED IS THE EL CENTO MAY 1940 CNE.(NORTH-SOUTH).....

LATERAL STIFFNESS MATRIX

0.4243E 06	-0.2589E 06	0.4530E 04
-0.2589E 06	0.5725E 06	-0.3174E 06
0.4530E 04	-0.3174E 06	0.3143E 06

DAMPING MATRIX

0.0	0.0	0.0
0.0	0.0	0.0
0.0	0.0	0.0

MASSSES

0.1369E 05 0.1294E 05 0.9310E 06

OUTPUT

TIME DISPLACEMENTS OF MASSES

0.3125E-01	-0.1109E-02	-0.1478E-02	-0.1584E-02
0.6250E-01	-0.2051E-02	-0.3503E-02	-0.4781E-02
0.9375E-01	-0.5277E-02	-0.8303E-02	-0.1040E-01
0.1250E 00	-0.9895E-02	-0.1608E-01	-0.2064E-01

0.1491E 02	0.1069E 01	0.1799E 01	0.2373E 01
0.1494E 02	0.9792E 00	0.1619E 01	0.2106E 01
0.1497E 02	0.7852E 00	0.1334E 01	0.1775E 01
0.1500E 02	0.6686E 00	0.1097E 01	0.1418E 01

MASS 1 MAX DISPLACEMENT= 0.2870E 01 AT TIME 0.4539E 01

MASS 2 MAX DISPLACEMENT= 0.4793E 01 AT TIME 0.4547E 01

MASS 3 MAX DISPLACEMENT= 0.6291E 01 AT TIME 0.4547E 01

STOP

/6

APPENDIX V

SUMMARY OF CALCULATIONS UNDERTAKEN IN MODELLING THE
THREE STOREY FRAME SHOWN IN FIGURE 6.1

Structural Member Sizes

Column 22 ins internal diameter. Wall thicknesses
 5/16 in 3/8 in and 7/16 in (top to bottom).

Rods Circular section mild steel, diameters
 2 $\frac{3}{8}$ in 2 $\frac{1}{8}$ in and 1 $\frac{3}{4}$ in (top to bottom).

Struts Channel Sections (See Figure 6.1)
 8 in 11.5 lb/ft, 9 in 13.4 lb/ft and
 10 in 15.3 lb/ft.

Derived Member Properties

Columns 5/16 in thick section

Cross sectional area	11 in ² ₄
Second Moment of area	673 in ⁴
<u>Total weight/column</u>	<u>1275 lb</u>

3/8 in thick section

Cross sectional area	13.4 in ²
Second Moment of area	820 in ⁴
<u>Total weight/column</u>	<u>1590 lb</u>

7/16 in thick section

Cross sectional area	15.3 in ²
Second Moment of area	948 in ⁴
<u>Total weight/column</u>	<u>1880 lb</u>

Rods

2.375 in diameter

Cross sectional area	4.43 in ²
Length	509 in
<u>Total weight/rod</u>	<u>640 lb</u>

2.125 in diameter

Cross sectional area	3.55 in ²
Length	530 in
<u>Total weight/rod</u>	<u>533 lb</u>

1.75 in diameter

Cross sectional area	2.41 in ²
Length	566 in
<u>Total weight/rod</u>	<u>386 lb</u>

Struts

Upper Strut

Total weight	630 lb
Second Moment of area	86.6 in ⁴

Lower Strut

Total weight	786 lb
Second Moment of area	118.0 in ⁴

Self Weight Distribution

Assuming the self weight of the tower is lumped at the ground, first strut, second strut and ring girder levels respectively,

Weight (lbs) at ground	5,304
first strut	13,688
second strut	12,942
ring girder	5,110

treating the full structure as a plane frame.

Geometry

Lengths of braces		Angle to horizontal
Bottom bay	566 in	53.367°
Middle bay	530 in	52.18°
Top bay	509 in	49.734°

Horizontal member lengths:

Lower strut	344 in
Upper strut	304 in
Ring girder	264 in

REFERENCES

1. Hurty, W.C. and Rubenstein, M.F.: Dynamics of Structures, Prentice-Hall, 1964, 455p.
2. Skinner, R.I.: Earthquake-Generated Forces and Movements in Tall Buildings, New Zealand D.S.I.R. Bulletin 166, 1964, 106p.
3. Housner, G.W.: The Plastic Failure of Frames During Earthquakes, Proceedings Second World Conference on Earthquake Engineering, Tokyo, 1960, II, 997-1012.
4. Shepherd, R.: The Design of Earthquake Resistant Multistorey Framed Structures, Journal of the Institution of Engineers, Australia, 1965, 37(12), 411-415.
5. Shepherd, R.: The Determination of Seismic Design Loads in a Framed Structure, N.Z. Engineering, 1967, 22(2), 56-61.
6. Shepherd, R.: Dynamic Elastic Analyses in the Design of Typical New Zealand High-Rise Buildings, Proceedings Fourth World Conference on Earthquake Engineering, Santiago 1969.
7. ——— New Zealand Standards Institute, NZSS 1900, Chapter 8: Basic Design Loads, 1965.
8. Blume, J.A., Newmark, N.M. and Corning, L.H.: Design of Multi-storey Reinforced Concrete Buildings for Earthquake Motions, Portland Cement Association, Chicago, Ill., U.S.A., 1961, 318 p.
9. ——— International Association for Earthquake Engineering, Tokyo, Earthquake Resistant Regulations, a World List, 1963.
10. Jacobsen, L.S.: Vibration Research at Stanford University, Bulletin, Seismological Society of America, 1929, 19(1), 1-27.
11. Brown, A.L.: Changed Elevated Tank Design Required for Safety Against Earthquakes, Engineering News-Record, 1934, Oct. 4, 424-426.
12. Westergaard, H.M.: Water Pressures on Dams During Earthquakes, Transactions, A.S.C.E., 1932, 418-471.

13. Hoskins, L.M. and Jacobsen, L.S.: Water Pressure in a Tank Caused by a Simulated Earthquake, Bulletin, Seismological Society of America, 1934, 24(1), 1-32.
14. Garder, D.S.: Observed Vibrations of Steel Water Towers, Bulletin, Seismological Society of America, 1936, 26(1), 69-88.
15. McLean, R.S. and Moore, W.W.: Computation of the Vibration Period of Steel Tank Towers, Bulletin, Seismological Society of America, 1936, 26(1), 63-67.
16. Williams, H.A.: Dynamic Distortion of Structures Subjected to Sudden Earth Shock, Transactions, A.S.C.E., 1936, 838-868.
17. Ruge, A.C.: Earthquake Resistance of Elevated Water Tanks, Transactions, A.S.C.E., 1938, 889-949.
18. Murphy, V.A.: New Zealand Earthquake Problem in Relation to Engineering Structures, Proceedings, N.Z. Institution of Engineers, 1946, 32, 302-337.
19. Ulrich, F.P. and Carder, D.S.: Vibrations of Structures, Proceedings, Symposium of Earthquake and Blast Effects on Structures, Los Angeles, 1952, 130-147.
20. Steinbrugge, K.V. and Moran, D.F.: An Engineering Study of the Southern Californian Earthquake of July 21, 1952 and its Aftershocks, Bulletin, Seismological Society of America, 1954, 44 (Appendix R), 436-453.
21. Moran, D.F. and Cheney, J.A.: Earthquake Response of Elevated Tanks and Vessels, Transactions, A.S.C.E., 1958, 503-516.
22. Steinbrugge, K.V. and Flores, R.A.: The Chilean Earthquakes of May 1960, A Structural Engineering Viewpoint, Bulletin, Seismological Society of America, 1963, 53, 225-307.
23. Clough, R.W. and Jenschke, V.A.: The Effect of Diagonal Bracing on the Earthquake Performance of a Steel Frame Building, Bulletin, Seismological Society of America, 1963, 53, 389-401.
24. Housner, G.W.: Limit Design of Structures to Resist Earthquakes, Proceedings, First World Conference on Earthquake Engineering, San Francisco, 1956, 5/1-11.
25. Housner, G.W.: Dynamic Pressures on Accelerated Fluid Containers, Bulletin, Seismological Society of America, 1957, 47, 15-35.

26. Jacobsen, L.S.: Impulsive Hydrodynamics of Fluid Inside a Cylindrical Tank and of Fluid Surrounding a Cylindrical Pier, Bulletin, Seismological Society of America, 1949, 39, 189-204.
27. Graham, E.W. and Rodriguez, A.M.: The Characteristics of Fuel Motion which Affect Air-Plane Dynamics, Journal of Applied Mechanics, 1952, 19(3), 381-388.
28. Housner, G.W.: The Dynamic Behaviour of Water Tanks, Bulletin, Seismological Society of America, 1963, 53, 381-387.
29. Cloud, W.K.: Period Measurements of Structures in Chile, Bulletin, Seismological Society of America, 1963, 53, 368-371.
30. Blume, J.A.: A Structural-Dynamic Analysis of Steel Plant Structures Subjected to the May 1960 Chilean Earthquakes, Bulletin, Seismological Society of America, 1963, 53, 439-480.
31. Shepherd, R.: Earthquake Resistant Design of Petroleum Storage Tanks, Proceedings, Second Australasian Conference on the Mechanics of Structures and Materials, Adelaide, 1969, 8.1-8.11.
32. Chandrasekaran, A.R. and Krishna: Water Towers in Seismic Zones, Proceedings, Third World Conference on Earthquake Engineering, New Zealand, 1965, IV, 161-171.
33. Ramiah, B.K. and Rajata Mohana Gupta, D.S.: Factors Effecting Seismic Design of Water Towers, Proceedings, A.S.C.E., 1966, ST4, 13-30.
34. Sonobe, Y. and Nishikawa, T.: Study on the Earthquake Proof Design of Elevated Water Tanks, Proceedings, Fourth World Conference on Earthquake Engineering, Santiago, 1969, B-4, 11-24.
35. Ifrim, M. and Bratu, C.: The Effect of Seismic Action on the Dynamic Behaviour of Elevated Water Tanks, Proceedings, Fourth World Conference on Earthquake Engineering, Santiago, 1969, B-4, 127-142.
36. Garcia, S.M.: Earthquake Response Analysis and Seismic Design of Cylindrical Tanks, Proceedings, Fourth World Conference on Earthquake Engineering, Santiago, 1969, B-4, 169-182.

37. Hanson, R.D. and Fan, W.R.S.: The Effect of Minimum Cross Bracing on the Inelastic Response of Multistorey Buildings, Proceedings, Fourth World Conference on Earthquake Engineering, Santiago, 1969, A-4, 15-30.
38. Naito, T.: Fifty Years of Earthquake Engineering Practice, Proceedings, Second World Conference on Earthquake Engineering, Tokyo, 1960, I, 127-132.
39. Vignola, S. and Arze, E.: Behaviour of a Steel Plant Under Major Earthquake, Proceedings, Second World Conference on Earthquake Engineering, Tokyo, 1960, I, 573 and 578.
40. Arias, S., Arze, V. and Banza, J.: Repairs on Power House and Boiler Support Structure Damaged by 1965 Earthquake, Ventanas 115 MW Steam Electric Station (Chile), Proceedings, Fourth World Conference on Earthquake Engineering, Santiago, 1969, B-6, 37-45.
41. Arze, E.: Seismic Failure and Repair of an Elevated Water Tank, Proceedings, Fourth World Conference on Earthquake Engineering, Santiago, 1969, B-6, 57-69.
42. Shepherd, R. and Reay, A.M.: Some Apparatus for the Small Amplitude Dynamic Testing of Multi-Storey Buildings. STRAIN, Journal of the British Society for Strain Measurement, 1967, 3(4), 16-21.
43. Shepherd, R.: A Comparison of Calculated and Measured Periods of a Tall Building. New Zealand Engineering, 1967, 22(9), 381-3.
44. Hunt, D.S.: A Dynamic Study of Structural Concrete. Unpublished M.E. Thesis, University of Canterbury, Christchurch, 1966.
45. Erasmus, L.A.: Factors Affecting the Tensile Flow Curve for Low Carbon Steel. Proceedings Second Australasian Conference on the Mechanics of Structures and Materials, Adelaide, 1969.
46. Kalpakjian, S.: 1967: Mechanical Processing of Materials. Van Nostrand.
- ✓ 47. ——— Lateral Forces of Earthquake and Wind. Transactions A.S.C.E., 117, Paper No. 2514. Proceedings Separate No. 66 April 1951.
48. Benioff, H.: The Physical Evaluation of Seismic Destructiveness. Bulletin, Seismological Society of America, 24, 398-403, 1934.

49. Biot, M.A.: A Mechanical Analyzer for the Prediction of Earthquake Stresses. Bulletin, Seismological Society of America, 31, 151-171, 1941.
50. Hudson, D.E.: Response Spectrum Techniques in Engineering Seismology. Proceeding, First World Conference on Earthquake Engineering, San Francisco, 4/1 - 4/12, 1956.
51. Merchant, H.C. and Hudson, D.E.: Mode Superposition in Multi-degree of Freedom Systems Using Earthquake Response Spectrum Data. Bulletin, Seismological Society of America 52, 405-416, 1962.
52. Berg, G.V. and Thomaidis, S.S.: Energy Consumption by Structures in Strong Motion Earthquakes. Proceedings, Second World Conference on Earthquake Engineering, Tokyo, II, 681-697, 1960.
53. Clough, R.W., Benuska, K.L. and Wilson, E.L.: Inelastic Earthquake Response of Tall Buildings. Proceedings, Third World Conference on Earthquake Engineering Wellington, N.Z., II, 68-84, 1965.
54. Walpole, W.R. and Shepherd, R.: Elasto-Plastic Seismic Response of a Reinforced Concrete Frame. Proceedings, A.S.C.E., 95, ST10, 2031-2055, 1969.
55. Shepherd, R.: The Dynamic Analysis of an Apartment Building. Bulletin, Seismological Society of America 56, 1, 13-34, 1966.
56. Shepherd, R.: Determination of Seismic Design Loads in a Framed Structure. N.Z. Engineering 22, 2, 56-61, 1967.
57. Wang, P.C.: Numerical and Matrix Methods in Structural Mechanics. Wiley, 1966.
58. Hudson, D.E.: Equivalent Viscous Friction for Hysteretic Systems with Earthquake-Like Excitations. Proceedings, Third World Conference on Earthquake Engineering. Wellington, N.Z., II, 185-203, 1969.
59. Rosenblueth, E.: Discussion on reference 59. *ibid.* II, 203-205, 1969.
60. Newmark, N.M.: A Method of Computation for Structural Dynamics. Proceedings A.S.C.E., 85, EM3, 67-93, 1959.

61. Arden, B.W.: An Introduction to Digital Computing. Addison Wesley, Massachusetts. 1963.
62. Nordsieck, A.: On Numerical Integration of Ordinary Differential Equations. Maths. Comput. 16, 22-49, 1962.
63. Shepherd, R. and McConnel, R.E.: Some Aspects of the Solution of Equations of Motion Using Numerical Integration Techniques. Australian Computer Journal, 3, 1, 18-22, 1971.
64. Biggs, J.M.: An Introduction to Structural Dynamics. McGraw Hill. New York, 1964, p.146.
65. Wang, P.C.: Numerical and Matrix Methods in Structural Mechanics, Wiley, New York, 1966, p.185.
66. Turner, M.J., Clough, R.W., Martin, H.C. and Topp, L.J.: Stiffness and Deflection Analysis of Complex Structures. Journal of the Aeronautical Sciences, 23 (9), 805-854, 1956.
67. Carr, A.J.: A Refined Finite Element Analysis of Thin Shell Structures Including Dynamic Loadings. Ph.D. Thesis, University of California, Berkeley, 1967.
68. Skinner, R.I.: Earthquake Generated Forces and Movements in Tall Buildings, Bulletin 166 D.S.I.R. Wellington, N.Z. 1964.
69. Walpole, W.R.: The Response of Structures to Earthquake Loading. Unpublished Ph.D. Thesis. University of Canterbury, 1968.
70. Berg, G.V.: Punched Card Accelerograms of Strong Motion Earthquakes. Report No. 2881-1-P, University of Michigan, September 1959.
71. Jennings, P.C. Housner, G.W. and Tsai, N.C.: Simulated Earthquake Motions for Design Purposes. Proceedings, Fourth World Conference on Earthquake Engineering, Santiago, 1969. A-1, 145-160.
72. Seed, H.B. and Idriss, I.M.: The Influence of Soil Conditions on Ground Motions during Earthquakes. Proc. A.S.C.E. 95, SM1, 99-137, (Jan.) 1969.
73. Shepherd, R. and Donald, R.A.M.: Seismic Response of Torsionally Unbalanced Buildings. Journal of Sound and Vibration, 6 (1) 20-37, 1967.

74. Garden, R.J.P., Shepherd, R. and Sharpe, R.D.: Notes on the Representation of Plastic Hinge Behaviour in Dynamic Analysis. New Zealand Engineering, 24(12), 386-391, 1969.
75. ————— Earthquake Resistant Design for Civil Engineering Structures, Earth Structures and Foundations in Japan. The Japan Society of Civil Engineers, Tokyo 1968.